Simulation of Water Transport through Nano-Foam Filter

A thesis submitted to Addis Ababa Institute of Technology, School of Graduate Studies, Addis Ababa University

In partial fulfillment of the requirement for degree of

Master of Science in Mechanical Engineering

(Mechanical Design Stream)

By

Tesfaye Gonite

Advisor

Professor Eyassu woldesenbet

Co-advisor

Dr. Daniel Tilahun

September 2015

Addis Ababa University

School of Graduate Studies

School of Mechanical and Industrial Engineering

Simulation of Water Transport through Nano-Foam Filter

A thesis submitted to Addis Ababa Institute of Technology, School of Graduate studies, Addis Ababa University

In Partial Fulfillment of the Requirement for Degree of

Master of Science in Mechanical Engineering

(Mechanical Design Stream)

By Tesfaye Gonite

Addis Ababa Institute of Technology, AAiT

Approved by Examining Board

Dr. Daniel Tilahun	_____
Chairman	Signature
Professor Eyassu woldesenbet	_____
Advisor	Signature
Dr. Daniel Tilahun	_____
Co-Advisor	Signature
Ato Mulugeta HabteMaryam	_____
External Examiner	Signature
Ato Araya Abera	_____
Internal Examiner	Signature

Acknowledgement

First of all I would like to thank the Almighty God, because it is impossible to finish this thesis without his blessings and help. Next I want to thank heartily my advisor professor Eyassu Woldesenbet for his unmeasured role in this thesis. He has been supportive from the selection of the title to this end. As I am new for nanotechnology and nanofiltration, his vast knowledge gave me insight to tackle the problems faced me during this paper work. I also got different life skills and good personality from him. I would not forget that he said "never give reason to solve problems; be knowledgeable person by fetching from different sources."

I would like to express my deep thank to my co-advisor Dr. Daniel Tilahun, the head of the school of mechanical and industrial engineering for his encouragement and willingness to support me by facilitating the way to get the simulation software. And also I want to say thank you for his customer handling and treatment.

I would like to thank Dr. Zewudu who supported me during the area selection by providing with papers and documents.

Finally I would like to thank my classmates especially those of who are advisees of Professor Eyassu Woldesenbet for their unlimited openness and constructive comments.

Abstract

Our world has shortage of water for household use especially potable water. People; researchers are putting their effort since early 4000 B.C. to find the solution. This time the world put trust on nanotechnology to alleviate the problem of drinking water. However there are challenges in the area. These are mainly related to membrane stability, lifetime, and lack of fundamental understanding of the process performance that can be translated in to modeling and simulation tools.

This study aimed to obtain the best composition and arrangement of polyurethane foam, activated carbon particle and silver nanoparticle in order to gage 2 to 3 L/h flow rate of water through simulation. Extensive literature reviews were made to know concepts, theories and previous findings in the area of Nanofiltration, specifically in water filtration. For the simulation, the finite element software COMSOL Multiphysics version 4.3 or 2012 release has been used. Simulation is done for 10PPI, 20PPI, 30PPI, 40PPI, 50PPI, 60PPI, 70PPI and, 90PPI polyurethane foam with different size, numbers and arrangements of activated carbon particles. Finally, nine best combinations of polyurethane foam with activated carbon particles and silver nanoparticles are identified based on the result of the simulation. Conclusions and some recommendations for future researchers are also made.

Key words: Flow rate, flow through porous media, polyurethane foam, activated carbon, silver nanoparticle, simulation

Table of Contents

Contents

List of tables

List of Figures

Nomenclatures

$(pb - pa)$ - Pressure drop across medium

μ - Fluid viscosity

A - Cross-sectional area of Porous medium

AC - Activated carbon

Al - Aluminum

ATR-FTIR - Attenuated total reflection-Fourier transform infrared,

CDC -Center of disease control and prevention

CIP - Cleaning in place

EDC - Endocrine disrupting compounds

EPA - United States Environmental Protection Agency

ESR - Electron spin resonance,

Fe - Ferrous

GAC- Granular activated carbon

L - Length of sample

NMR - Nuclear magnetic resonance

NOM- Natural organic matter

NP - Nanoparticle

OC - Dissolved organic matter

PAC- Powdered activated carbon

Ph.D.-Doctoral philosophy

PPCPs - Pharmaceutically active compounds and personal care products

PPI- Pores per inch

PU - Polyurethane

q - Darcy flux

Q - Volumetric flow rate

Re - Reynolds number

UV - Ultra violet

v - Fluid velocity

WHO - World health organization

XPC - X-ray photoelectron spectroscopy

κ - Permeability of porous medium

ρ - Density

ϕ - Porosity

CHAPTER ONE

INTRODUCTION

1.1. History of water filtration

Water treatment originally focused on improving the aesthetic qualities of drinking water. Methods to improve the taste and odor of drinking water were recorded as early as 4000 B.C. [20, 21]. Ancient Sanskrit and Greek writings recommended water treatment methods such as filtering through charcoal, exposing to sunlight, boiling, and straining. Visible cloudiness (later termed turbidity) was the driving force behind the earliest water treatments, as many source waters contained particles that had an objectionable taste and appearance [21, 52]. To clarify water, the Egyptians reportedly used the chemical alum as early as 1500 B.C. to cause suspended particles to settle out of water. During the 1700s, filtration was established as an effective means of removing particles from water, although the degree of clarity achieved was not measurable at that time. By the early 1800s, slow sand filtration was beginning to be used regularly in Europe. During the mid to late 1800s, scientists gained a greater understanding of the sources and effects of drinking water contaminants, especially those that were not visible to the naked eye [21, 32]. In Paisley, Scotland, the first municipal water treatment plant was constructed in 1804 [18]. In 1855, epidemiologist Dr. John Snow proved that cholera was a waterborne disease by linking an outbreak of illness in London to a public well that was contaminated by sewage. In the late 1880s, Louis Pasteur demonstrated the "germ theory" of disease, which explained how microscopic organisms (microbes) could transmit disease through media like water [21, 31].

During the late nineteenth and early twentieth centuries, concerns regarding drinking water quality continued to focus mostly on disease-causing microbes (pathogens) in public water supplies [21, 32, 48]. Scientists discovered that turbidity was not only an aesthetic problem; particles in source water, such as fecal matter, could harbor pathogens. As a result, the design of most drinking water treatment systems built in the U.S. during the early 1900s was driven by the need to reduce turbidity, thereby removing microbial contaminants that were causing typhoid, dysentery, and cholera epidemics. In order to reduce turbidity, some water systems in U.S. cities (such as Philadelphia) began to use slow sand

filtration. While filtration was a fairly effective treatment method for reducing turbidity, it was disinfectants like chlorine that played the largest role in reducing the number of waterborne disease outbreaks in the early 1900s. In 1908, chlorine was used for the first time as a primary disinfectant of drinking water in Jersey City, New Jersey. The use of other disinfectants such as ozone also began in Europe around this time [16, 19]. In the 1970s and 1980s, improvements were made in membrane development for reverse osmosis filtration and other treatment techniques such as ozonation. Some treatment advancements have been driven by the discovery of chlorine-resistant pathogens in drinking water that can cause illnesses like hepatitis, gastroenteritis, legionnaire's disease, and cryptosporidiosis. Other advancements resulted from the need to remove more and more chemicals found in sources of drinking water [18]. However, newer treatment techniques (e.g., reverse osmosis and granular activated carbon) are also being employed by some modern drinking water facilities.

Nanofiltration was introduced in the late 1980s, mainly aiming at combined softening and removing of organics. Since then, the application range of nanofiltration has extended tremendously [8].

New possibilities were discovered for drinking water production, providing answers to new challenges such as arsenic removal, removal of pesticides, endocrine disruptors and chemicals, and partial desalination.

During the last two decades, the interest in the use of membrane technology in general and nanofiltration in particular has emerged in wastewater treatment as well as drinking water and process water production. This growth can be explained by a combination of growing demand for water with high quality, growing pressure to reuse wastewater, better reliability and integrity of the membranes, lower prices of membranes due to enhanced use, and more stringent standards, e.g., in the drinking water industry [8]. T. Pradeep [59] also gives short summary of history of water purification (1800–2007) from the perspective of noble metal nanoparticles in water treatment as depicted by (table 1) [59].

Table 1: History of water purification (1800-2007) [59]

Year	Milestone
1804	Setup of world's first city-wide municipal water treatment plant (Scotland, sand-filter technology)
1810	Discovery of chlorine as a disinfectant
1852	Formulation of Metropolis Water Act (England)
1879	Formulation of Germ Theory (L. Pasteur)
1902	Use of chlorine as a disinfectant in drinking water supply (calcium hypochlorite,)
1906	Use of ozone as a disinfectant (France)
1908	Use of chlorine as a disinfectant in municipal supply, New Jersey
1914	Federal regulation of drinking water quality (USPHS)
1916	Use of UV treatment in municipal supplies
1935	Discovery of synthetic ion exchange resin
1948	Nobel Prize to Paul Hermann Muller (insecticidal properties of DDT)
1959	Discovery of synthetic reverse osmosis membrane
1962	Silent Spring published first report on harmful effects of DDT (R. Carson)
1965	World's first commercial RO plant launched
1974	Reports on carcinogenic by-products of disinfection with chlorine Formulation of Safe Drinking Water Act (USEPA)
1975	Development of carbon block for drinking water purification
1994	Report on use of zero valent iron for degradation of halogenated organics
1997	Report on use of zero valent iron nanoparticles for degradation of halogenated organics
1998	Drinking Water Directive applied in EU
2000	Adoption of Millennium Declaration during the UN Millennium Summit (UN Millennium Development Goals)
2003	Report on use of noble metal nanoparticles for the degradation of pesticides
2004	Stockholm Convention, banning the use of persistent organic pollutants
2007	Launch of noble metal nanoparticle-based domestic water purifier

Even though many extensive work and study have been done, the problem of drink water is still serious issue for the world [38]. WHO estimates that, in 2008 diarrheal disease claimed the lives of 2.5 million people. For children under five, this burden is greater than the combined burden of HIV/AIDS and malaria [66]. According to CDC report 2,195 Children die daily of diarrhea, that is like losing nearly 32 school buses full of children each day [55].

A total of 58 countries from all continents reported a cumulative total of 589,854 cholera cases in 2011, representing an increase of 85% from 2010. The greatest proportion of cases was reported from the island of Hispaniola and the African continent [64]. Aasif Mujtaba [1] also presented the problem of drinking water in a table as follows:

Table 2: Problem of drinking water [1]

884 million	people lack access to safe water supplies, approximately one in eight people
6 kilometers	is the average distance African and Asian women walk to fetch water
3.6 million	people die each year from water-related disease
98 per cent	of water-related deaths occur in the developing world
84 per cent	of water-related deaths are in children ages 0–1
43 per cent	of water-related deaths are due to diarrhea
65 million	People are at risk of arsenic poisoning in the Bangladesh, India and Nepal area

Ethiopia boasts a population of about 83 million people and which only 38 percent have access to safe drinking water sources and only 12 percent of the population use improved sanitation facilities [28]. Therefore the problem of drinking water needs the maximum effort of all people interested in the wellbeing of the Ethiopian population. It also motivates someone to do best as much as he/she can.

1.2. Statement of the problem

The problem addressed in this study was the flow rate of the water through polyurethane foam combined with activated carbon nanoparticle and silver nanoparticle composite filter using a suit computer simulation. In addition the phenomena of flow around the activated carbon particles and filtration mechanism of the nanoparticles will be addressed.

The number of applications for nanofiltration increases steadily; nevertheless, several challenges remain to be solved to allow the use of nanofiltration in more demanding applications. Drinking water production currently faces new challenges [8].

Drawbacks in this area are of a different kind; for solvent filtration, one of the emerging applications, these are mainly related to membrane stability and lifetime, and the lack of fundamental understanding of the process performance that can be translated to modeling and simulation tools. Challenges that were identified by B. Van der Bruggen, 2008 [8] are membrane fouling, its causes and possibilities to remediate, separation between solutes that can be achieved, further treatment of concentrates, chemical resistance of membranes, insufficient rejection in water treatment, and the need for modeling and simulation tools. It must be stressed that many applications are already running regardless of these suggested improvements. In addition the cost of different water filter systems is not affordable especially for most people who live in developing countries as shown in (table 3).

Table 3: Name of filters and their cost [41]

No.	Name of filter	Cost of filter
1	Ion exchange	$400-$1000 (plus installation).
2	Distillation	$300(counter-top)-$1700(automatic), plus electricity to run
3	Reverse osmosis	$100 (under sink) - $400 (whole house) (plus installation)
4	Chlorination	cost (continuous chlorinator): $500 - $1300
5	UV Radiation	$250 (under sink) - $1000+ (whole house)
6	Ozonation	$250 (portable) - $2000 (whole house)
7	Activated Carbon	$30 (faucet mount) - $450 (whole house)
8	Mechanical	$35 (single faucet) - $550+ (whole house)

Herewith there are many types of water treatment systems available, but no one type of treatment can address every water quality problem [41]. Nowadays, cost effective nanocomposite (polyurethane foam combined with activated carbon nanoparticle and silver nanoparticle composite filter, that is well efficient to remove waterborne pathogenic and organic and inorganic contaminants) water filter is on progress to take part in solving the above problem [20]. But the simulation of the filter is not yet performed. Hence the simulation of water transport

through the filter was performed to provide an efficient combination and arrangement of materials for the achievement of a solution.

1.3. Objective of the study

The main objective of the study was to obtain the best composition and arrangement of polyurethane foam, activated carbon nanoparticle and silver nanoparticle in order to get 2 to 3 L/h flow rate of water through simulation. Auphedeous Y. Dang-i, and Winston. O. Soboyejo [6] did experimental study for two kinds of ceramic filters; one without hydroxylapatite and the other with hydroxylapatite. They obtained the flow rate between 1-2 liters per hour (L/h), which is the acceptable flow rate for all ceramic filters. The pore size of the filters is 1μm as they obtained by X-Ray diffraction (XRD) and Energy Dispersive X-ray Spectroscopy (EDS). But the pore size of the polyurethane foam is greater than 1μm, which is 0.133mm and above [16]. Flow rate and cross section area of flow have direct proportional relationship. That is why my objective is to obtain 2 to 3 L/h flow rate.

The specific objectives were:-

- ✓ To simulate using *COMSOL multiphysics*.
- ✓ To analyze the flow rate.
- ✓ To study the effect of the particles size and arrangement on the flow of water
- ✓ To identify the best suit size and amount of activated carbon particle, and silver nanoparticle

1.4. Strategy of the study

In order to achieve the study objective, the following strategies are utilized. First I have extensively reviewed literatures to know: the basic parameters used during simulation, properties of foam, activated carbon particle, silver nanoparticles, the mechanism of adsorption and immobilizing of activated carbon in the support matrix and action of silver nanoparticles on microbes, bonding mechanism of activated carbon particles to the foam, and the size and the amount of particles essential for the efficient water filter.

Software simulation was used to obtain the result of the flow rate. The finite element software COMSOL Multiphysics 4.3 was used. Then the simulation result is analyzed to identify the best

type of composition. Finally, the results were compared with other results that were previously studied.

1.5. Scope of the study

In this particular study the simulation of water transport through polyurethane foam based activated carbon silver nanocomposite filter is presented.

1.6. Significance of the study

This study will have the following importance:

1. It will provide the potential in achieving a better design of the filter.
2. It will have important role in speeding up the application of the project. Therefore the implementation period will be shortened. If it is so the people who suffer of waterborne diseases will be saved in the next few years.
3. It will be used as reference for other study.

1.7. Organization of the thesis

Chapter one: introduction part, which contains the history of water filtration from early 4000BC to this modern era. The statement of the problem, the objective of the thesis, strategy and scope of the study, and the significance of the study are found in this chapter.

Chapter two: back ground of the study, in this chapter the brief and basic concepts of nanofiltration such as; flow through porous media, nanofiltration membranes, membrane characterization, performance parameters, and morphology parameters, nanocomposite filter, adsorption of particles to polyurethane foam, colloid filtration theory are presented.

Chapter three: literature survey here more than thirteen articles are reviewed and the motivation of the thesis also presented in this chapter.

Chapter four: Simulation and analysis in this part of the study the highlight of COMSOL Multiphysics simulation software, the assumed working conditions of the filter simulated, the result of simulation and analysis of result are presented.

Chapter five: conclusion and recommendations, the summary of the thesis drown from the simulation and analysis result is briefly presented in this chapter. The recommendations for future researchers are also discussed here.

CHAPTER TWO

BACKGROUND OF THE STUDY

2.1. Flow through porous media

Many daily processes involve the movement of fluids across porous medium. For example, sponge, drying of wood, filtration of water by using sand and/or other porous materials. As commonly observed, some fluid flows through the media while some mass of the fluid is stored in the pores present in the media. The knowledge of how the fluid diffuses through these materials and what are the factors upon which the diffusion depends is really useful for engineering practices. Four sets of equations that apply under different conditions form the basis for these application modes are [13]:

- Darcy's law describes low-velocity flows of one or more fluids.
- For porous media, the Brinkman equations cover high-velocity flows.
- Richards' equation governs the wetting and drying of rocks or soils.
- The Navier-Stokes equations describe free flows within a river or well, for example.

2.1.1. Darcy's Law

The basic law governing the flow of fluids through porous media is Darcy's Law, which was formulated by the French civil engineer Henry Darcy in 1856 on the basis of his experiments on vertical water filtration through sand beds. Darcy's law applies when the gradient in hydraulic potential drives fluid movement in the porous medium [67].

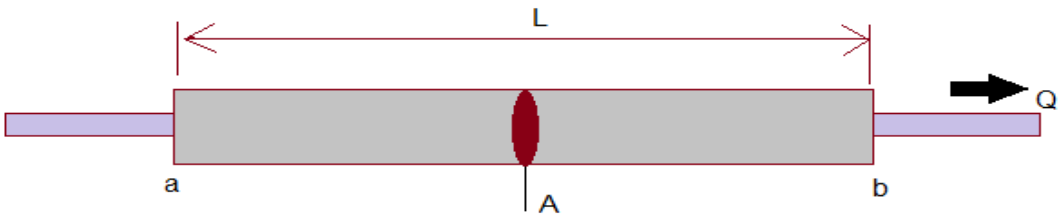

Figure 1: Diagram showing definition and direction of Darcy`s law [15]

According to which (Wikipedia authors, 2015 and Zimmerman, D.R., 2002-2003) [15, 67],

$$Q = \frac{-\kappa A}{\mu}\frac{(\mathrm{pb} - \mathrm{pa})}{L} \tag{2.1}$$

Where;

Q = Volumetric flow rate [m^3/s]

κ = Permeability of porous medium [m^2]. The permeability is a function of material type, and also varies with stress, temperature, etc.

μ = Fluid viscosity [Pa.s]

A = Cross-sectional area of Porous medium [m^2]

$(pb - pa)$ = Pressure drop across medium [Pa]

L = Length of sample[m]

The negative sign is needed because fluid flows from high pressure to low pressure. Note: the elevation head must be taken into account if the inlet and outlet are at different elevations. If the change in pressure is negative (where $pa > pb$), then the flow will be in the positive 'x' direction. Dividing both sides of the equation by the area and using more general notation leads: [15]

$$q = \frac{-k}{\mu}\nabla p \tag{2.2}$$

Where q is the flux (discharge per unit area, with units of length per time, m/s) and ∇p is the pressure gradient vector (Pa/m). This value of flux, often referred to as the Darcy flux, is not the velocity which the fluid traveling through the pores is experiencing. The fluid velocity (v) is related to the Darcy flux (q) by the porosity (ϕ). The flux is divided by porosity to account for the fact that only a fraction of the total formation volume is available for flow. The fluid velocity would be the velocity a conservative tracer would experience if carried by the fluid through the formation [67].

$$v = \frac{q}{\phi} \tag{2.3}$$

Darcy's law is a simple mathematical statement which neatly summarizes several familiar properties that groundwater flowing in aquifers exhibits, including:

- If there is no pressure gradient over a distance, no flow occurs (these are hydrostatic conditions),
- If there is a pressure gradient, flow will occur from high pressure towards low pressure (opposite the direction of increasing gradient - hence the negative sign in Darcy's law),
- The greater the pressure gradient (through the same formation material), the greater the discharge rate, and
- The discharge rate of fluid will often be different
    - Through different formation materials (or even through the same material, in a different direction)
    - Even if the same pressure gradient exists in both cases.

Darcy's law is only valid for slow, viscous flow. Typically any flow with a Reynolds number less than one is clearly laminar, and it would be valid to apply Darcy's law. Experimental tests have shown that flow regimes with Reynolds numbers up to 10 may still be Darcian, as in the case of groundwater flow. The Reynolds number (a dimensionless parameter) for porous media flow is typically expressed as [15]

$$Re = \frac{\rho v}{\mu} d_{30} \tag{2.4}$$

Where ρ is the density of water (units of mass per volume), v is the specific discharge (not the pore velocity with units of length per time), d_{30} is a representative grain diameter for the porous media (often taken as the 30% passing size from a grain size analysis using sieves with units of length), and μ is the viscosity of the fluid.

For transient processes in which the flux varies from point to-point, the following differential form of Darcy's law is used [15].

$$Q = \frac{-\kappa A}{\mu} \left(\frac{dp}{dx}\right) \tag{2.5}$$

According to Darcy's law, the net flux across a face of porous surface is [13]:

$$u = -k/\eta \, (\nabla p + \rho f g \nabla D) \tag{2.6}$$

In this equation, u is the Darcy velocity or specific discharge vector (m/s); κ is the permeability of the porous medium (m^2); η is the fluid's dynamic viscosity ($Pa \cdot s$); p is the fluid's pressure (Pa) and ρf is its density (kg/m^3); g is the magnitude of gravitational acceleration(m/s^2); and D is a unit vector in the direction over which g acts. Here the permeability κ represents the resistance to flow over a representative volume consisting of many solid grains and pores.

2.1.2. Brinkman Form of Darcy's Law

Is extension to the traditional form of Darcy's law is the Brinkman term, which is used to account for transitional flow between boundaries (introduced by Brinkman in 1949) [15],

$$\beta \nabla^2 q + q = -\kappa p \tag{2.7}$$

Where β is an effective viscosity term, this correction term accounts for flow through medium where the grains of the media are porous themselves.

D.D. Joseph, D.A. Nield and G. Papanicolaou [14] have formulated a nonlinear extension of Brinkman's self-consistent theory for the flow of viscous fluid through a swarm of spherical particles. They equated the drag per unit volume given by the right hand side of the first of Darcy's equation ($\nabla p = -(\mu/k)\, V - (pc\ /\ (k^{1/2}))|v|v$, div V=0) to the total drag ND on the N particles contained with in the unit volume, in an infinite region Ω where D is the drag on a single partice placed in a velocity field Vsubjected to $\rho(V.\nabla)V + grad\, p = \mu\nabla^2 V - (\mu/k)V - (cp/k^{1/2})|v|v$, div V=0, V $|_{\partial\Omega}$ is prescribed constant, μ is the viscosity.

2.1.3. Darcy-Forchheimer Law

For very high velocities in porous media, inertial effects can also become significant. Sometimes an inertial term is added to the Darcy's equation, known as Forchheimer term. This term is able to account for the non-linear behavior of the pressure difference versus velocity data [14].

$$\frac{\partial p}{\partial x} = -\frac{\mu}{\kappa} q - \frac{\rho}{\kappa 1} q2 \tag{2.8}$$

Where, the additional term κ_1 is known as inertial permeability.

2.1.4. Non-Darcy Flow in Porous Media

Non-Darcy behavior is important for describing fluid flow in porous media in situations where high velocity occurs. Two types of criteria, the Reynolds number and the Forchheimer number,

have been used in the past for identifying the beginning of non-Darcy flow. Because each of these criteria has different versions of definitions, consistent results cannot be achieved. Darcy's law is an approximation in describing the phenomenon of fluid flow in porous media, and is valid under a limited range of low velocities. Experimentally, fluid flow deviations from Darcy's law have long been observed [27]. Various terms, such as non-Darcy flow, turbulent flow, inertial flow, high velocity flow, etc., have been used to describe this behavior. Forchheimer (1901) added a second order of the velocity term to represent the microscopic inertial effect, and corrected the Darcy equation into the Forchheimer equation: [27]

$$-\frac{dp}{dX} = \frac{\mu v}{k} + +\beta\rho v^2 \tag{2.9}$$

Many researchers intensively studied to gate the value of Reynolds number where non-Darcy flow is started [24]. But due to inconsistency in definitions and thus in critical values, no widely accepted criterion for non-Darcy flow in porous media is available. Zhengwen Zeng and Reid Grigg [27] have recommend Forchheimer Number criterion. The Forchheimer number has the advantage of clear definition, sound physical meaning, and wide applicability than Reynolds number criterion [27].

$$Fo = \frac{k\beta\rho v}{\mu} \tag{2.10}$$

In the Forchheimer equation, Equation (2.9), the left-hand-side term,$-(dp/dX)$, is the total pressure gradient. The first term in the right-hand side, $(\mu v/k)$, can be considered as the pressure gradient required overcoming viscous resistance. Similarly, the second term $\beta\rho v^2$ is the pressure gradient needed to overcome liquid–solid interactions. The ratio of the liquid-solid interaction pressure gradient to that by viscous resistance leads to $(k\beta\rho v/\mu)$, which is the Forchheimer number defined in Equation (2.10). Therefore, the Forchheimer number is the ratio of liquid–solid interaction to viscous resistance.

2.2. The Navier-Stokes Equations

An equation, when the forces acting in or on the fluid are those of viscosity, gravity, and pressure, is called the Navier–Stokes equation. The Navier-Stokes equations are employed to represent steady state creeping incompressible flow conditions, i.e. [27].

$$-\frac{\partial p}{\partial i} + \mu.\nabla^2 vi + \rho w g i = 0 \quad \text{i=x, y, z}$$

$$\nabla.\underline{v} = 0 \tag{2.11}$$

where p is the pressure (Pa), μ is the dynamic viscosity of the water (Pa.s), vx, vy, vz are the vector components for the velocity ($\underline{v} = vx\vec{\imath} + vy\vec{j} + vz\vec{k}$) of the water (m/s), ρw is the density of the water (kg/m^3), and gx, gy, gz are the vector components for the gravitational acceleration (9.81 m/s^2). The Navier–Stokes equation is difficult to solve in a given flow problem to obtain spatial distributions of velocities and pressures and shear stresses. Basically the reasons are that the acceleration term is nonlinear, meaning that it involves products of partial derivatives, and the viscous-force term contains second derivatives, that is, derivatives of derivatives. Only in certain special situations, in which one or both of these terms can be simplified or neglected, can the Navier–Stokes equation be solved analytically. But numerical solutions of the full Navier–Stokes equation are feasible for a much wider range of flow problems, now that computers are so powerful. Equation (2.11) is valid for Reynolds number much less than one. The Reynolds number is defined as:

$$Re = \frac{\underline{v}\, d\rho w}{\mu} \tag{2.12}$$

Where d is the diameter of the collector (m).

2.3. Flow past a spherical collector at low Reynolds numbers

Consider flow of a viscous fluid past a sphere by restricting consideration to low Reynolds numbers $\rho UD/\mu$ (where, as before, *U* is the uniform approach velocity and *D* is the diameter of the sphere).

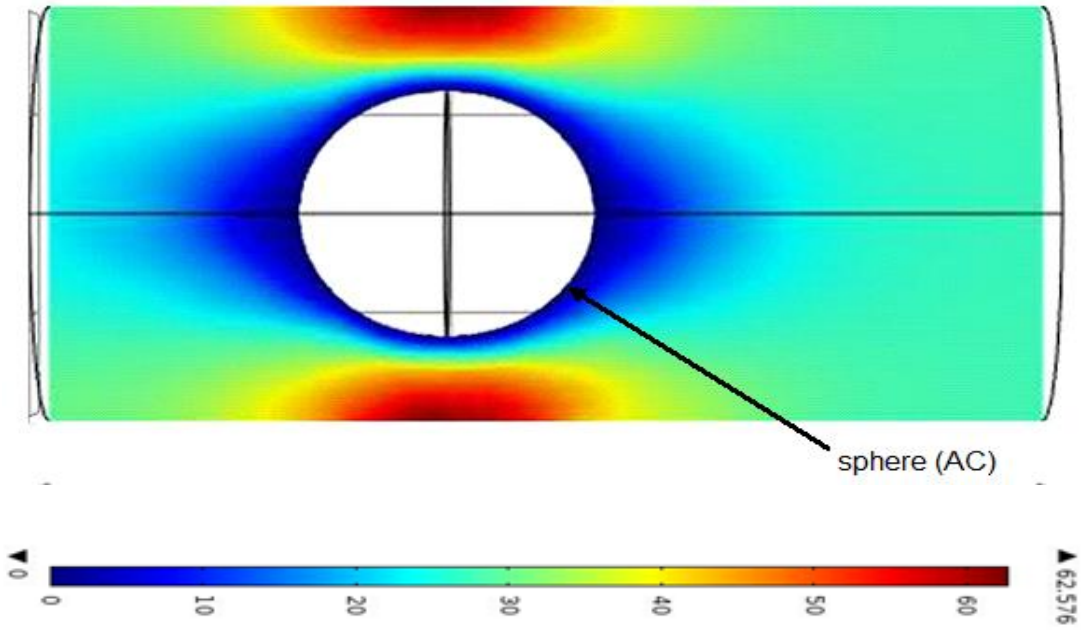

Figure 2: Steady flow of a viscous fluid at very low Reynolds numbers ("creeping flow") past a sphere

At very low Reynolds numbers, Re << 1, the flow lines relative to the sphere are about as shown in Figure 2. The first thing to note is that for these very small Reynolds numbers the flow pattern is symmetrical front to back. For a relatively large distance away from the sphere surface the dark blue flow stream gradually become light blue, indicating that the fluid velocity is less than the free-stream velocity. For very low Reynolds numbers, however, the effect of "crowding", which acts to increase the velocity, is more than offset by the effect of viscous retardation, which acts to decrease the velocity.

The velocity of the fluid is everywhere zero at the sphere surface (the no-slip condition) and increases only slowly away from the sphere, even in the vicinity of the midsection: at low Reynolds numbers, the retarding effect of the sphere is felt for great distances out into the fluid. The zone of retardation shrinks greatly as the Reynolds number increases, and the "crowding" effect causes the velocity around the midsection of the sphere to be greater than the free-stream velocity except very near the surface of the sphere.

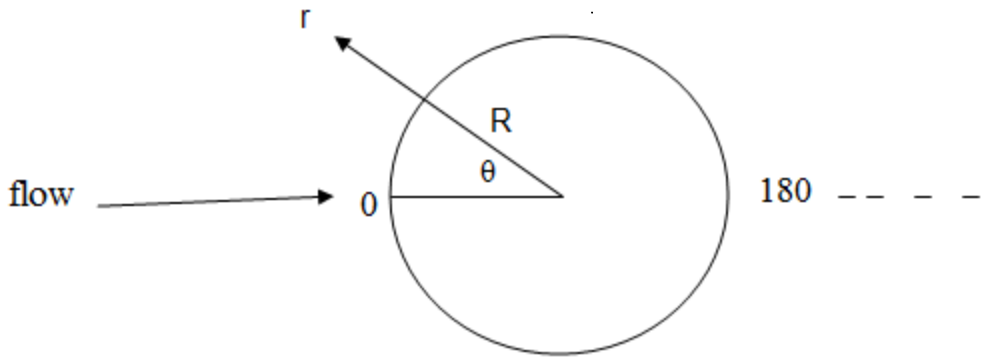

Figure 3: Coordinate for description of the theoretical distribution of velocity in flow past a sphere at very low Reynolds numbers (creeping flow)

Equations 2.13 give the theoretical distribution of velocity v, as a function of distance r from the center of the sphere and the angle θ measured around the sphere from 0° at the front point to 180° at the rear point (Figure 3) [47]:

$$\left.\begin{aligned} Ur &= -U\cos\theta\left\{1-\frac{3R}{2r}+\frac{R\text{^}3}{2r\text{^}3}\right\} \\ U\theta &= U\sin\theta\left\{1-\frac{3R}{4r}+\frac{R\text{^}3}{4r\text{^}3}\right\} \end{aligned}\right\} \quad (2.13)$$

"This result was obtained by Stokes (1851) by specializing the Navier–Stokes equations for an approaching flow that is so slow that accelerations of the fluid as it passes around the sphere can be ignored, resulting in an equation that can be solved analytically" [47]. Fluid density ρ is needed as a variable to describe the drag force on a sphere because accelerations are produced in the fluid as the sphere moves through it. If these accelerations are small enough, however, it is reasonable to expect that their effect on the flow and forces can be neglected. Flows of this kind are called creeping flows. The reason, to which is that in the Navier–Stokes equations the term for rate of change of momentum becomes small faster than the two remaining terms, for viscous forces and pressure forces, as the Reynolds number decreases.

You can see from Equations 2.13 that as $r \to \infty$ the velocity approaches its free-stream magnitude and direction. The $\frac{1}{r}$ dependence in the second terms in the parentheses on the right-hand sides of (Equations 2.13) reflects the appreciable distance away from the sphere the effects of viscous retardation are felt.

At every point on the surface of the sphere there is a definite value of fluid pressure (normal force per unit area) and of viscous shear stress (tangential force per unit area). These values also come from Stokes' solution for creeping flow around a sphere. For the shear stress, you could use Equations 2.13 to find the velocity gradient at the sphere surface. For the pressure, Stokes found [47] a separate equation,

$$P - Po = \frac{3}{2}\frac{\mu UR}{r^2}cos\theta \tag{2.14}$$

Where, Po = the free-stream pressure

(Figures 4 and 5) give an idea of the distribution of these forces. It is easy to understand why the viscous shear stress should be greatest around the midsection and least on the front and back surface of the sphere, because that is where the velocity near the surface of the sphere is greatest. The distribution of pressure, high in the front and low in the back, also makes intuitive sense. It is interesting, though, that there is a large front-to-back difference in pressure despite the nearly perfect front-to-back symmetry of the flow.

You can imagine adding up both pressures and viscous shear stresses over the entire surface, remembering that both magnitude and direction must be taken into account, to obtain a resultant pressure force and a resultant viscous force on the sphere. Because of the symmetry of the flow, both of these resultant forces are directed straight downstream. You can then add them together to obtain a grand resultant, the total drag force F_D. Using the solutions for velocity and pressure given above (Equations 2.13 and 2.14), Stokes obtained the result for the total drag force on the sphere [47].

$$F_D = 6\pi\mu UR \tag{2.15}$$

Density does not appear in Stokes' law because it enters the equation of motion only the mass-time-acceleration term, which was neglected. For Reynolds numbers less than about one, the result expressed by (Equation 2.15), called Stokes law is in nearly perfect agreement with experiment. "It turns out that in the Stokes range, for $Re << 1$, exactly one-third of F_D is due to the pressure force and two-thirds is due to the viscous force"[44].

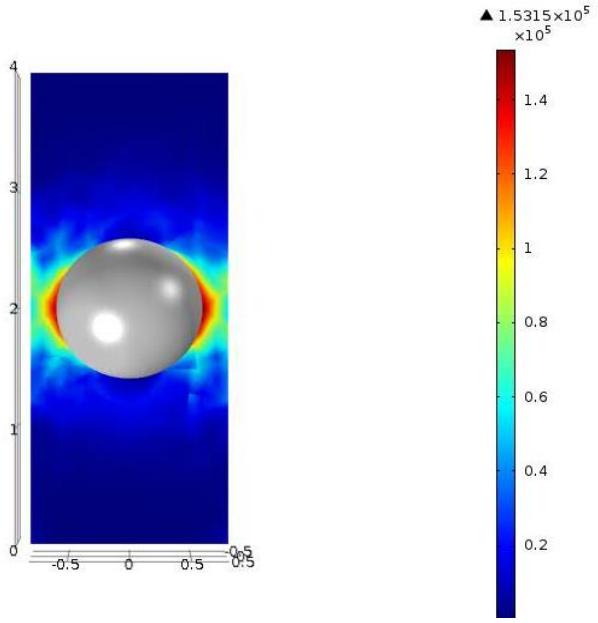

$$\tau_o = \frac{3}{2}\frac{\mu U sin\theta}{R}$$

Figure 4: Distribution of shear stress on the surface of a sphere in a flow of viscous fluid at very low Reynolds numbers (creeping flow).

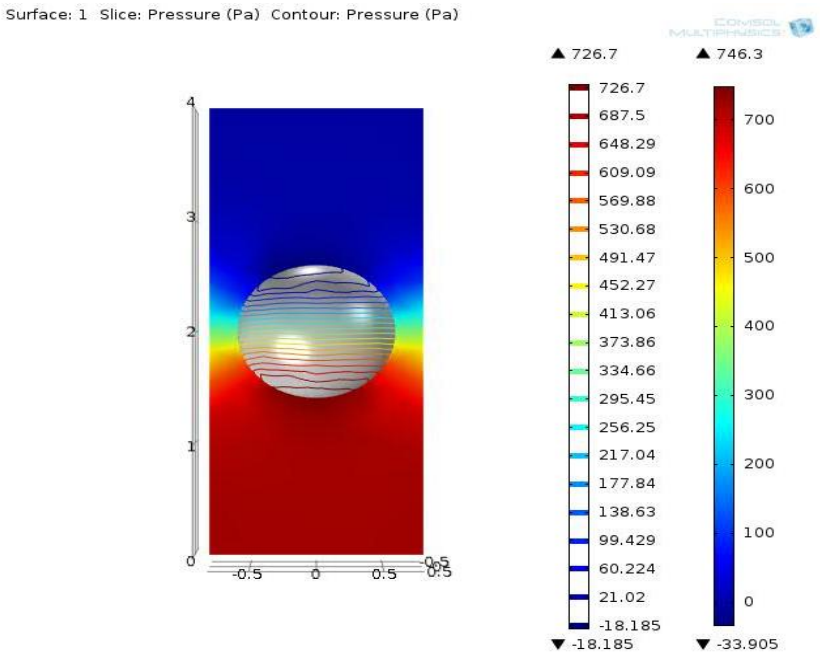

Pressure, P= $-\frac{3}{2}\frac{\mu U cos\theta}{R}$

Figure 5: Distribution of pressure on the surface of a sphere in a flow of viscous fluid at very low Reynolds number (creeping flow).

In a porous medium, fluid flow around a spherical collector is affected by the presence of other collectors around it. Therefore, a proper flow model for porous media is needed to reflect the disturbance of the flow field around the individual collectors. Among the various theoretical models Happel's fluid shell model is the most commonly used model.

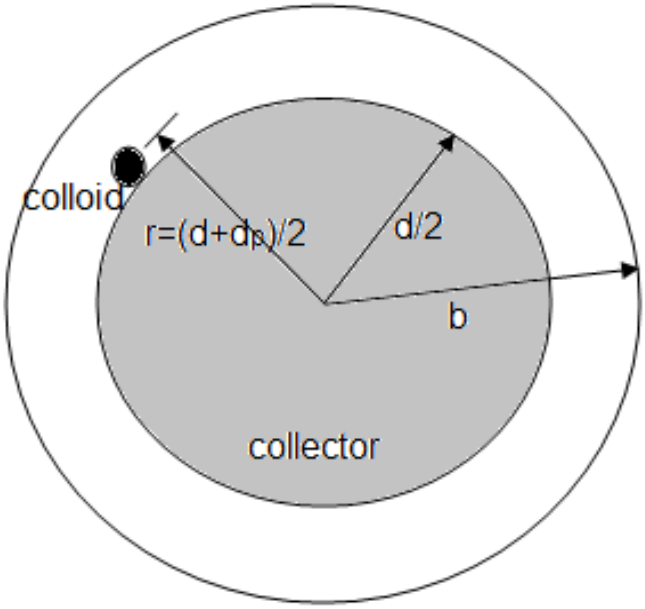

Figure 6: Schematic representation of a unit collector, and Happel's fluid shell [11]

In Happel's model, the porous medium is constructed of identical spherical collectors, each of which is in a fluid shell (Figure 6). In order to maintain the overall porosity of the porous medium for a single collector, the thickness of the shell, b, is defined as:

$$b = \frac{d}{2}(1 - \varepsilon)^{1/3} \tag{2.16}$$

Where, ε = the porosity of the porous medium

2.4. Convection-Diffusion Equation

Once the velocity field is determined, the distribution of colloids within the pore space of a porous medium can be found by solving the convection-diffusion equation for steady state conditions. The convection-diffusion equation is given by [11]:

$$(\underline{v} \,.\nabla C) - (D\,\nabla^2 C) - \sum_i \left(1 - \frac{\rho w}{\rho p}\frac{mgi}{3\pi\mu dp}\frac{\partial C}{\partial Xi}\right) \tag{2.17}$$

Where C is the concentration of the colloids ($number\ of\ colloids/m^3$); D is the diffusion coefficient of the colloids calculated by Einstein's equation (m^2/s), ρp is the density of an individual colloid (kg/m^3), m is the mass of the colloids (kg), and dp is the diameter of the colloids (m). The terms in the equation represent (left to right) the colloid transport processes of convection, diffusion, and gravitational settling.

When colloids make contact with a collector surface it is assumed that they disappear into the collector by specifying the collector surface as being a perfect sink. This means that all colloids arriving at the collector surface are irreversibly captured. The condition for a perfect sink can be achieved by setting the concentration in the vicinity of the collector surface to zero, i.e. [11],

$$C = 0 \text{ at } r = (d + dp)/2 \tag{2.18}$$

Where r represents the radius of an imaginary spherical surface displaced slightly outward from the surface of the collector (m) (Figure 6).

At an infinite distance from the collector center the colloid concentration is assumed to be equal to the free stream concentration, C_0

$$C = C0 \text{ at } r = \infty \tag{2.19}$$

In previous analyses that used Happel's model for the flow velocity field, the above boundary condition is specified at the surface of the fluid shell, i.e.

$$C = C0 \text{ at } r = b \tag{2.20}$$

The diffusion coefficient in the convection-diffusion equation is calculated by Einstein's equation [11]:

$$D = \frac{KT}{3\pi\mu dp} \tag{2.21}$$

Where k is the Boltzmann's constant (J/K), and T is the absolute temperature (Kelvin).

2.5. Deposition (Collision) Efficiency

Solution of equations (2.11) and (4.17) subject to the corresponding boundary conditions will yield the mass of particles entering the shell, the concentration of particles within the spherical

shell, and the mass of particles leaving the shell. Also, the flux of particles passing into the ideal sink will also be determined from that solution. The solution can then be used to determine the particle deposition efficiency, η, which is calculated as: [11]

$$\eta = \frac{I}{\upsilon o \, Co \frac{\pi dp2}{4}} \tag{2.22}$$

Where I is the total particle deposition rate onto a collector, obtained by integrating the particle flux over the surface of the collector, υo is the free stream (initial) water velocity

2.6. Nanofiltration membranes

NF is a pressure driven membrane process and the convective transport of associated components occurs with the water flux through the membrane owing to the pressure difference between the feed and the permeate sides in the system.

Membrane manufacture process, material type, and membrane structure plays an important role in selective character of membrane. Two structural categories can be given: symmetric and asymmetric membranes. The latter one is the mostly used structure in the commercially available membranes and consists of two subgroups: integrally skinned asymmetric membranes and composite membranes. Integrally skinned asymmetric membranes are produced by phase inversion technique, which is a controlled transformation of a polymer solution from a liquid into a solid state.

The most widely used methods to produce composite membranes are dip coating and interfacial polymerization. In dip coating, the support layer is dipped into a low concentration polymer solution. Afterwards, it is dried in an oven where solvent evaporates and a thin (up to 1 μm) active layer forms dependent on the concentration of the polymer solution. Interfacial polymerization, the most currently used method, produces ultrathin layers (< 50 nm). In this technique, polymerization occurs at the interface between two immiscible monomer solutions. The developments in membrane material technology are ongoing in line with industrial demands. One of the approaches is to develop polymeric composite membranes with controllable surface chemistry and charge and tight pore size distribution.

2.6.1. Membrane module of Nano filter

In applications of NF processes, membrane module gains importance since the flux obtained from a membrane material depends on the available total membrane area and module characteristics. Hence, the membrane area per unit volume for a given element (packing density) is an important consideration among other factors such as fouling, in selecting a module for an application. Today NF membranes are produced in spiral wound, plate and frame, hollow fiber, capillary and tubular configurations from a range of materials, including cellulose derivatives, synthetic polymers, inorganic materials and organic / inorganic hybrids.

Table 4: Comparison of different membrane module types [5]

Module	Packing density (m^2/m^3)	NF Application	Limitation for NF
Tubular	80-450	+	None
Plate and frame	100-1000	+	Pressure containment
Spiral wound	500-1000	++	None
Hollow	500-5000	-	Burst pressure of fiber

++ = major application, + = some application, - =rare application

2.6.2. Current applications

Due to its charge and thus selective separation, NF is utilized in diverse industrial fields and finds increasingly new application areas. A predominant field is water treatment, scarcity. It has been a state of the art process in the pre-treatment of wastewater for the removal of refractory materials before the biological treatment. Moreover, it is gradually more applied in the drinking water production fields since the undesired components can be removed in one step unlike to conventional treatment, which makes it even cheaper in some cases. It is generally expected to remove from 60 % to 80 % of hardness (e.g. Ca^{2+}, Mg^{2+}), greater than 90 % of colour and all turbidity if applied in water treatment processes. Approximately 65 % of the NF market constitutes water treatment, 25 % the food and dairy industries and 10 % the chemical industry.

Table 5: A general overview of current and future NF application [5]

Industry	Application
Water	Softening, removal of NOM from surface waters, removal of EDC / PPCPs from natural water and wastewater, removal of DOC and pesticides from surface water and wastewater, removal of nitrate ion from natural water, water removal of heavy metals from industrial wastewater, sulphate removal, seawater pre-treatment, desalination by dual stage, partial demineralization of seawater to prepare personal body washing solutions (salinity near $9g/L$)
Food	Centration and demineralization of whey/UF whey, treatment of vapour condensate in milk processing, concentration of dairy matter, recycle of process waters in dairy industry, Food recovery of cleaning agent from CIP discharge in dairy industry, purification of dextrose syrup, decolorization of sugar solutions, demineralization of colored brine from anion-exchange resin elution, concentration of glycoside sweeteners from stevial leaves, concentration of xylose reaction liquor or manufacturing xylitol sweetener
Beverage	grape juice concentration for wine processing
Textile	removal of organics, color, turbidity in wastewater
Pulp and paper	Pulp and paper treatment of effluents to reuse water
Leather	✓ recovery and recycle of tannins in the leather industry ✓ removal of sulphate and chromium from wastewater
Pharmaceutical	recovery and concentration of antibiotics
Diverse	✓ sulfate removal from brine feed to the electrolyzers in chloralkali plants, dewaxing organic solvent by solvent resistant NF membranes, in production processes of organic acids, Diverse removal of caustic in aggressive wastewater streams, recovery of precious metals such as gold and silver, catalyst recovery by solvent resistant NF membranes, in tissue engineering and orthopaedics, DNA and protein separation

Abbreviations: NOM = natural organic matter, EDC = endocrine disrupting compounds, PPCPs = pharmaceutically active compounds and personal care products, DOC = dissolved organic matter, CIP = cleaning in place

2.7. Membrane characterization

Membrane characterization parameters can be categorized into three groups:

- Performance parameters
- Morphology parameters
- Charge parameters

2.7.1. Performance parameters

Performance parameters are usually defined in terms of rejection and permeate flux [5].

$$R = (1 - \frac{Cp}{\mathrm{CF}}).100 \tag{2.23}$$

Permeate flux is a result of a driving force acting on the components. It is determined by both the driving force and the total resistance of the membrane as well as the interfacial region adjacent to it. In industrial applications, fouling and accordingly the applied cleaning procedure affect the permeate flux. Depending on the reason in flux increase, i.e. through pressure or cross-flow velocity, rejection may increase or decrease based on the concentration polarization phenomenon and the module design. Performance characterizations are basically composed of pure water permeability along with rejection measurements of uncharged and / or charged solutes. Characterization of membranes in terms of their performance parameters is performed in this work by the above mentioned standard measurements, i.e. pure water permeability, uncharged and charged solute filtration measurements.

2.7.2. Morphology parameters

Membrane characterization is also essential for performance description, prediction and optimization modelling studies. AFM is relatively new technique which can be used basically to quantify NF membrane properties such as pore size distribution, thickness and surface morphology, to obtain surface electrical properties, to investigate surface adhesion membrane fouling behavior and to correlate membrane characteristics with process behavior.

Table 6: Morphology characterization methods for NF membranes [5]

Method	Characteristic (s)
Gas adsorption/desorption	Pore size, surface area
Permporometry	Pore size/porosity
Microscopy Field emission microscopy (FEM),Scanning electron microscopy (SEM),Atomic force microscopy (AFM)	pore size, porosity Surface roughness, pore size, porosity
Spectroscopy ATR-FTIR, ESR/NMR, Ramen spectroscopy, XPS	Chemical composition
Contact angle Captive bubble method, Sessile drop method	Hydrophobicity

ATR-FTIR = Attenuated total reflection-Fourier transform infrared, ESR = Electron spin resonance, NMR = nuclear magnetic resonance, XPC = X-ray photoelectron spectroscopy

Hydrophilic / hydrophobic character of the membrane has influence on the membrane wettability and gives clues about the fouling tendency and the chemical as well as the mechanical stabilities of the membrane. For instance, hydrophobic membranes have good chemical and mechanical stabilities but show more fouling tendency than hydrophilic membranes. Hydrophilic membranes usually have more functional groups that can dissociate and generate a charge on the membrane and show generally higher fluxes.

Another important parameter is the chemical structure of a membrane. Some post-treatment methods in the membrane manufacturing can introduce functional groups to the surface or change the membrane hydrophilicity. Charge is certain to be an important physicochemical parameter in respect of the rejection mechanisms and fouling tendency of a membrane.

2.8. Nanocomposite Filter

The definition of a nanotechnology, as defined by the Environmental Protection Agency (EPA) [21], is as follows: "research and technology development at the atomic, molecular, or macromolecular levels using a length scale of approximately 1−100 nm in any dimension; the creation and use of structures, devices, and systems that have novel properties and functions because of their small size, and the ability to control or

manipulate matter on an atomic scale." Specifically, a nanoparticle is defined as a particle consisting of 10 to 105 atoms that is utilized for its unique size characteristics, which can fulfill a variety of functions, such as serving as biosensors, nano electric materials, and also antibacterial consumer products [10].

Composite materials (composites) are inherently heterogeneous and represent a defined combination of chemically and structurally different constituent materials, ensuring the required properties such as mechanical strength, stiffness, low density, or other specific characteristics depending on their purpose. Therefore, composite material is a system composed of two or more physically distinct phases whose combination produces a synergistic effect and aggregate properties that are different from those of its constituents. Favorable characteristics of composite materials were known to the people even in the period BC and were used in order to improve the quality of human daily life. Significant development and application of composites began in the second half of the 20^{th} century, wherein their diversity and areas of application are constantly increasing. Development of composite materials is resulted mainly from the increasing need for materials with better mechanical characteristics that would be used as components in various constructions. For this purpose, such composites should have an adequate strength, stiffness, good oxidation resistance and low weight.

Modern composites can be said to have "designed micro-and nanostructures" which means that the constituents of composites have much more finely divided structures and tend to have sizes in the micrometer or nanometer range.

Taking into consideration that available supplies of fresh water are limited (due to population growth, extended deficiency, stringent health regulations, and competing demands from a variety of users/consumers) the world is facing with challenges to satisfy demands on high water quality standards and quantities (volumes). Benefits and trends in Nano-scale science, chemistry and engineering impose that many of the current problems regarding green chemistry may be resolved using nano-sorbents, nano-catalysts, nanoparticles and nanostructured catalytic membranes. Dhermendra K. Tiwari, J. Behari and Prasenjit Sen [17] have written as "In the area of water purification, nanotechnology offers the possibility of an efficient removal of pollutants and germs. Today nanoparticles, nano membrane and nano powder used for detection and removal of chemical and biological substances include metals (e.g. Cadmium, copper, lead,

mercury, nickel, zinc), nutrients (e.g. Phosphate, ammonia, nitrate and nitrite), cyanide, organics, algae (e.g. cyanobacterial toxins) viruses, bacteria, parasites and antibiotics."

Nano-materials are characterized by a number of key physicochemical properties being particularly attractive for water purification treatments [38]. Nanomaterials have:

- ✓ Much large specific surface area than bulk respect particles (mass to volume ratio),
- ✓ They can be functionalized with reactive chemical groups specific in affinity to a given model compound.
- ✓ These materials may possess redox features and take part in shape- and structural-dependent catalyzed reactions of water purification.
- ✓ In aqueous solutions, they can serve as sorbents/catalysts for toxic metal ions, radionuclides, organic and inorganic solutes/anions.
- ✓ Moreover, nano-materials can be used in selective targeting of biochemically constituents of aquatic bacteria and viruses.

The Nano-materials seems to be key components in future environmental friendly and cost-effective functional materials to desalinate public and polluted water world-wide, for purification of water contaminated by pesticides, pharmaceuticals, phenol and other aromatics as well as microorganisms such as bacteria, virus. Therefore the Nano foam filter that I simulated is composed of polyurethane foam, silver nanoparticle, and activated carbon particles.

2.9.1. Polyurethane foam

Polyurethane (PU) stands for a group of products within the family of polymers or plastics. It is the generic name for a wide range of foam types [50, 51]. The structure of PU foam consists of a network of dodecahedron cells which behave as micro-springs. The cell is 12-dimensional, formed by 125-angeled windows and 30 ribs.

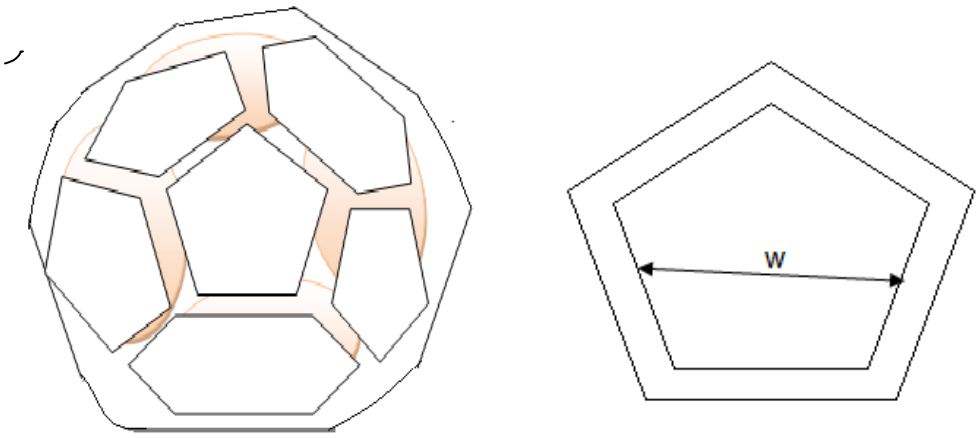

Figure 7: Network of dodecahedron cells [50]

The morphology and the chemical structure of the ribs characterize the final properties of the foam. That's why the analysis of the cell is an important approach to develop and design new foam varieties based to specific demands.

The properties of PU depend on:

- The chemical composition and thickness of the cell walls.
- The volume-solid matter/air ratio.
- The concentration of the cell membranes (air permeability/open cell structure).

In the production of polyurethane foam three basic raw materials play a key role: polyol, di-isocyanate and water. Agents, such as catalysts and stabilizers, are used to support the chemical process. Supplementary, further additives can be added to obtain specific product properties [50]. Polyurethane polymers are traditionally and most commonly formed by reacting a di- or polyisocyanate with a polyol. Both the isocyanates and polyols used to make polyurethanes contain on average two or more functional groups per molecule [51].

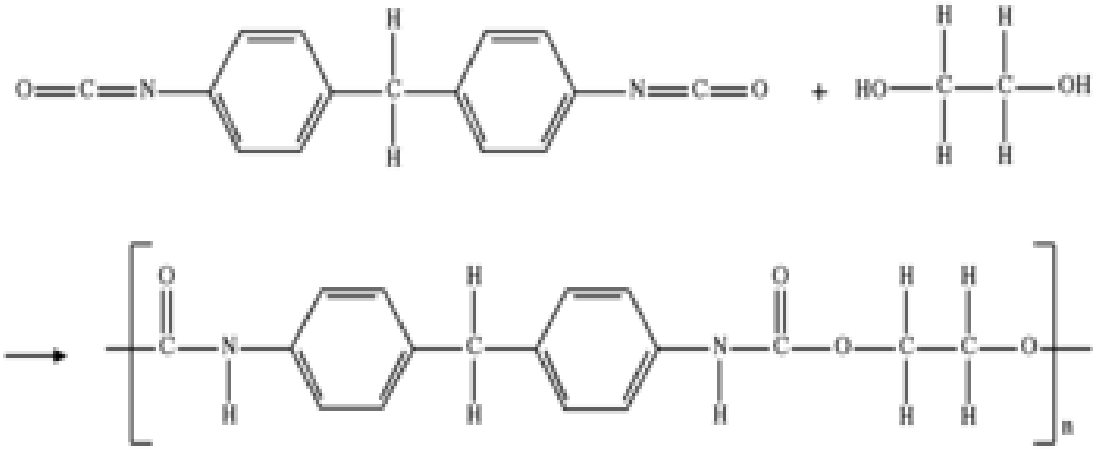

Figure 8: Polyurethane synthesis, where in the urethane groups (NH-(C=O)-O-) link to the molecular unit [51]

Foam is produced in blocks that can be sliced to give thicknesses from 3 to 200 mm, and form sheets 2 m × 1 m [14]. 50×50×6mm PU foam was used through experiment for bacteria removal from water by combining with silver nanoparticles by Nguyen [46]. Prashant Jain also use 20cm×25cm of thickness 8mm foam and he got 100% efficiency water filter experimentally [53].

Composite materials composed of polymers and adsorbents show potential for purification applications. Polyurethane (PU) foams have been used as adsorbents in the treatment of contaminated water and effluent because they are cheap and can be used without prior treatment. In addition, PU foams have important properties for this purpose. These are:

- PU foams are able to retain different classes of substances because of the presence of both polar and nonpolar groups in their structures.
- PU foams can possess a high surface area because of their open porous structures and thus can be used as matrices to immobilize various adsorbents such as AC, biomass, clays, and hydroxyapatite that are used to treat aqueous solutions containing heavy metal ions.

Polyurethane has the following important characteristics; compressibility, cushioning, energy absorption, fabricatibility, flexibility, light-weight, low thermal conductivity, low water vapor transmission, mildew-resistance, resiliency, sound absorption, vibration dampening. The

polyurethane foam used for water filter purpose has 10 to 90 PPI porosity and 25kg/m^3 density [48]. The porosity 10 to 45 PPI is offered [20]. The nominal pore size ranges of polyurethane foam are depicted in (table 7) [57]. Average pore diameters versus pores per linear inch in polyurethane foam is shown figure 9.

Table 7: Nominal pore size range of polyurethane foam

Porosity Grade (pores/inch)	Minimum Porosity	Maximum Porosity
100	80	110
80	70	90
60	55	65
45	40	50
30	25	35
25	20	30
20	15	25
10	8	15

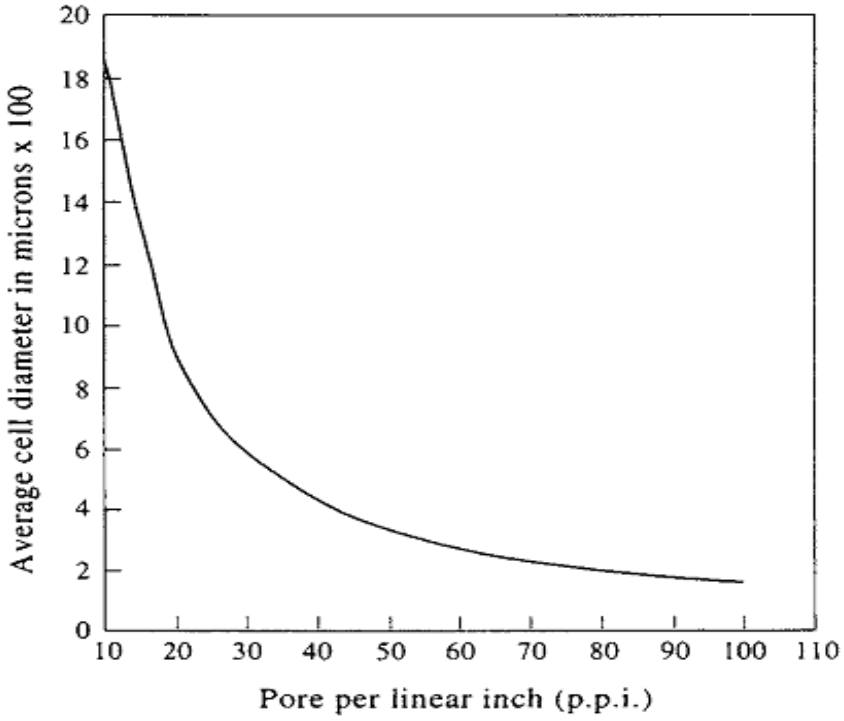

Figure 9: Average pore diameters versus pores per linear inch in polyurethane foam [16].

2.9.2. Activated carbon

Carbon is the sixth most common element in the universe and the fourth most common element in the solar system. It is the second most common element in the human body after oxygen. About 18 percent of a person's body weight is due to carbon. The black color of smoke is caused by unburned specks of carbon. Carbon is the 17^{th} most common element in the Earth's crust. Its abundance has been estimated to be between 180 and 270 parts per million. It rarely occurs as a diamond or graphite [33].

Activated carbon (AC) has been proven to be an effective adsorbent for the removal of a wide variety of organic and inorganic pollutants from aqueous or gaseous media. It is widely used, due to its exceptionally high surface area (ranges from 500 to 1500 $m^2.g^{-1}$), well-developed internal micro porosity, and wide spectrum of surface functional groups [2]. Activated carbons normally have surface areas greater than 1000 m^2g^{-1}, mainly because of the high micro porosity rather than the external surface area (A_{ext}) [44].

Activated carbon has also proven to remove bacteria like Pseudomonas aeruginosa and Escherichia coli from fresh and potable water systems. Despite electrostatic repulsion between negatively charged microorganisms and carbon surfaces, microorganisms attach to activated carbon particles through strong Lifshitzvan derWaals forces. Potable water systems are considered low in ionic strength so electrostatic interactions can offer the possibly of enhancing the efficiency of activated carbon to remove microorganisms from water by positive charge modification of the carbon surfaces. Once there is a charge reversal, the electrostatic attraction between negatively charged microbial cell surfaces and positively modified carbon particles [36].

The process of contaminant adsorption to activated carbon, in a system containing free water is generally thought to involve three steps: macro transport, micro transport, and sorption. Macro transport involves movement of an organic compound through water to the liquid-solid interface by advection and diffusion. Micro transport involves diffusion of the organic compound through the macro pores system of GAC to adsorption sites in the microspores and submicropores of GAC. The term sorption is used because it is difficult to differentiate between chemical and physical adsorption. Sorption results in the accumulation of a chemical species on the interface between the two distinct phases. Solute adsorption from liquid solution on a solid surface can be

thought of the net result of the competition between the surface and the solvent for solute molecules [40].

Activated carbons are complex products which are difficult to classify on the basis of their behavior, surface characteristics and other fundamental criteria. However, some broad classification is made for general purpose based on their size, preparation methods, and industrial applications [3].

Powdered activated carbon

Normally, activated carbons are made in particulate form as powders or fine granules less than 1.0 mm in size with an average diameter between 0.15 and 0.25 mm. Thus they present a large surface to volume ratio with a small diffusion distance.

Granular activated carbon (GAC)

Granular activated carbon has a relatively larger particle size compared to powdered activated carbon and consequently, presents a smaller external surface. GAC typically has a diameter ranging between 1.2 to 1.6 mm and an apparent density ranging between 25 and $31 lb/ft^3$, depending on the material used and manufacturing process [62]. These carbons are suitable for absorption of gases and vapors, because they diffuse rapidly. Granulated carbons are used for water treatment, deodorization and separation of components of flow system and are also used in rapid mix basins. GAC can be either in granular or extruded form.

Extruded activated carbon (EAC)

Extruded activated carbon combines powdered activated carbon with a binder, which are fused together and extruded into a cylindrical shaped activated carbon block with diameters from 0.8 to 130 mm. These are mainly used for gas phase applications because of their low pressure drop, high mechanical strength and low dust content.

Bead activated carbon (BAC)

Bead activated carbon is made from petroleum pitch and supplied in diameters approximately from 0.35 to 0.80 mm. Similar to EAC; it is also noted for its low pressure drop, high mechanical strength and low dust content, but with a smaller grain size. Its spherical shape makes it preferred for fluidized bed applications such as water filtration.

Impregnated carbon

Porous carbons containing several types of inorganic impregnate such as iodine, silver, cations such as Al, Mn, Zn, Fe, Li, and Ca have also been prepared for specific application in air pollution control especially in museums and galleries. Due to its antimicrobial and antiseptic properties, silver loaded activated carbon is used as an adsorbent for purification of domestic water.

Polymer coated carbon

This is a process by which a porous carbon can be coated with a biocompatible polymer to give a smooth and permeable coat without blocking the pores. The resulting carbon is useful for hemoperfusion. Hemoperfusion is a treatment technique in which large volumes of the patient's blood are passed over an adsorbent substance in order to remove toxic substances from the blood.

Others

Activated carbon is also available in special forms such as cloths and fibers. The "carbon cloth" for instance is used in personnel protection for the military.

Adsorption process using granular activated carbon (GAC) or powdered activated carbon (PAC) have been used extensively as the final stage in water, groundwater, and wastewater treatment to remove trace levels of hazardous organic contaminants [40].

2.9.3. Silver nanoparticle

Silver nanoparticle can be produced using different methods. V. Hoek [30] in 2009 has stated three method**s.**

1. Chemical reduction: it is the most common method of producing silver by the process of a silver salt dissolved in water with a reducing compound such as NaBH4, citrate, glucose, hydrazine, and ascorbate. In order to generate silver nanoparticles with controlled sizes, a two-step method is usually utilized. In this method, nuclei particles are prepared using a strong reducing agent and they are enlarged by a weak reducing agent.
2. Biological methods involve the production of silver nanoparticles utilizing extracts from bio-organisms as reductant, capping agents or both. Such extracts can include proteins,

amino acids, polysaccharides, and vitamins. Plant extracts such as apian (a glucoside compound) and leaf extract from magnolia, Persimmon, geranium, and Pine leaf have also been used as reducing agents of Ag+ to produce silver nanoparticles.

3. Solvated metal atom dispersion (SMAD) method. In this method, a metal is co-vaporized with a solvent onto a liquid nitrogen cooled surface, as liquid nitrogen is removed the metal atoms and solvent warms causing the aggregation of metal atoms.

Many new applications for AgNPs have recently been developed, including AgNP embedment in bacterial cellulose wound dressings, water filters, and surface coatings for biofilm prevention [4]. The use of silver ions as antimicrobial agents is limited by the solubility of silver ions in biological and environmental media containing Cl^-, because AgCl has a very low solubility and rapidly precipitates out of solution. In some cases, silver salts are stabilized with hyper branched polymers or dendrimers that act as nanoreactors, wherein silver ions are initially complexed with a specific moiety in the polymeric structure and then reduced to form silver nanoparticles within the polymeric matrix. Silver nanoparticles coated onto polyurethane and silver–magnetite composite nanoparticles (Fe3O4@Ag); both of these hybrids are utilized for water disinfection [30].

2.9.3.1. Bactericidal activity of silver nanoparticle

Silver, in the form of nanoparticles (Ag NP) and ions, is a common antimicrobial agent. It interacts with cell components (e.g., DNA, RNA, and ribosomal units), deactivating them and effectively stopping microbial life processes. It has been observed that Ag NP can puncture cell membranes and penetrate deep into the cell interior. Silver ion and silver-based compounds are highly toxic to microorganisms, showing strong biocidal effect against as many as 16 species of bacteria, including Escherichia coli [17, 37]. Inhibitory effect of Ag+ is due to its sorption to the negatively charged bacterial cell wall, deactivating cellular enzymes, disrupting membrane permeability, and ultimately leading to cell lysis and death [1].

Spherical shape and the sizes from 7 – 11 nm; 7 – 14 nm; 6 – 11 nm; 6 – 12 nm are suitable for killing bacteria, virus, and fungus [43]. Although the mechanisms behind the activity of nano-scaled silver on bacteria are not yet fully elucidated, the three most common mechanisms of toxicity proposed to date are: (1) uptake of free silver ions followed by disruption of ATP

production and DNA replication, (2) silver nanoparticle and silver ion generation of ROS, and (3) silver nanoparticle direct damage to cell membranes [1, 4, 7, 30, 54].

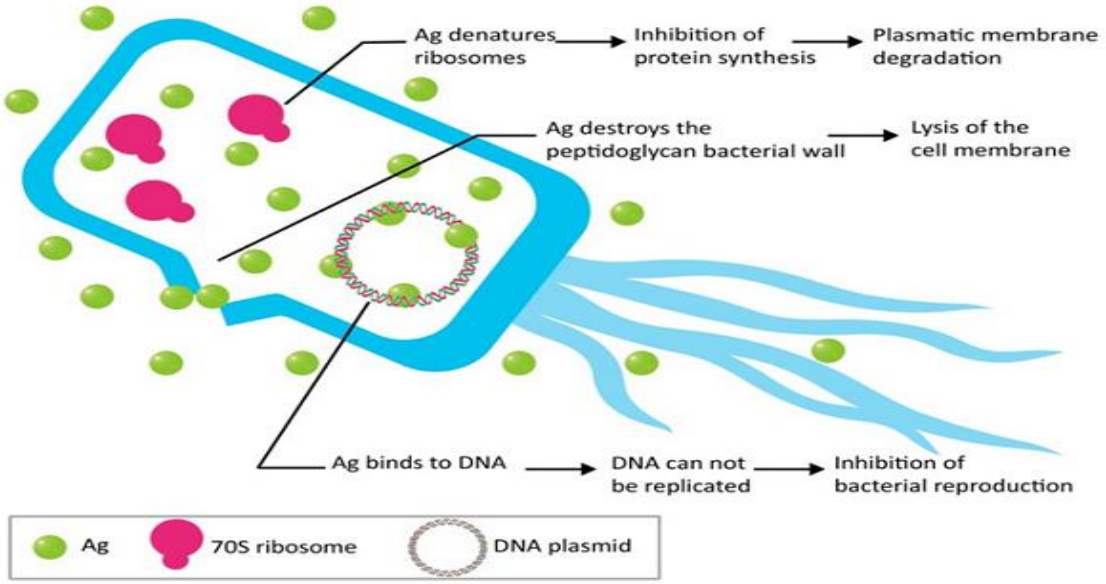

Figure 10: Mechanism for antibacterial activity of silver [7, 30]

2.10. How to compose polyurethane foam, activated carbon particle and silver nanoparticle?

To produce Silver Nanoparticle-Coated Polyurethane Foam, Flexible PU foams soaked in silver colloidal solutions for specified time, then washed and air-dried at room temperature [46]. Repeated washing and air-drying yields uniformly coated PU foam, which can be used as a drinking water filter where bacterial contamination of the surface water is a health risk. The nanoparticle binding is due to its interaction with the nitrogen atom in the ─NH─ bond of the PU [26, 53]. This prepared filter can kill E. coli after 15 min. with the antibacterial efficiency of over 95% and after 5hr with antibacterial efficiency of 100% for the content of silver nanoparticles (g) of polyurethane sheets (kg) from 0.25 to 2.80g/kg [46]. At a flow rate of 0.5 L/min, in which contact time of the order of a second, the output count of Escherichia coli was nil when the input water had a bacterial load of 10^5 colony-forming units (CFU) per mL [49].

To coat AC, activated carbon granules should impregnated in silver nanoparticles solution under vigorous stirring at room temperature overnight to make sure the coating is complete. The

activated carbon coated with silver was then cured in a vacuum oven at 110°C for at least 2h to allow full coating of the silver nano-particles onto the activated carbon [2].

PU foam/AC composite adsorbents can be prepared by adding granular AC during the preparation of PU foam. The composite foams prepared in this way possess well-developed open cell structures with a non-uniform distribution of AC [35]. A higher carbonization temperature promoted the formation of pore structures.

2.11. Water Contaminants

a. Pathogens

Bacteria are commonly found in water; it is when they start to increase in numbers that are above safe levels that water contamination occurs. Two of the most common pathogen pollutants are Coliform and E. coli bacteria. Coliforms are normally present in the environment in safe levels and can actually be used to detect other pathogens in water. However, Water Filter Review reports that if coliforms increase in numbers, it can be dangerous for the health of the environment. The presence of E. coli bacteria indicates that water has been contaminated with human or animal wastes. It has rod length 1.0-3.0µm and rod or coccus diameter 0.5 µm.

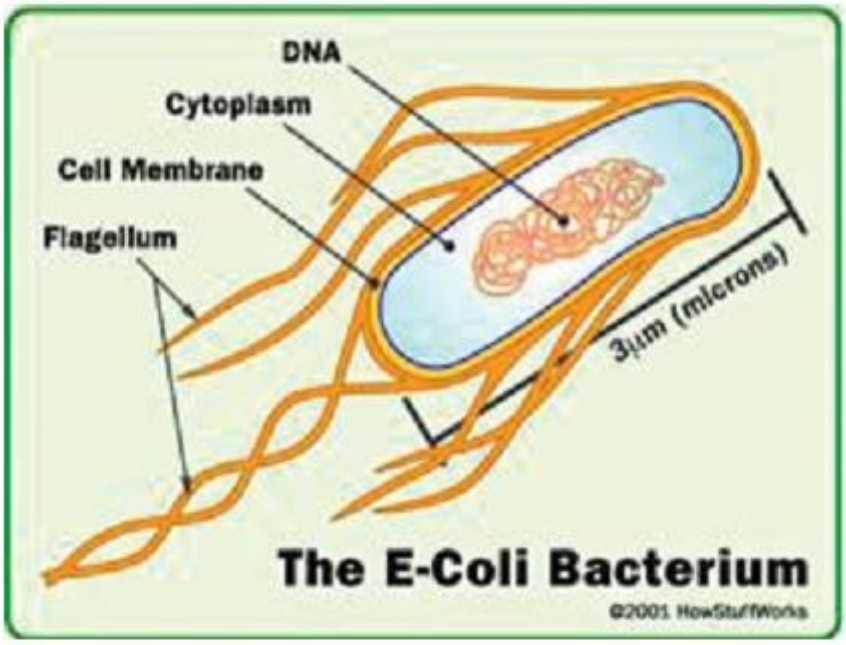

Figure 11: Escherichia coli (E.coli) [57]

b. Inorganic Material

Inorganic materials such as heavy metals--arsenic, mercury, copper, chromium, zinc and barium, for example--though harmless in small concentrations, act as pollutants when they end up in the water due to heavy industrialization or industrial accidents. This kind of water pollution can cause severe health problems and can even be fatal.

c. Organic Materials

These materials contain molecules which have carbon in their make-up. One of the most frequently detected volatile organic chemicals is Methyl Tertiary Butyl Ether (MTBE). MTBE was used as an air-cleaning gas additive, and was once added to gasoline. Although it is now a banned chemical, it will take years before MBTE is thoroughly removed from contaminated water systems. Water contaminated with this organic chemical can cause leukemia, lymphoma and tumors in testicles, the thyroid glands and kidneys.

d. Macroscopic Pollution

Macroscopic pollution is when large, visible items pollute the water. The first common pollutant is trash--paper, plastic or food waste. It is either thrown directly into the water or washed away by the rain into a body of water. Other types of macroscopic pollution include nurdles (small waterborne plastic pellets); pieces of wood; metals; and even obvious things like shipwrecks. This form of pollution is the most manageable; however, these pollutants must be removed in order to avoid loss of life in aquatic animals and contamination upon the chemical breakdown of these objects. See table. In the appendix A. Table of contaminants [20]

CHAPTER THREE

LITERATURE SURVEY

3.1. Literature Review

Using Nanocomposite filter in water filtration has attracted the global interest in recent year. This is because of their high reactivity due to the large surface area to volume ratio.

Due to the wide use of nanocomposite filter in water cleaning from different contaminants; organic, inorganic as well as microorganisms such as E.coli, and great promising for the future application to solve the scarcity of drinking water has receive a widespread attention and has been extensively investigated by many researchers. Some of the researchers` outputs which are related to this thesis are discussed below.

Nguyen Thi Phuong Phong, N. V. (2009) [46] fabricated silver-coated polyurethane foams and used it as a bacterial filter for contaminated drinking water. They soaked flexible PU foams in silver colloidal solutions for 10 h, then they washed and air-dried at room temperature. The prepared silver colloidal solutions and silver-coated PU materials were characterized by TEM, FESEM/EDS, UV-VIS, ICP-AAS, and Raman spectroscopy. They got from TEM images that the size of silver nanoparticles in colloidal solutions varies from 6 to 12nm. The Raman, FE-SEM/EDS and ICP-AAS data illustrated that silver nanoparticles were stable on the PU foam and were not washed away by water. Furthermore, they carried out microbiological tests (tube tests and flow test) on silver-coated PU materials with the Coliforms, E. coli, and B. subtilis. They obtained results that the bacteria were killed completely with antibacterial efficiency of 100%. Their research suggests that silver-coated polyurethane foams can be used as excellent antibacterial water filters and would have several applications in other sectors. But they did not use activated carbon as additional component.

Auphedeous Y. Dang-i, a. W. (2013) [6] studied and evaluated ceramic water filters, to provide information that will help to improve their performance and promote their use. They fabricate two kinds of ceramic filters, one without hydroxyapatite and the other with hydroxylapatite. They determined the filters flow rates and ability to remove E.coli through

experiment. Finally they obtained the result of flow rates between 1-2 liters per hour (L/h) and from the E.coli test, E.coli removal was successful.

Luying Wang [63] used non equilibrium molecular dynamics (NEMD) simulations to investigate pressure-driven water flow passing through carbon nanotube (CNT) membranes at low pressures (5.0 MPa) typical of real nanofiltration (NF) systems. He modeled CNT membrane as a simplified NF membrane with smooth surfaces, and uniform straight pores of typical NF pore sizes. His final Results show that water flow through a CNT membrane under a pressure difference has the unique transport properties of very fast flow and a non-parabolic radial distribution of velocities. Density distributions along radial and flow directions show that water molecules in the CNT form layers with an oscillatory density profile, and have a lower average density than in the bulk flow.

Mehmet Ekrem Cakmak [11] simulated the colloidal deposition on a solid grain and air bubble based on the colloidal filtration theory using finite element based computational modeling and simulation software package named COMSOL Multiphysics® (COMSOL, Inc., Burlington, MA, USA). He mainly used Navier-Stokes Equations and Convection-Diffusion Equation. He concluded that pore water velocity and the disturbances in the flow field have a substantial effect on the deposition and transport paths of the colloids.

Mehmet Ekrem Cakmak [11] also simulated the effect of surface roughness on possible colloid retention by comparing pathways created by micron-scale surface asperities with those around smooth grains by solving the Stokes equation using the finite element method. He found that at the collector scale, micron-sized surface asperities led to the formation of vorticities and enhanced stagnant/low flow spots around the near sand grain region, at the surface scale, flow vorticities could also be formed among the asperities, where colloids could easily get trapped on the surface of a rough sand grain, The formation of vorticities was dependent on the direction of fluid flow. It is believed that this information will help to clarify the potential effect of micron-sized surface roughness on colloid behavior under favorable saturated conditions in porous media.

Mark W. Kennedy, K. Z. (2012) [39] done experiment and simulation to Determine and Verify the Forchheimer Coefficients for Ceramic Foam Filters Using COMSOL CFD Modelling. They

conduct their experiments with water at velocities from ~0.015-0.77 m/s to determine the permeability of 50 mm thick commercially available 30, 40, 50 and 80 Pores per Inch (PPI) alumina Ceramic Foam Filters (CFF) used for liquid metal filtration. In their output a high level of agreement was achieved between the experimental and the 2D axial symmetric CFD FEM results. The agreement obtained between the FEM model of the 49 mm filter apparatus, using the analytically derived Forchheimer coefficients and the experimental data, indicated that there was negligible bypassing of the filter media by the water during the experiments.

Mohan Noronha, V. M. (2003) [43] used a steady-state process simulation, NF-PROJECT to determine the membrane parameters permeability, transmembrane flux, membrane rejection based on feed-side concentration on the membrane surface, permeate concentration, the hydraulic and osmotic differential pressure, the retentate permeate ratio as well as the membrane element recovery. They dealt with a practice-related, stationary process simulation for industrial two-stage nanofiltration processes (feed and bleed operation), termed NF-PROJECT and based on a numerical calculation of the individual membrane elements (8-inch spiral wound elements). In their sequential element-by-element analysis they obtained volume flow, concentration, and hydraulic pressure at the inlet and outlet of each membrane element. They averaged these values to determine the aforementioned parameters. The result illustrating the successive reduction in permeability and rejection between the elements arranged inside the pressure vessel.

Thomas R.R. Pintelon, S. A. (2010) [60] studied "Validation of 3D Simulations of Reverse Osmosis Membrane Biofouling". They dealt with the spiral wound module reverse osmosis membrane which consists of two 0.15 mm thick membrane sheets separated by a 0.77 mm thick nylon mesh spacer sheet contained within a $40\times16\times1.07$ mm^3 PVC cavity. They performed their study by using a modified lattice Boltzmann (LB) platform (adapted to enable larger more realistic velocities), which is applied to a 2D RO membrane analog and 3D imaging of the membrane fouling simulation (MFS) using magnetic resonance imaging (MRI) permits provision of a simulation lattice. Then they compare resultant simulated velocity fields with (MRI) velocity images acquired for the MFS as a function of biofouling extent. Finally they got a very good agreement between simulation and experiment both in terms of the velocity probability distributions and in terms of the displacement propagators.

Dzmitry Hlushkou [29] has simulated fluid flow and mass transport in (electro) chromatographic systems for his Ph.D. thesis. He presented his thesis by combining the coupled numerical treatment of the Poisson and Nernst-Planck problems by traditional finite-difference techniques, as well as the Navier-Stokes problem by the relatively novel lattice-Boltzmann equation (LBE) method. His work gave solution for electroosmotic flow (EOF) in a straight open capillary with non-uniform distribution of the ζ-potential; electroosmotic flow/EOF in slit micro-channels with non-uniform surface charge density which depends on the local chemical environment; electroosmotic flow/EOF through a simple cubic array of spherical particles; Hydrodynamic dispersion in random closed packings of porous particles; electroosmotic flow/EOF through confined random packings of spherical nonporous particles. He finally compared the primary simulated data for a simplified or approximated problem to the published one before his work and got good agreement.

F. El Azhar, N. E. (2013) [23] used ROSA software in their feasibility study of Nanofiltration process in dual stage in desalination of the seawater to predict the performances of NF membranes for seawater desalination utilization. In their system configuration the first stage included a nanofiltration membrane, but the second included a nanofiltration or reverse osmosis (BW) membranes in order to produce potable water (TDS less than 1000mg/l). They examined the effect of membranes type and seawater salinity and compared energy requirements of NF–NF and NF–BW to single stage RO desalination. Their result showed the energy consumed by the system NF / BW is still below that of consumed by reverse osmosis membrane and gave confirmation of the feasibility of NF membrane in dual stage in seawater desalination.

John Palmeri and Xavier Lefebvre [34] did extensive study on Modeling of neutral solute and ion transport in charged nanofiltration membranes using computer simulation programs. They did practical experiment and simulated using a nanofiltration simulation code**;** NanoFlux on six different nanocomposites filters (NTR-7450 nanofilter, Desal5DK and NTR-729 (HN-PVD1) nanofilter, Comparative study of NF200, Desal5DL, and Membraloxnanofilters, Homemade Hafnia ceramic nanofilter, and Homemade Titania ceramic nanofilter. From their experiment they determined a limited number of single salt model parameters, such as effective pore radius and effective membrane thickness and (volumetric) charge density. When they used these effective transport model parameters to perform NF simulations of Multi-electrolyte

mixtures, they showed and concluded as “it is possible to obtain good agreement with experiment, not only for ternary and quaternary ion mixtures, but even real drinking water containing seven predominant ionic species”.

Mohammed Amine Kendouci, B. K. (2013) [32] did on Simulation of water filtration in porous zone based on Darcy's law. They used sand dune as porous medium. They used experimental device for the testing of filtration, the driver was a glass column of 5 cm diameter and 100 cm height and cylindrical shape and the actual height of the filter bed 60cm, 30 cm. They conducted a simulation based on experimental data obtained in the laboratory, using the computer code FLUENT and got agreement between the experimental and simulated flow which is about 4.3% difference.

Bastian Schäfera, M. H. (2009) [9] studied on the title “Agglomeration and filtration of colloidal suspensions with Derjaguin-Landau-Verwey-Overbeek (DVLO) interactions in simulation and experiment”. They used a combined stochastic rotation dynamics (SRD) and molecular dynamics (MD) methodology to simulate the cake formation. They investigated permeability with lattice Boltzmann (LB) simulations of flow through the discretized cake, depends on the particle size and porosity, and thus on the agglomeration of the particles. Their results agreed qualitatively with experimental data obtained from colloidal boehmite (a light gray to dark red-brown mineral consisting of hydrous aluminum oxide) suspensions.

Guillem Portella Carbó [12] in his PhD thesis; “Determinants of water and ion permeation through nanopores studied by Molecular Dynamics simulations” used the atomistic molecular dynamics simulations, GROMACS 3.3.1 simulation software to characterize the critical fundamental factors that determine water and ion permeation through channels of molecular dimensions. His final conclusion showed the extension of the channel is found to have no impact on the water mobility; the polarity of the channels strongly influences the water permeability, ranging from almost empty pores to tightly adsorbed water molecules; The water mobility within a given water-pore affinity remains invariant with the length; the strong effect of the pore radius and polarity on the water pore occupancy and water permeability over a range of radii of 0.4 nm.

3.2. Motivation

Most researchers in the above literature review did their simulation on the preexisting filters which were used by developed nations and in particular organizations. Some of them did in general matters of filtration process; means they did not perform on the specific filter. Herewith no one perform simulation on the nano-composite filter (polyurethane foam based activated carbon and silver nanoparticle composite), which is the concern of this thesis. As mentioned in the problem statement, if it is necessary to give solution for the world serious problem of drinking water, a well efficient in all pollutant rejection and affordable (to economical disadvantaged people) filter should be produced and manufactured in sufficient amount and must be distributed. Even though it is not the only solution for such serious problem, this day a new composite nanofilter which is composed of polyurethane foam, silver nanoparticle and activated carbon particles is in progress. Someone will expect that it is hopeful in the future and also it is good news for the people especially for the concerned researchers. Therefore any concerned researchers should support this project by contributing their knowledge. That was why I am motivated to do the simulation of this filter.

CHAPTER FOUR

SIMULATION AND ANALYSIS

Simulation of nanofiltration is important; membrane stability, lifetime, and the lack of fundamental understanding of the process performance problems will be answered through simulation [8, 58]. Currently there are different softwares which are used to simulate nanofiltration, such as Lattice Boltzmann simulation, NanoFlux, HYDRUS, Rosa, and COMSOL Multiphysics software etc. Among those softwares COMSOL Multiphysics is used in this thesis, because of its availability and suitability for this particular work.

4.1. COMSOL Multiphysics

COMSOL Multiphysics (formerly FEMLAB) is a finite element analysis, solver and Simulation software / FEA Software package for various physics and engineering applications, especially coupled phenomena, or multiphysics. COMSOL Multiphysics also offers an extensive interface to MATLAB and its toolboxes for a large variety of programming, preprocessing and post processing possibilities. The packages are cross-platform (Windows, Mac, Linux, Unix.) In addition to conventional physics-based user-interfaces, COMSOL Multiphysics also allows for entering coupled systems of partial differential equations (PDEs) [13].

How to create a new model in COMSOL?

1. Start COMSOL Multiphysics
2. Work through the COMSOL Model Wizard which will require you to select the coordinate system for the model, the relevant physics to the problem, and the type of study you wish to perform (Time dependent or stationary).
3. Define the parameters, equations and variables pertinent to the model (sub directory (Global Definitions).
4. Define the geometry of the model (Geometry).
5. Select the materials you wish to use in your model (Materials).
6. Select the boundary, bulk and initial conditions for your system for each physics you are using (This will be entered separately for each different physics you are using e.g. you

will need to enter these for Laminar Flow and again for Heat Transfer if you are using both).

7. Choose the element size to be used (Mesh).
8. Adjust solver parameters and compute (Study).
9. Display the desired results in the most meaningful way (Results).

Not all of these steps are always necessary when building a model. The order is also variable depending on the complexity of the model.

4.2. Working condition of the filter

By assuming the filter for house and office use; it can be enough if it has a container volume of 5 Lt. Again if we assume it has circular shape with diameter of 20 cm therefore, the height will be $h = 16\,cm$ (by equation 4.1). The filter plate is 5cm thick (i.e. the polyurethane foam thickness). For cylinder the volume is its cross sectional area multiplied by its height.

$$Volume = \pi r^2 \times h \tag{4.1}$$

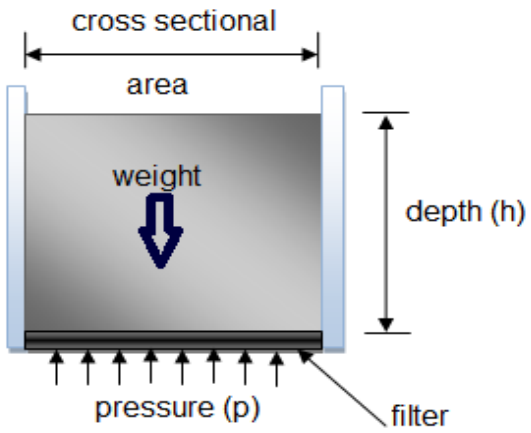

Figure 12: Schematic representations of the filter apparatus

Here the pressure on the filter due to the water load is given by

$$P = \rho g h \tag{4.2}$$

And if it is vent or open at the upper part

$$P = \rho g h + \text{Atmospheric pressure} \tag{4.3}$$

Where ρ is density of water which is 1000kg/m^3 and g is gravity constant which is 9.81m/s^2.

Table 8: Pressure of water at different height of the container (no vent)

Height(cm)	1	2	4	6	8	10	12	14	16	Average
Pressure(Pa)	98.1	196.2	392.4	588.6	784.8	981	1177.2	1373.4	1569.6	716.13

The pressure will decrease with h until zero at h zero, and if there is vent or open until 101.325kPa. But in this thesis work the closed one has been considered.

A 25kg/m^3 density with porosity 10-90PPI (pores per inch) polyurethane foam will be used in water filter application. The size of activated carbon is granular activated carbon (GAC) with diameter from 1.2 to 1.6 mm, powder activated carbon (PAC) from 0.15 to 0.25mm, and bead activated carbon (BAC) from 0.35 to 0.80mm.However granular activated carbon (GAC) and powder activated carbon (PAC) are extensively used in water filtration. Spherical shape and the sizes from 6 to 14 nm silver Nano particles are suitable for killing bacteria, virus, and fungus. This is taken from the background of this thesis. Based on this information the following alternatives are drawn as depicted by table 9.

Table 9: Alternative combinations of foam with AC particles

Alternative	Porosity Grade (pores/inch)	Pore size (mm) Diameter	Particle size or spherical collector size, diameter (mm)		Remark Total alternative
			GAC	PAC	
1	100	0.133	0	0	0
2	90	0.166	0	0.15	1
3	70	0.2	0	0.15 to 0.19	5
4	60	0.233	0	0.15 to 0.2	6
5	50	0.2833	0	0.15 to 0.25	11
6	40	0.45	0	0.15 to 0.25	11
7	30	0.6	0	0.15 to 0.25	11
8	20	0.9	0	0.15 to 0.25	11
9	10	1.95	1.2 to 1.6	0.15 to 0.25	17
Sum of Total alternative					**73**

From the previous table we can see that there are 73 alternatives, and also more alternatives fall under 10 to 40 PPI polyurethane foam. Among the alternatives I selected 34 alternatives based on the following criteria; one basic thing we have to know is that each water molecule should make contact with the activated carbon and silver Nano particles in order to get the water purified. Therefore we have to minimize the area difference between the pore of the polyurethane foam and the particles.

Table 10: Selected combinations

Alternative	Porosity Grade (pores/inch)	Pore size (mm) Diameter	Particle size or spherical collector size, diameter (mm)		Remark Total alternative
			GAC	PAC	
1	100	0.133	0	0	0
2	90	0.166	0	0.15	1
3	70	0.2	0	0.17 to 0.19	3
4	60	0.233	0	0.2 to 0.22	3
5	50	0.2833	0	0.25	1
6	40	0.45	0	0.15,0.16,0.17,0.21,22	5
7	30	0.6	0	0.15,0.16,0.17,0.18,0.19,0.2,0.22,0.25	8
8	20	0.9	0	0.15,0.16,0.17,0.18,0.19,0.2,0.22,0.25	8
9	10	1.95	1.2 to 1.6	0	5
Sum of Total combinations					**34**

4.7. Simulation Results and Analysis

Assumptions for the simulation:

- The flow is a steady-state system (no transient effects);
- The system is isothermal (in particular, there are no Joule heating effects);

- ❖ Porous medium is represented by an assemblage of perfect spherical solid grains (collectors). The solid grain in this paper is activated carbon particle coated by silver nanoparticles.
- ❖ The water is evenly distributed through the porous media
- ❖ The silver nanoparticles are assumed to be coated on the activated carbon and polyurethane foam.
- ❖ The pores of polyurethane foam are perfect cylindrical
- ❖ The surface of the fluid is specified as a symmetry boundary to take the effect of neighboring activated carbon particles on fluid flow into account. The symmetry boundary means that the velocity of the water normal to the boundary is zero at that boundary, and that the tangential component of the viscous force vanishes.
- ❖ A no-slip boundary condition is specified at the surface of the activated carbon where the water velocity equals zero.

4.7.1. Simulation procedures

1. Selecting the space dimension-3D

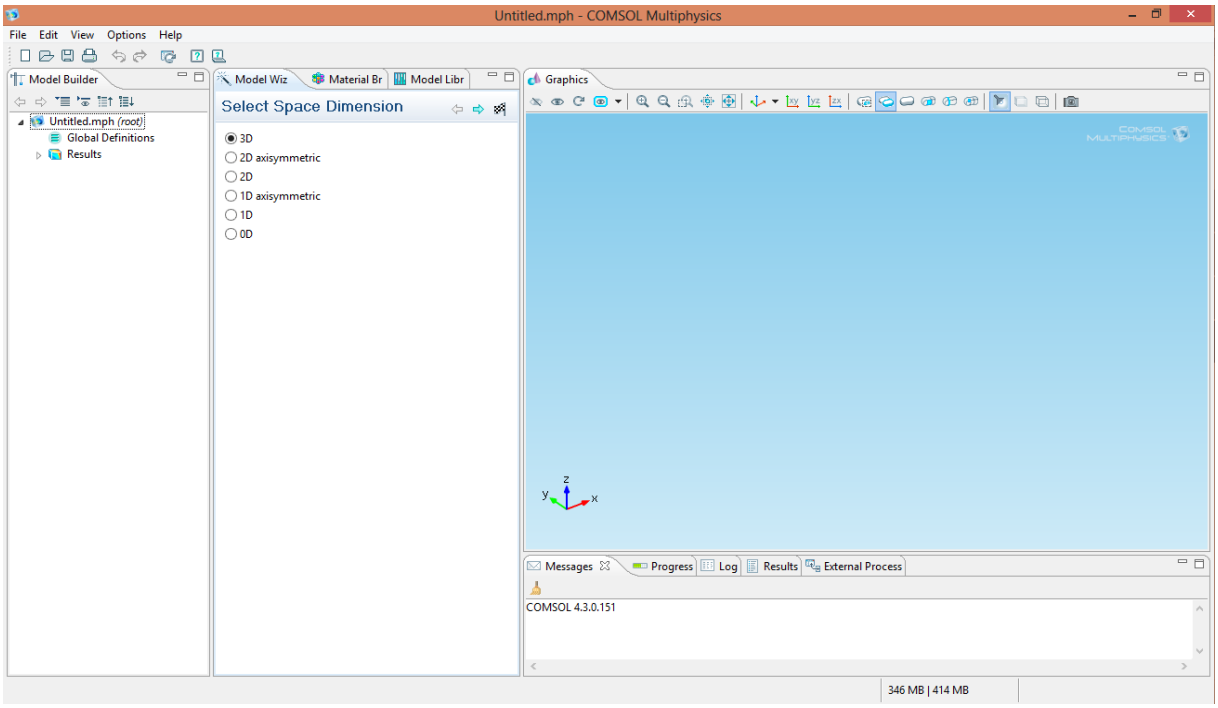

Figure 13: Selection of space dimension

2. Select the physics to the problem

For the problem of flow in filter media, creeping flow is selected. The Creeping Flow interface is used for simulating fluid flows at very low Reynolds numbers for which the inertial term in the Navier-Stokes equations can be neglected. This single-phase flow type is also referred to as Stokes flow and occurs in systems with high viscosity or small geometrical length scales**.** The equations solved by the Creeping Flow interface are the Stokes equations for conservation of momentum and the continuity equation for conservation of mass.

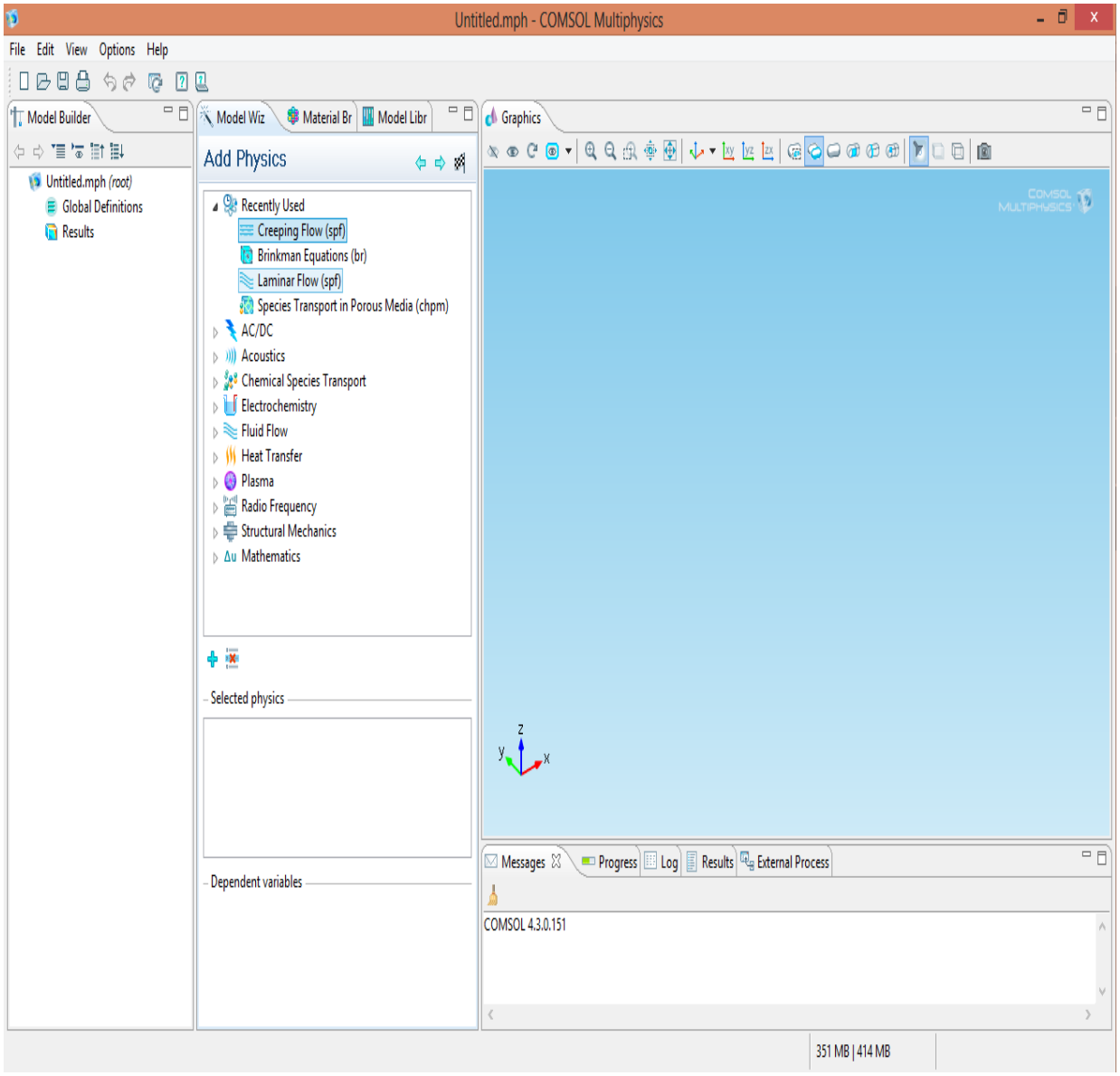

Figure 14: Adding physics

3. Select the study type then specify unit

For this particular study steady state is selected. The Stationary study is used when field variables do not change over time. In fluid flow it is used to compute the steady flow and pressure field.

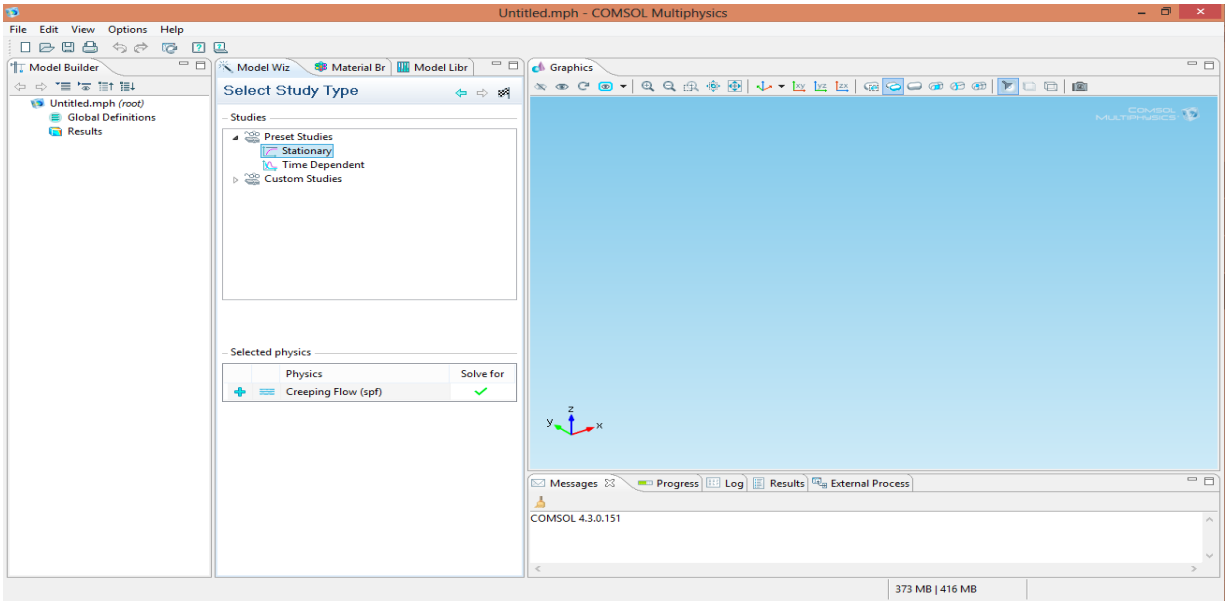

Figure 15: Selecting study type

4. Build sphere to represent the activated carbon particle, cylinder to represent the pore of the polyurethane foam and the water.

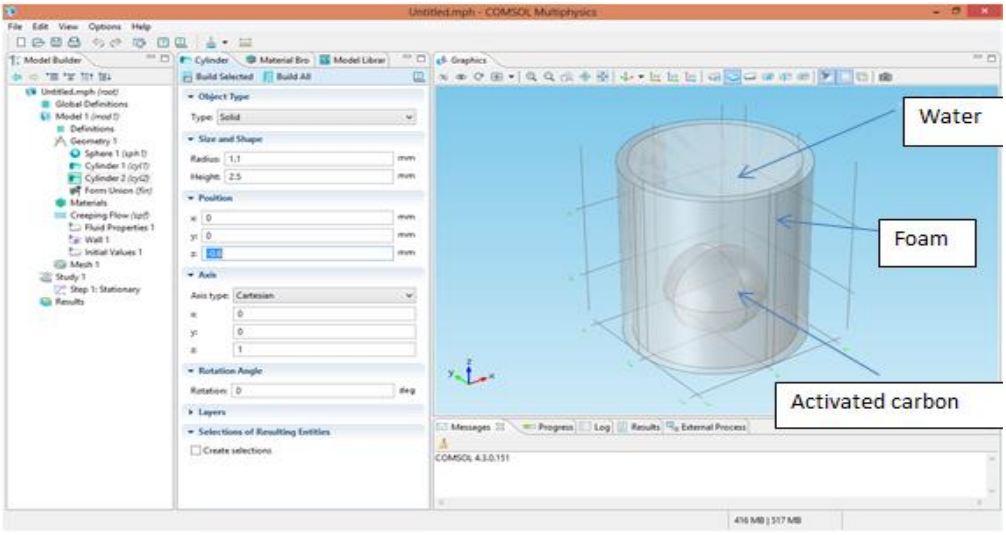

Figure 16: Building geometry

5. Select the respective materials from the material library. Then inlet, outlet and symmetry also assigned.

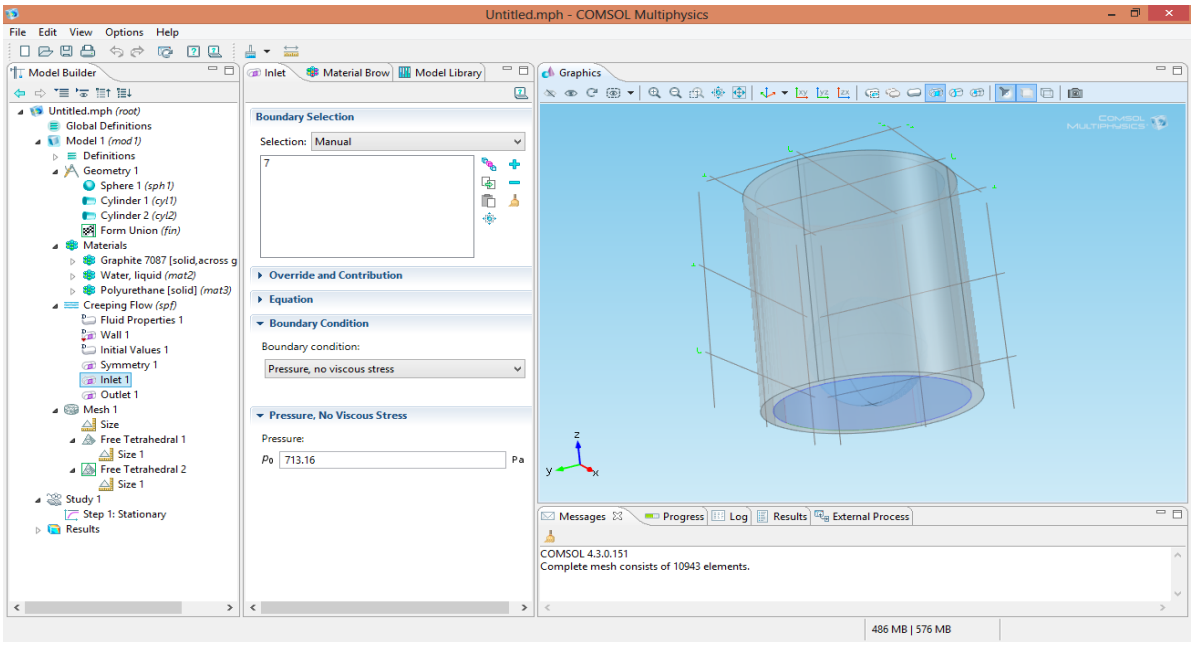

Figure 17: Material selection

6. Building mesh

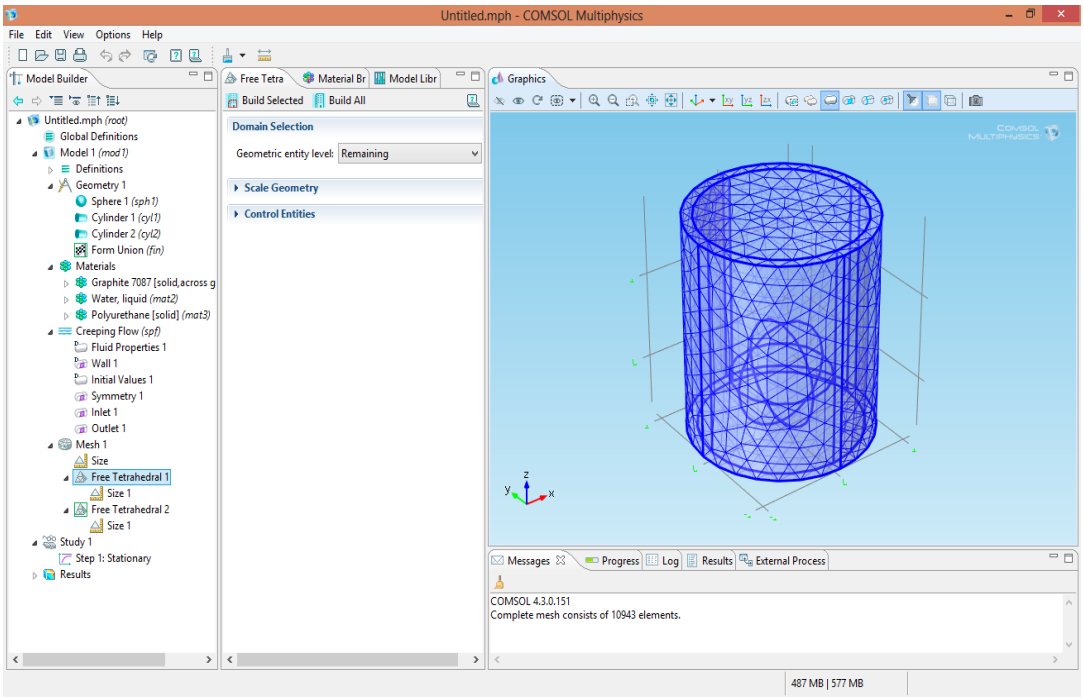

Figure 18: Building mesh

7. Compute the study and read the result. The result can be displayed in slice velocity (a), volume velocity (b), isosurface velocity field (c), arrow volume velocity field (d), and streamline forms. The dark red indicates the highest velocity and the dark blue indicates the lowest velocity (see figure 19).

a) slice velocity	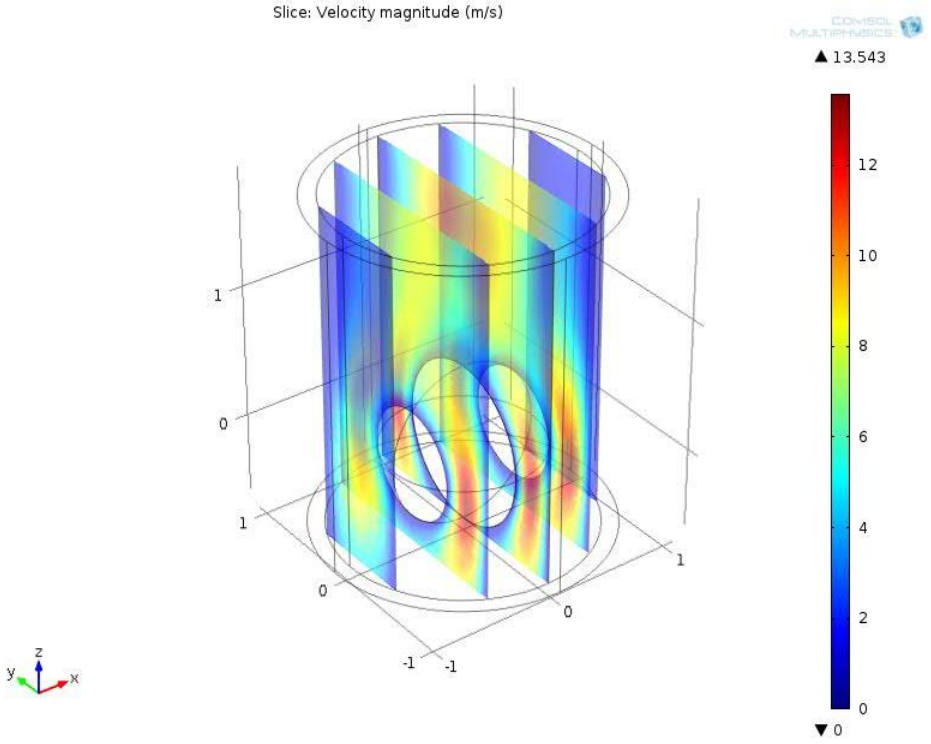
b) volume velocity	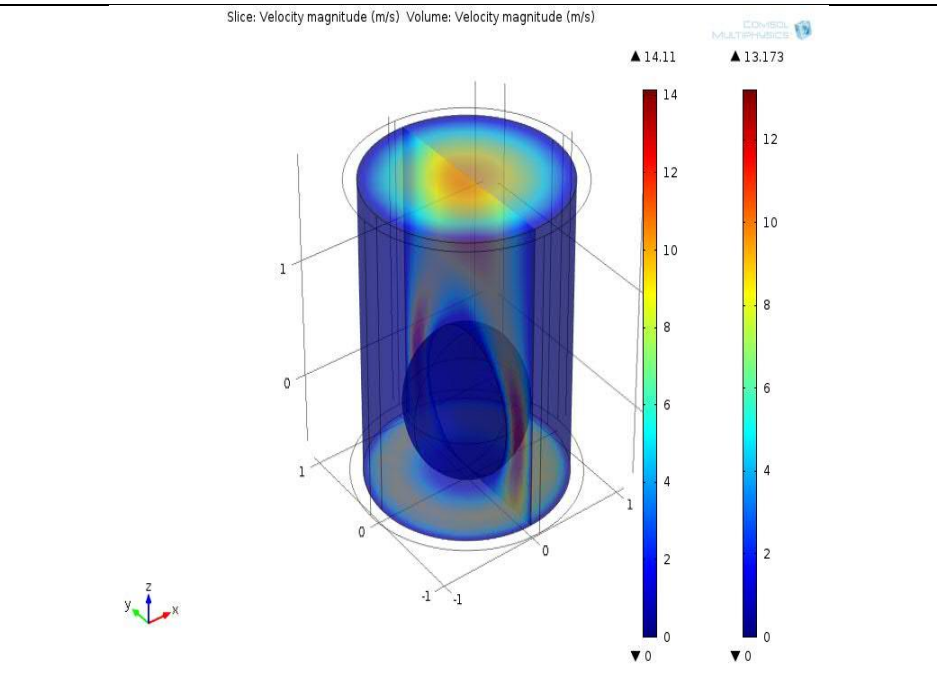

c) isosurface velocity field	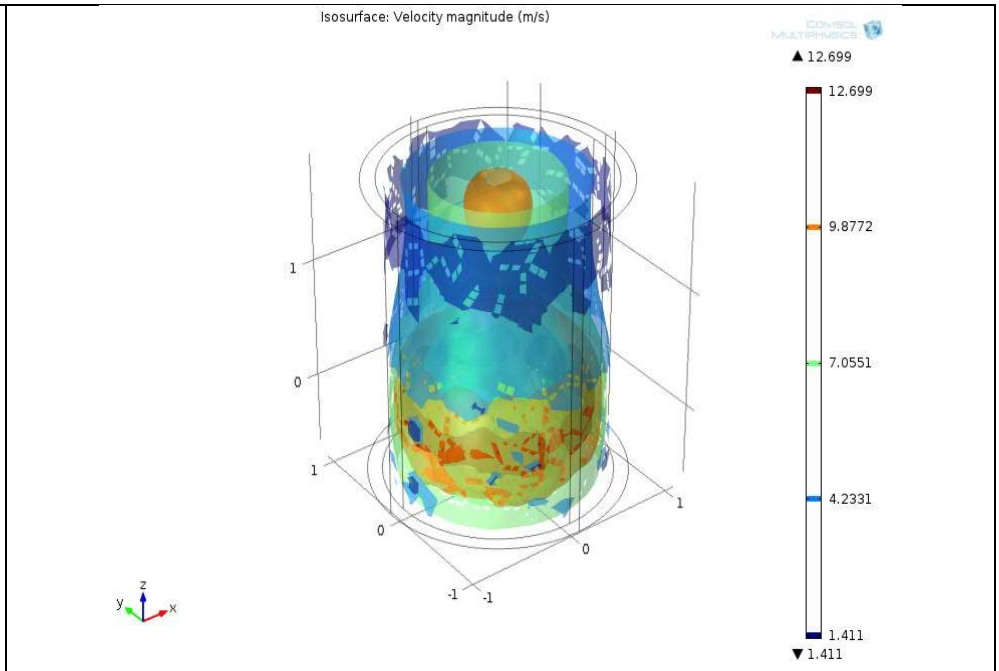
d) Arrow volume velocity field	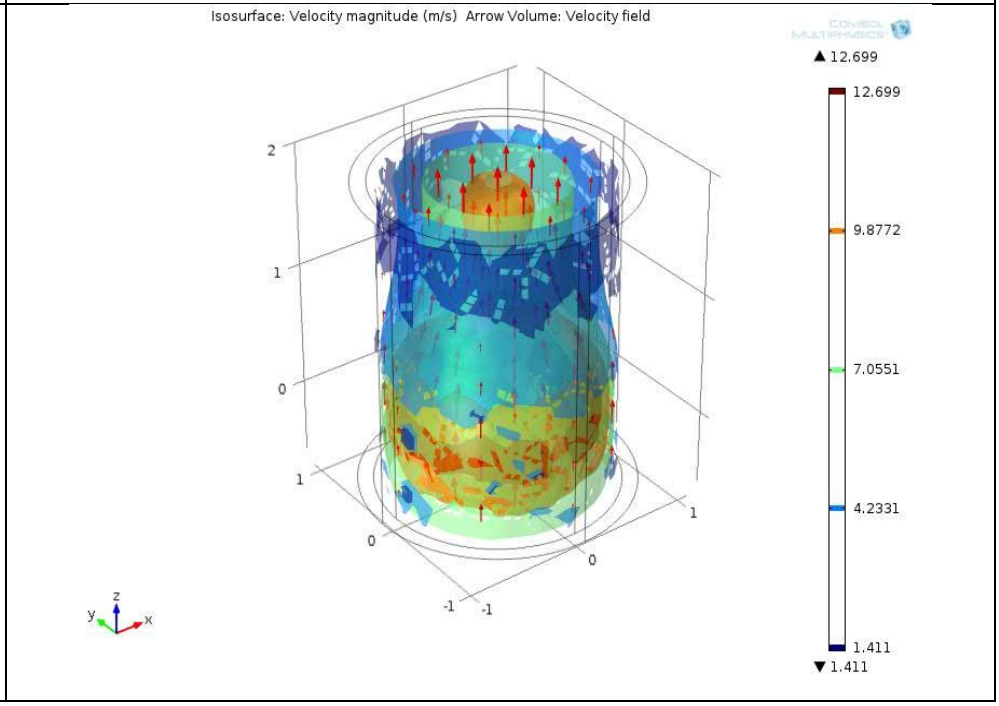

Figure 19: results

Based on the procedure 60 simulations are simulated. Among them four are unique because the particles used are combination of granular activated carbon and powdered activated carbon particle.

4.7.2. Simulation Result

The velocity result was simulated for both the 2.5mm and 5mm thick foam. Then this result is translated to 50mm thickness. Lastly the flow rate is calculated by multiplying the velocity by the total area. The graphical results are presented in appendix B.

$$\text{Ratio}=\frac{velocity\ at\ pore\ height\ 5mm}{velocity\ at\ pore\ height\ 2.5mm} \tag{4.2}$$

To translate the result for 50mm thick foam, taking the ratio of 50mm to 2.5mm:

$$50mm/2.5mm = 20 \tag{4.3}$$

Then to get the average velocity for 50mm thickness foam multiply the average velocity at 2.5mm by the $(Ratio)^{20}$. Then, the total flowrate can be calculated based on the following step.

1. Find the area difference between the pore and the particles.

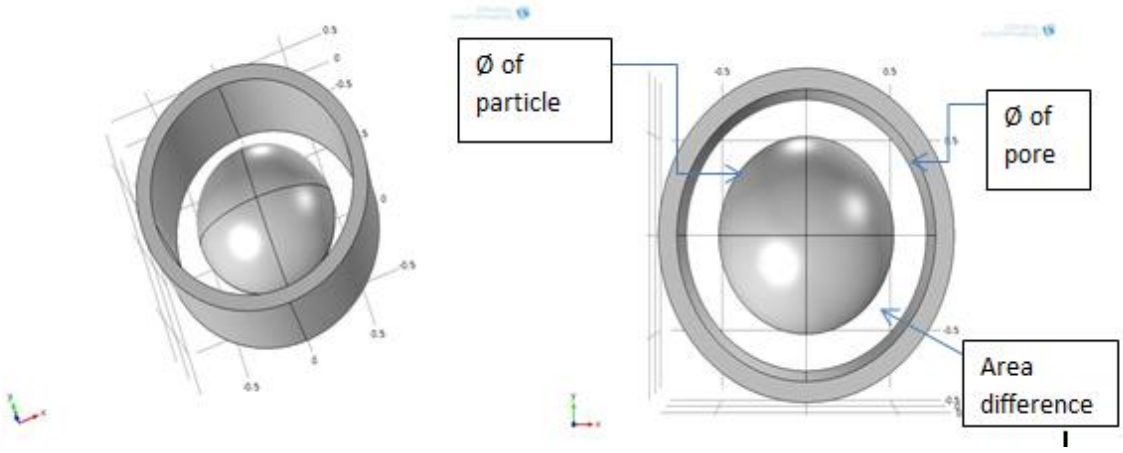

Figure 20: Area difference

2. Find the total number of pores in the foam used

   For this study as described at the beginning of this chapter the total number of pores is calculated for 20cm diameter foam plate with respect to the PPI.

3. Multiply area difference by total number of pores to get total area that the water flow through
4. Finally multiply total area by average velocity for 50 mm thick foam to find flow rate of the filter. (See appendix A).

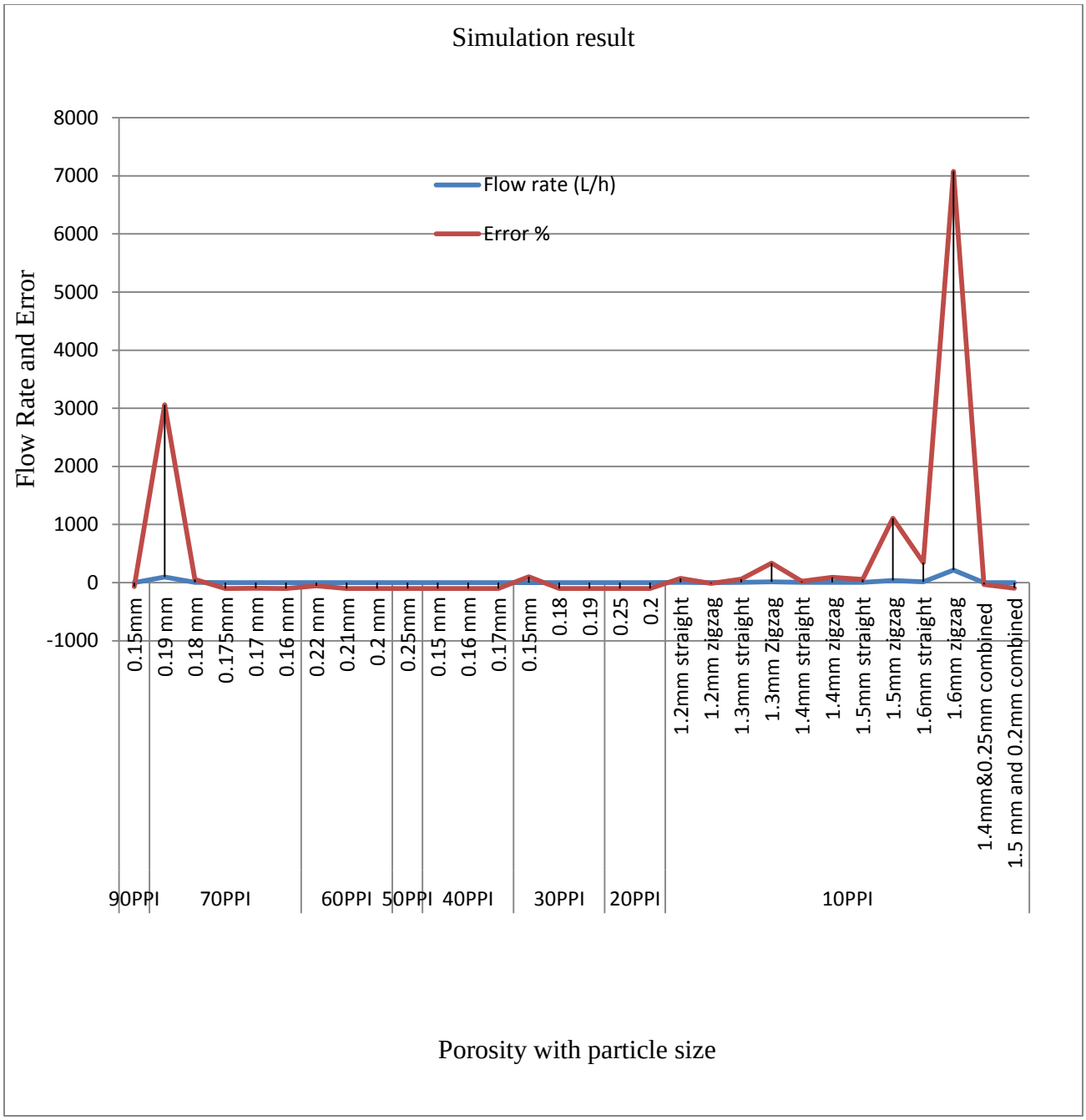

Figure 21: Graph of simulation results

4.7.3. Simulation Result Analysis

From the result it can be seen that the area and the thickness (the height of pore) are the main determinant factors for the flow rate. That is, as the area difference increases the flow rate increases. Whereas increasing thickness of foam decrease the flow rate because there is a lot of contact of water with particles.

We can also observe that one third of the result of ratio (equation 4.2) is less than half and two third of the result is greater than half. This means there is relatively high contact of water with particles for those of ratio less than half. From the flow rate result two third of the result is less than two and one third of the result is greater than three (See appendix A). There are flow rates with -99.99% to +7076.6 % errors with respect to the objective of this study. Among these I am interested to dealing with error less than ±100% specially those are high contact probability with the particles.

Table 11: Results error up to +/- (100%)

No.	Particle size		Porosity PPI	Error %
1	0.15mm		90	-71
3	0.18 mm		70	+53.3
4	0.175mm		70	-99.9
5	0.17 mm		70	-98.8
6	0.16 mm		70	-99.75
7	0.22 mm		60	-56.3
8	0.21mm		60	-99.58
9	0.2 mm		60	-99.81
10	0.25mm		50	-99.99
11	0.15 mm		40	-99.98
12	0.16 mm		40	-99.6
13	0.15mm		30	100
14	0.18 mm		30	-99.89
15	0.19 mm		30	-99.88
17	0.25 mm		20	-99.95
18	0.2 mm		20	-99.91
19	1.2mm	straight	10	+72
20		zigzag	10	-14
21	1.3mm	straight	10	+60.6
22	1.4mm	straight	10	+25
23		zigzag	10	+92.3
24	1.5mm	straight	10	+56.3
25	1.4mm&0.25mm combined		10	-30.5
26	1.5 mm and 0.2mm combined		10	-97

As we see from table 11 there is no perfect result. But we can try other alternatives by reducing thickness of foam for the negative errors and reducing radius of foam used for the positive error results. (See appendix A)

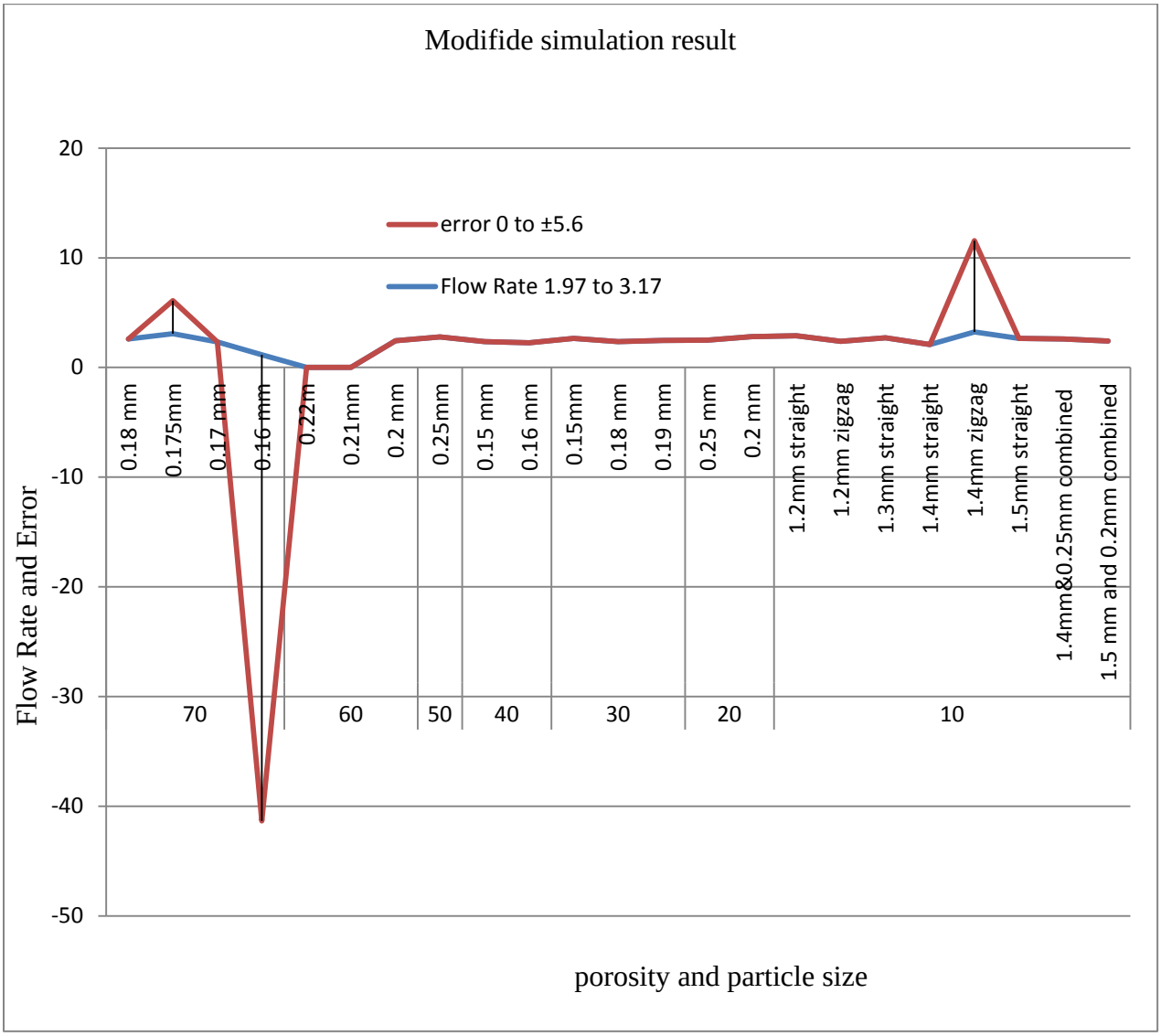

Figure 22: Graph of modified simulation result

Now we also consider the area difference between the pore and the activated carbon particles to select the suitable filter. Because, the smaller area difference is more reliable than, greater area difference for better purification.

Table 12: Area difference between pores and activated carbon particles

No.	Particle size		Porosity PPI	Area difference
1	0.15mm		90	3.96896*10^-3
3	0.18 mm		70	5.966*10^-3
4	0.175mm		70	7.35*10^-3
5	0.17 mm		70	8.71*10^-3
6	0.22mm		60	4.62*10^-3
7	0.21mm		60	7.99*10^-3
8	0.2 mm		60	0.01122
9	0.25mm		50	0.01394
10	0.15 mm		40	0.05298
11	0.16 mm		40	0.03838
12	0.15mm		30	0.1236
13	0.18 mm		30	0.05636
14	0.19 mm		30	0.02755
15	0.25mm		30	0.08635
16	0.25 mm		20	0.14522
17	0.2 mm		20	0.2276
18	1.2mm	Straight	10	1.8545
19		Zigzag	10	1.8545
20	1.3mm	Straight	10	1.6583
21	1.4mm	Straight	10	1.4463
22	1.5mm	Straight	10	1.2487
23	1.4mm&0.25mm combined		10	0.8576
24	1.5 mm and 0.2mm combined		10	0.71631

For effective purification of water relatively high thickness and low area difference is preferred. Because it can increase the contact time of water with activated carbon particles. Therefore, the two variables are evaluated out of 10. Thickness is evaluated out of 6 and the area difference is

out of 4. This decision is made based on the result shown in table 12; the change in velocity in thickness difference is greater than the velocity change due to area difference.

Table 13: selection of alternatives

Porosity PPI	Particle Size	Height Value (6%)	Area Value (4%)	Total Value (10%)	Rank
90	0.15mm	4.22	3.9999	8.2199	2
70	0.18 mm	6	3.995	9.995	1
70	0.175mm	1.8	3.992	5.792	20
70	0.17 mm	1.92	3.9897435	5.909744	18
60	0.22mm	2.4	3.9985842	6.398584	12
60	0.21mm	1.92	3.9912998	5.9113	17
60	0.2 mm	2.1	3.984318	6.084318	14
50	0.25mm	2.1	3.9784387	6.078439	15
40	0.15 mm	3	3.8940523	6.894052	7
40	0.16 mm	3.3	3.9256107	7.225611	5
30	0.15mm	1.2	3.7414045	4.941405	22
30	0.18 mm	3	3.8867463	6.886746	8
30	0.19 mm	3	3.9490201	6.94902	6
20	0.25 mm	3	3.6946721	6.694672	10
20	0.2 mm	2.88	3.5166047	6.396605	13
10	1.2mmstraight	6	8.5*10^-7	6	16
10	1.2mm Zigzag	5.856	8.5*10^-7	5.856	19
10	1.3mmstraight	6	0.4240936	6.424094	11
10	1.4mmstraight	6	0.8823394	6.882339	9
10	1.5mmstraight	6	1.3094592	7.309459	4
10	1.4mm&0.25mm combined	5.7	2.1548363	7.854836	3
10	1.5mm and 0.2mm combined	2.88	2.4602399	5.34024	21

The results in above table are compared and ranked 1 up to 12 are taken as best. But it is clear that the value less than half may be rejected. The alternatives in particle size column 1.5mm straight, 1.3mm straight, 1.4mm straight are less than half in the area difference value. Therefore these are dropped.

Table 14: best alternatives

Porosity PPI	particle size	Height value (6%)	Area value (4%)	Total (10%)	Rank
70	0.18 mm	6	3.995	9.995	1
90	0.15mm	4.22	3.9999	8.2199	2
10	1.4mm&0.25mm combined	5.7	2.1548363	7.854836	3
40	0.16 mm	3.3	3.9256107	7.225611	5
30	0.19 mm	3	3.9490201	6.94902	6
40	0.15 mm	3	3.8940523	6.894052	7
30	0.18 mm	3	3.8867463	6.886746	8
20	0.25 mm	3	3.6946721	6.694672	10
60	0.22mm	2.4	3.9985842	6.398584	12

In the background already stated that from 10PPI to 45PPI polyurethane foams are mostly used for water filtration purpose. Hence, even though all the nine alternatives have good agreement with the objective of this thesis, the lists ranked from 3 to 10 (table 14) can be more recommended. The COMSOL graphics of these selected alternatives are plotted as follows (in table 15).

Table 15: figures of COMSOL graphics for selected alternatives

0.22mm particle size by 0.233mm pore size 70ppi PU height 2.5mm	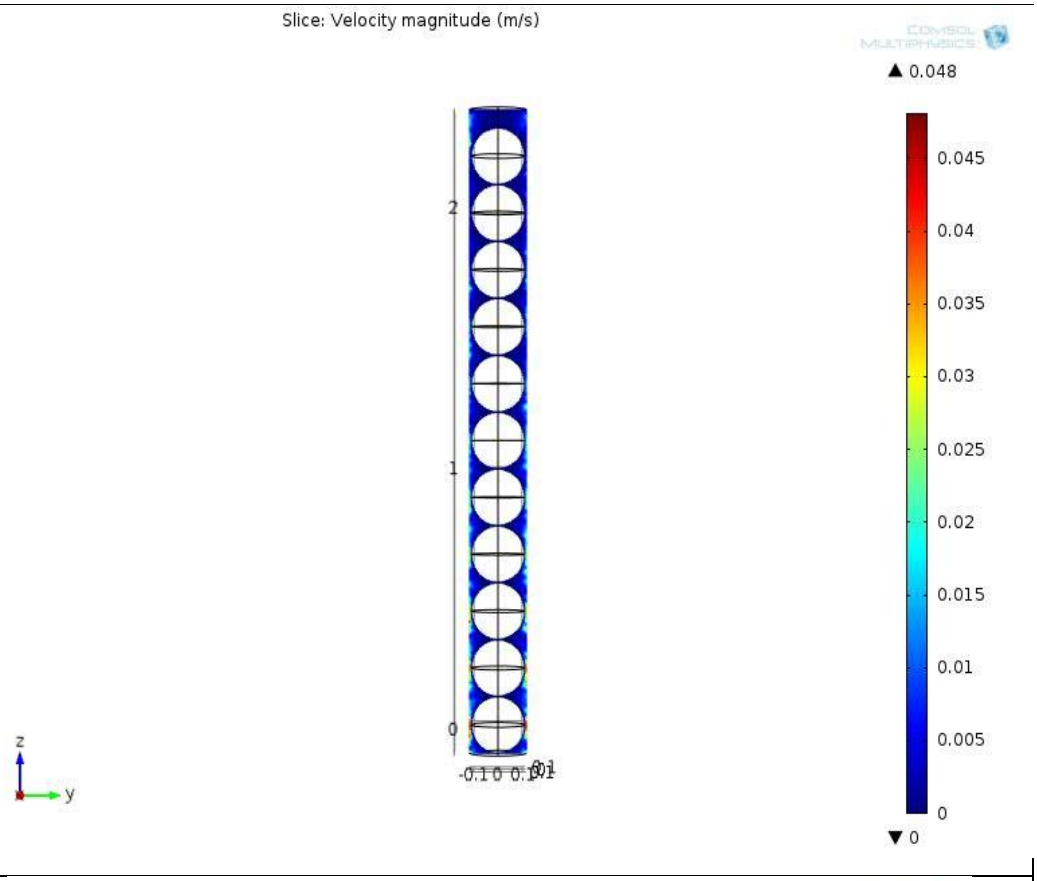
0.25mm particle size arrangement in 0.9mm pore size 20PPI PU	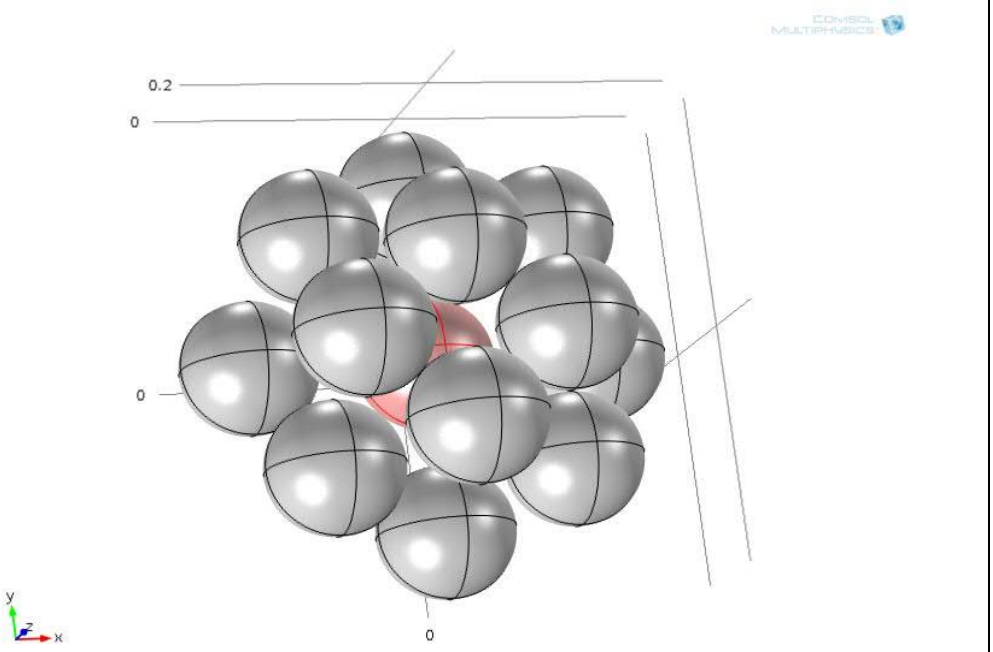

0.25mm particle size & 0.9mm pore size 20PPI PU	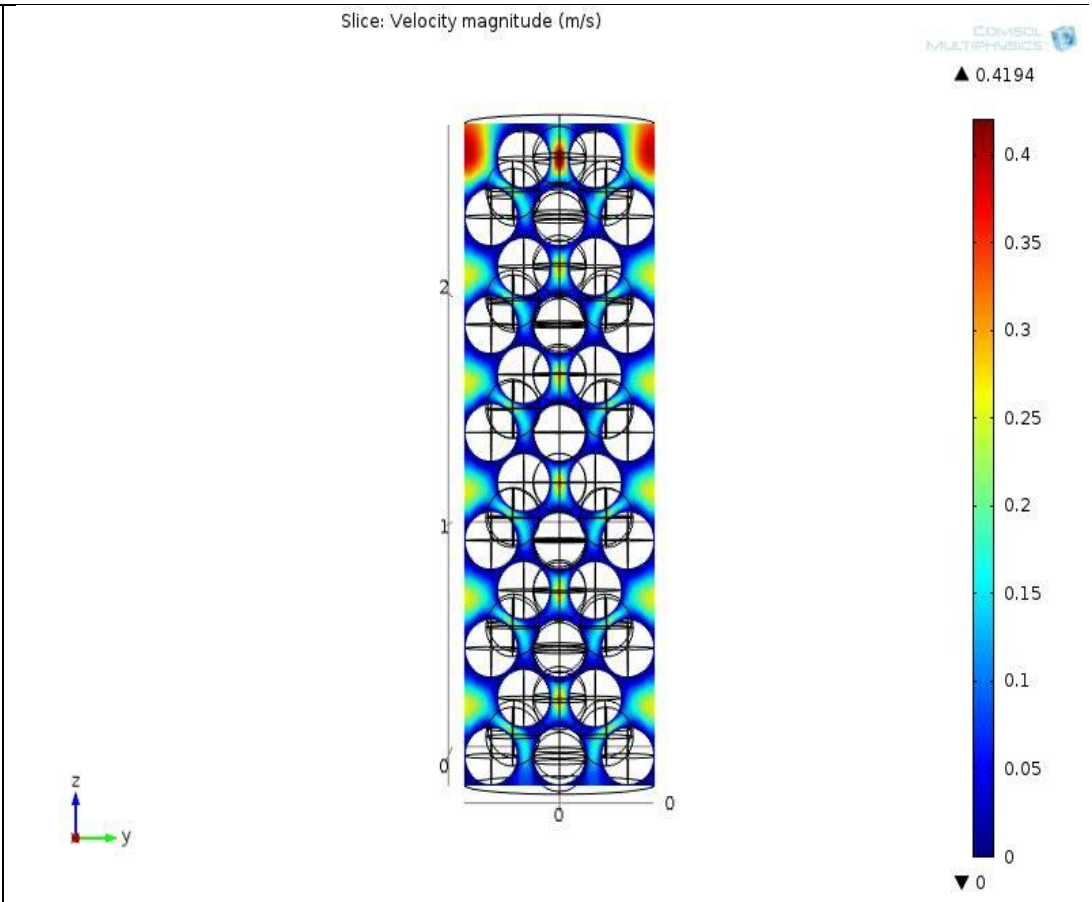
1.4mm and 0.25mm particle size in 1.95mm pore size 10ppi	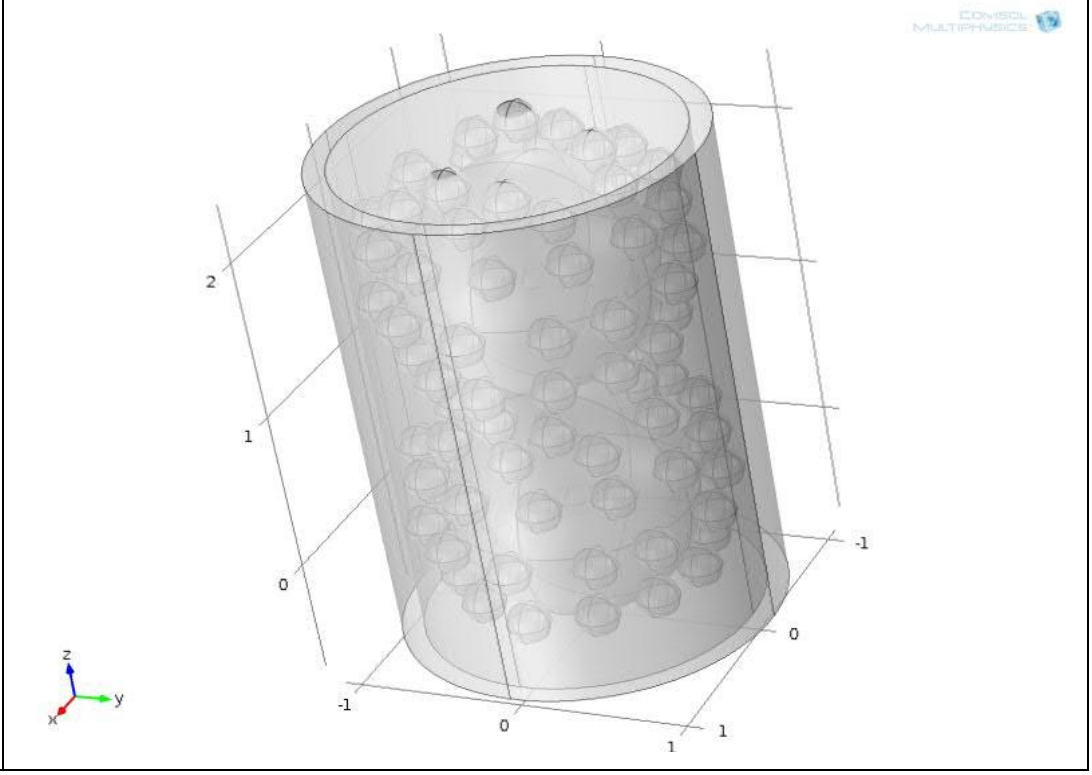

1.4mm and 0.25mm particle size in 1.95mm pore size 10ppi	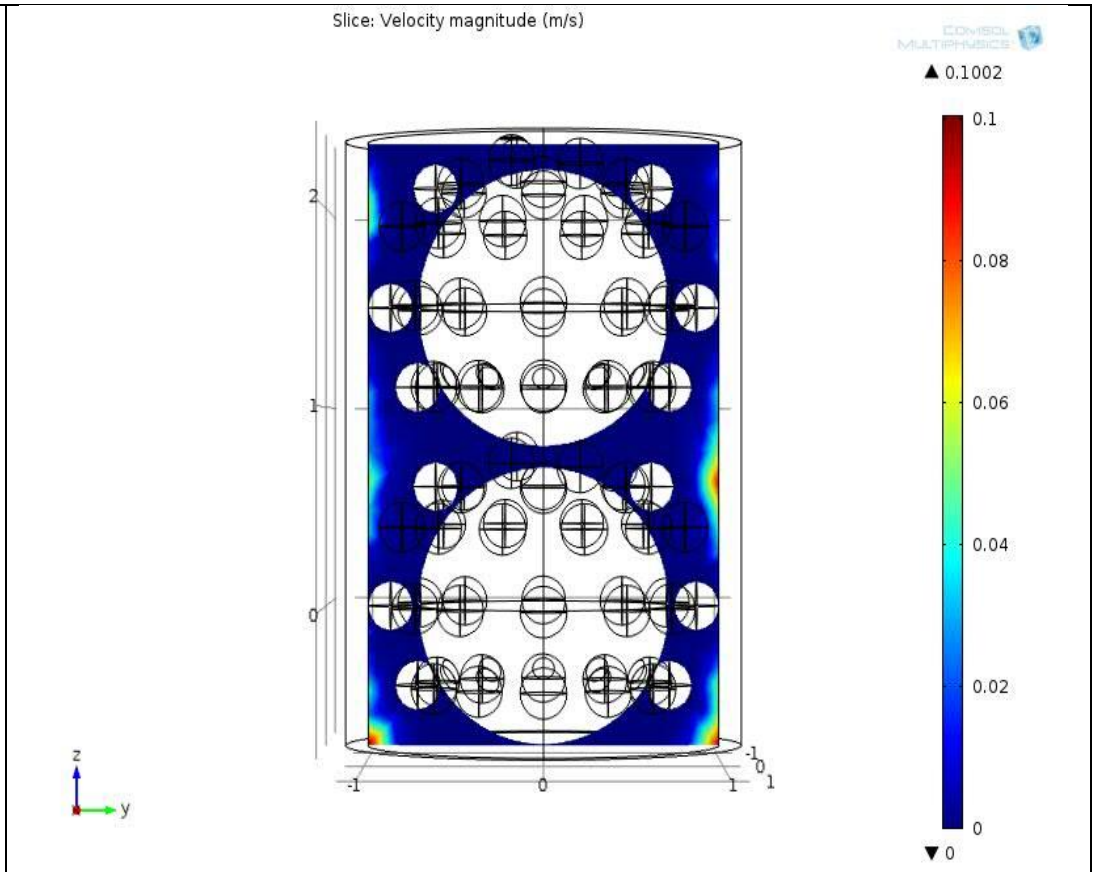
0.15 mm particle size in 0.166mm pore size 2.5mm thickness 90PPI PU	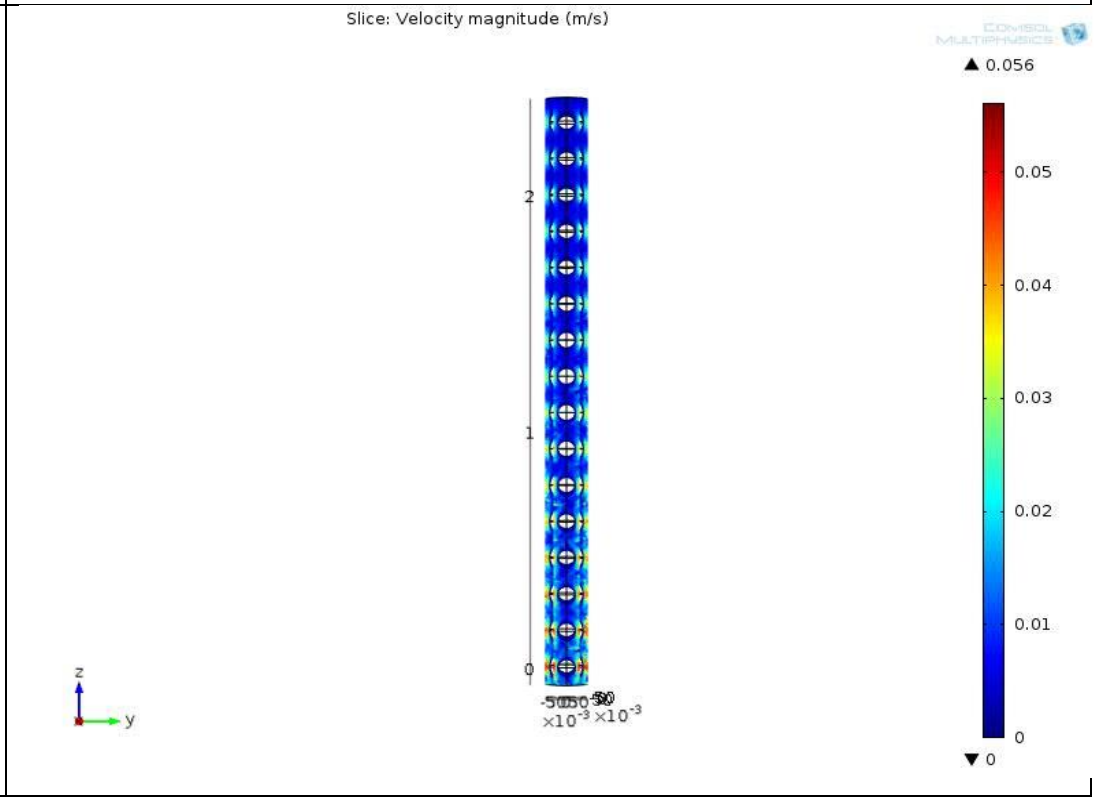

0.18mm particle size in 0.2mm pore size 70ppi with height 2.5mm PU	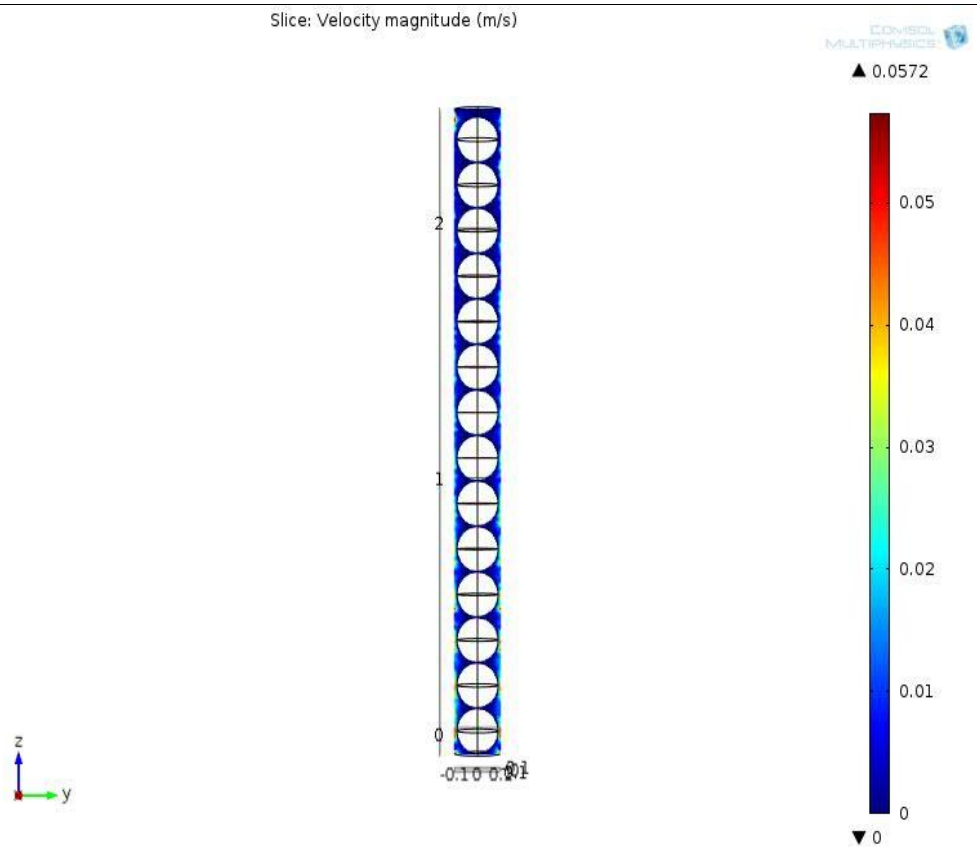
0.15mm particle size in 0.45mm pore size 40ppi	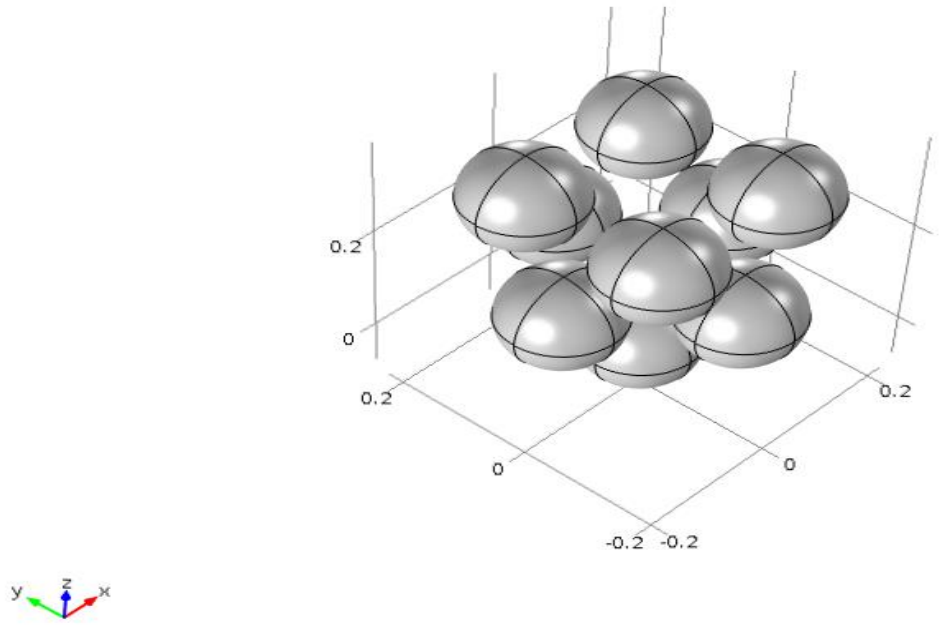

0.15mm particle size in 0.45mm pore size 40PPI PU	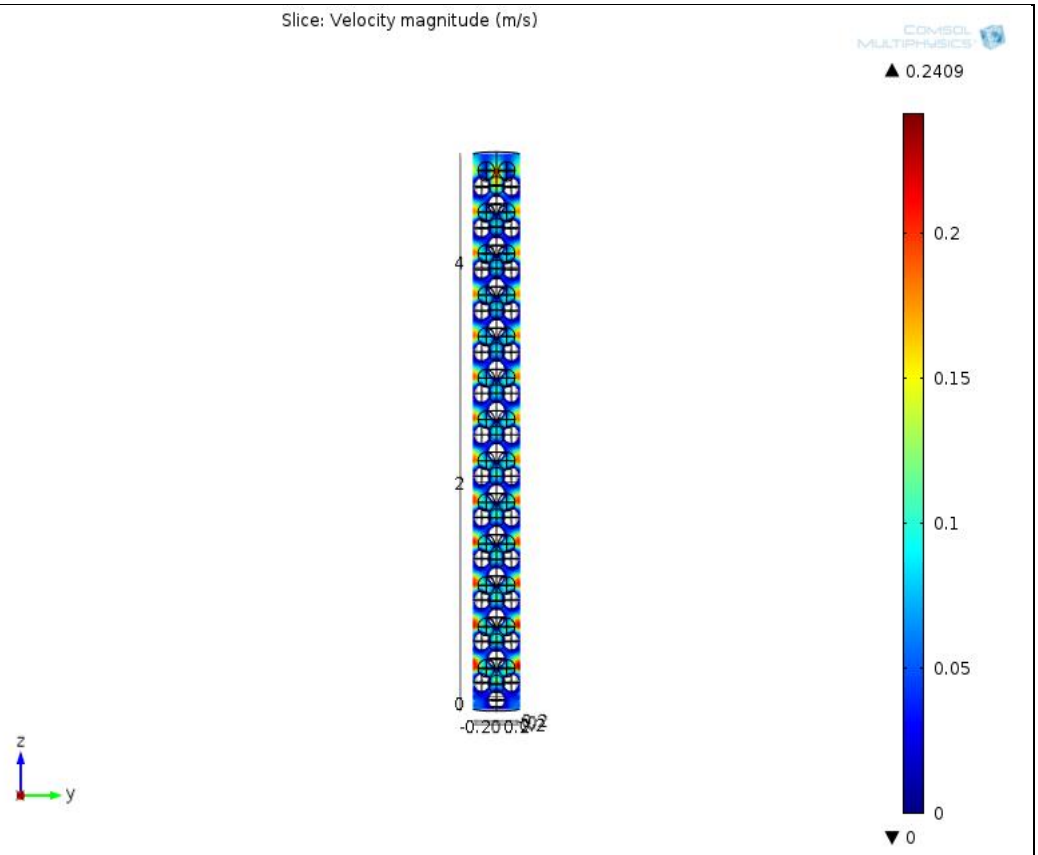
Arrangement of 0.18mm particle size in 0.6mm pore size 30PPI PU	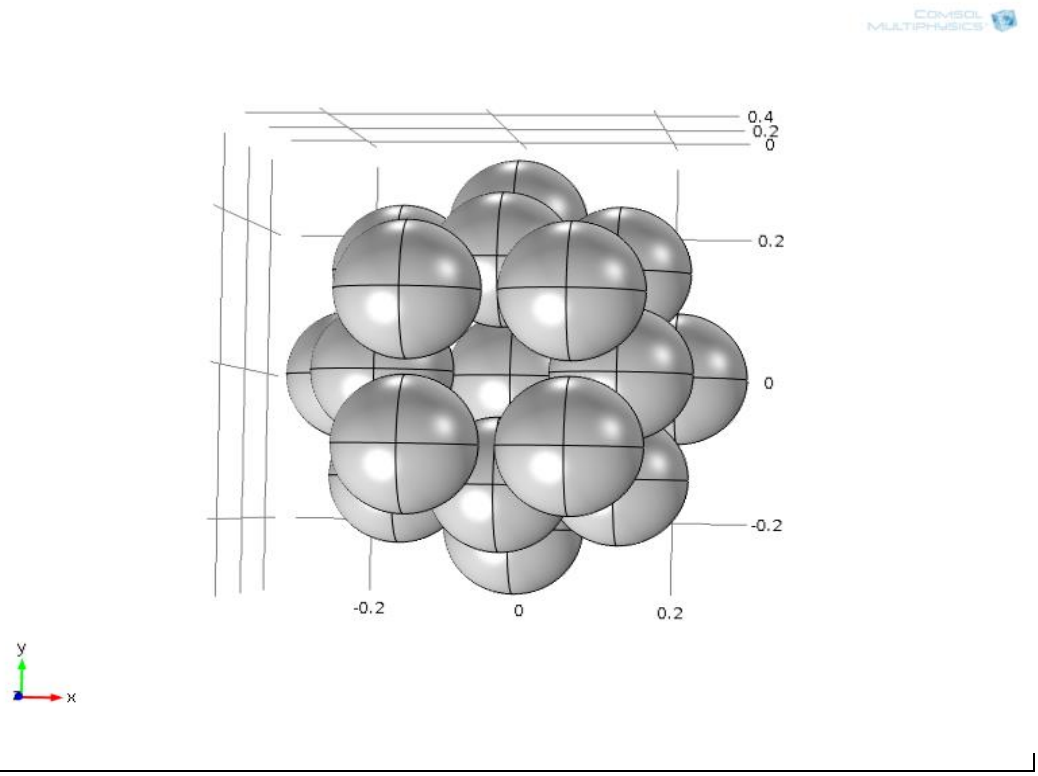

0.18mm particle size in 0.6mm pore size 30PPI PU	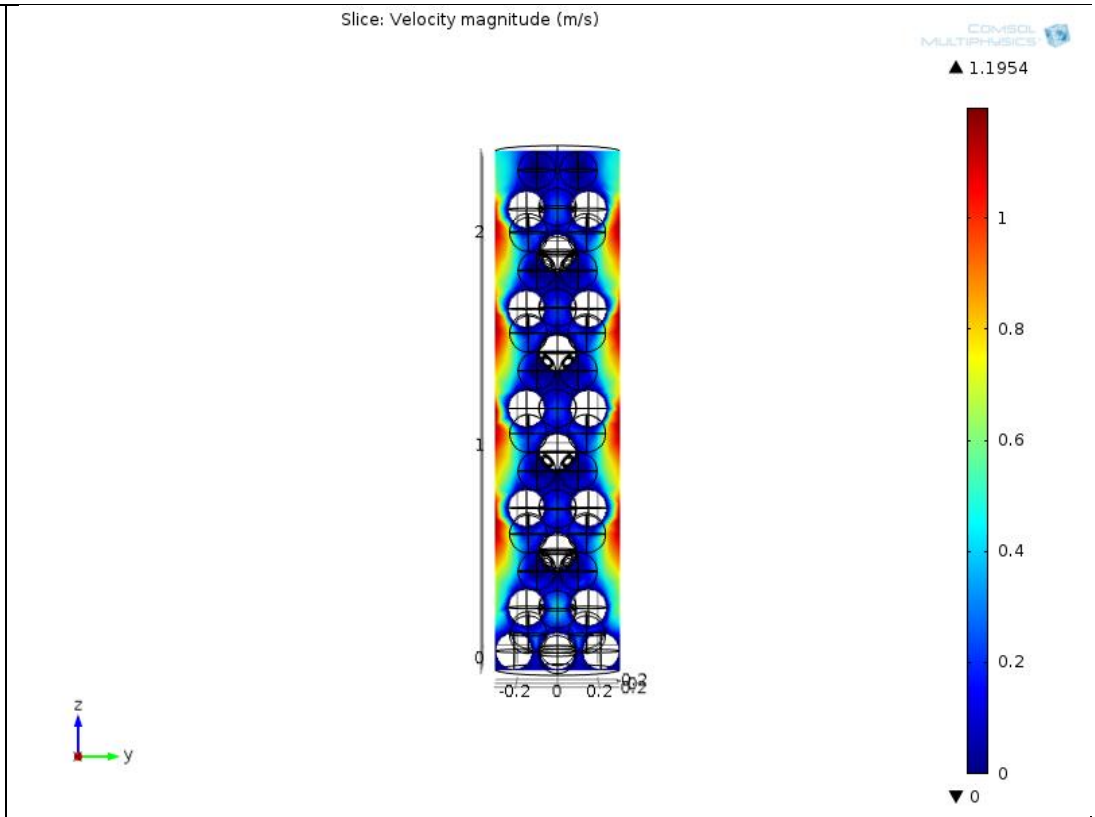
0.19mm particle size in 0.6mm 30PPI PU	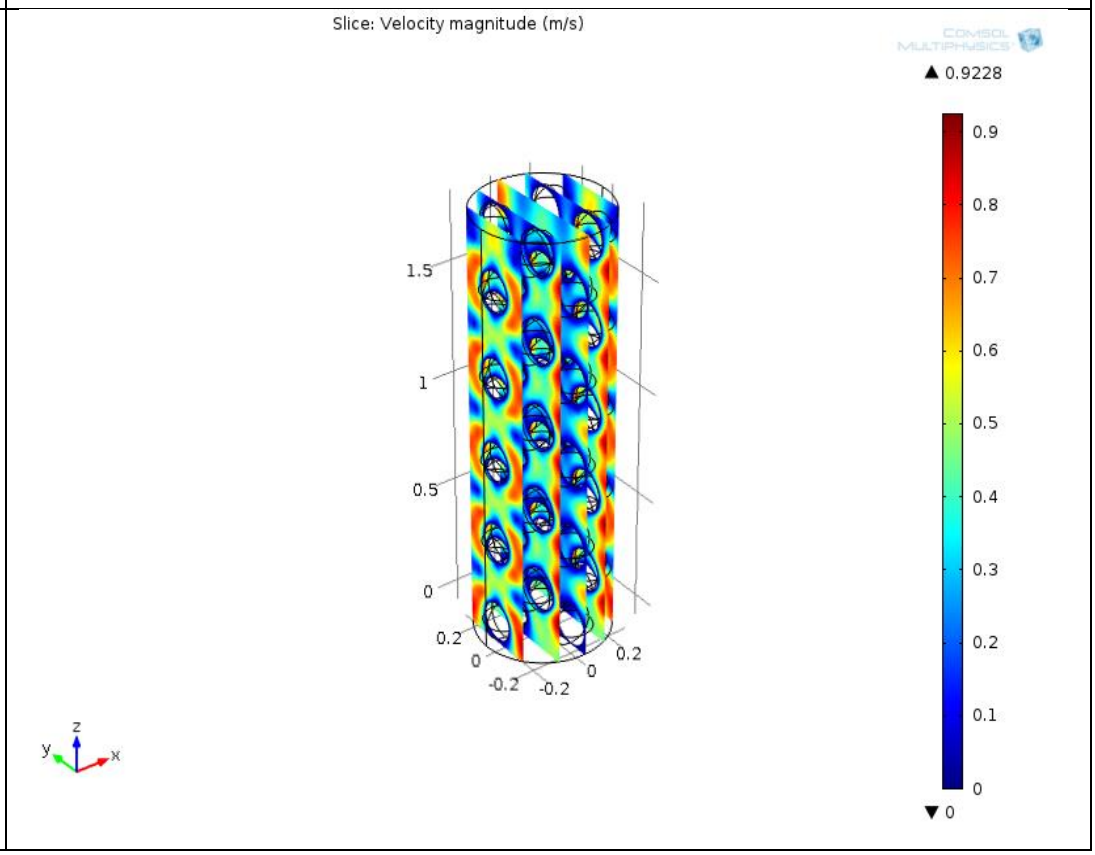

CHAPTER FIVE

CONCLUSION AND RECOMMENDATION

5.1 Conclusion

The flow of water through polyurethane foam based activated carbon and silver Nano particles composite filter is studied. At the end of the simulation and analysis nine alternative results which have 2 to 3L/h flow rate were obtained. This result is agreed with the objective of this research. It also agreed with the experimental result of Prashant Jain, T. Pradeep [53] as well as the simulation result of Mark W. Kennedy (2012) [39]. Their work has already discussed in the literature review and the background of this paper. Finally the following conclusions are drawn:

1. As the thickness of foam increases the velocity of water decreases.
2. As the area difference between the pore of foam and the particles increases the flow rate increases.
3. The arrangement of the particles in pores has significant influence on the flow rate of water.
4. Smaller size particles have more probability to contact with water in the course of flow than bigger sized particles in the same thickness of foam.
5. Using Combination of powder activated carbon and granular activated carbon gives good result relative to using one type of activated carbon alone.

5.2 Recommendation

In this thesis simulation of water flow through the polyurethane foam based activated carbon and silver; Nano particles composite Nano filter is studied through simulation. The main focus was on the flow rate of the filter. In order to use this filter the research in this paper is not enough. Further studies experimentally as well as computer modeling is necessary on:

1. The efficiency of the filter in terms of water quality must be studied.
2. Since membrane fouling is one of the challenges in the area of water filtration, it also carefully studied for this filter.
3. Chemical resistance and the life time of the filter also should be investigated.

There for I recommend further study on the aforementioned points by respective researcher

BIBLIOGRAPHY

1. Aasif Mujtaba, C. K., & Bassin, a. J. (2011). *Nano-Technology for Water Purification – Nano Silver and Titanium Dioxide.* Delhi: Term Paper Water and Wastewater Technologies.

2. Abdel Hameed M. El-Aassar, M. M.-G. (2013). Using Silver Nanoparticles Coated on Activated Carbon Granules in Columns for Microbiological Pollutants Water Disinfection in Abu Rawash area, Great Cairo, Egypt . *Australian Journal of Basic and Applied Sciences, 7(1)*, 422-432.

3. *Activated carbon.* (2015, February 15). Retrieved February 25, 2015, from google: http:// index.php?title=Activated_carbon&oldid=647262255

4. Arnaout, C. L. (2012). *Assessing the Impacts of Silver Nanoparticles on the Growth, Diversity, and Function of Wastewater Bacteria.* Duke University: unpublished.

5. Artuˇg, G. (October 2006). *Modelling and Simulation of Nanofiltration Membranes, thesis report.*

6. Auphedeous Y. Dang-i, a. W. (2013). Removal ofF E.Coli from Drinkink water using Hydroxyapatite Modified Clay Filter. *Journal of Scientific Innovations for Development Volume 1(1)*, 41-53.

7. B. Domènech, M. M. (2013). Polymer-Silver Nanocomposites as Antibacterial materials. *Microbial pathogens and strategies for combating them: science, technology and education (A. Méndez-Vilas, Ed.)*, 630-640.

8. B. Van der Bruggen, M. M. (2008). Drawbacks of applying nanofiltration and how to avoid them: A review. *Separation and Purification Technology*, 251-263.

9. Bastian Schäfera, M. H. (2009). *Agglomeration and filtration of colloidal suspensions with DVLO interactions in simulation and experiment* . Retrieved February 21, 2015, from google: http://arxiv.org/ftp/arxiv/papers/0907/0907.1551.pdf

10. Bhushan, B. (2010). Introduction to Nanotechnology. In B. E. Bhushan, *Handbook of* (pp. 1-13). Berlin Heidelberg: Springer .

11. Cakmak, M. E. (January 2011). *Computational Fluid Flow and Transport of Ccolloidal Pparticles in Soil Ppores.* Cornell: unpublished.

12. Carbó, G. P. (2008). *Determinants of water and ion permeation through nanopores studied by Molecular Dynamics simulation.* Göttingen: Georg-August-Universität zu Göttingen.

13. COMSOL AB. (2008). *Earth Science Module User's Guide ver.-3.5.* unpeblished.

14. D.D. Joseph, D. N. (August 1982). nonlinear equation governing flow in saturated poruse medium . *water resource research,Vol. 18 No. 4*, 1049-1052.

15. *Darcy's law*. (2015, January 17). Retrieved February 2, 2015, from Wikipedia, The Free Encyclopedia: http://en.wikipedia.org

16. Derek B. Purchas, K. S. (November 2002). *Handbook of Filter Media.* Boulevard, Langford Lane, kidlilngton, Oxford, UK: Elsevier Science & Technology Books.

17. Dhermendra K. Tiwari, J. B. (2008). Application of Nanoparticles in Waste Water Treatment. *World Applied Sciences Journal 3 (3)*, 417-433.

18. Edward H. Winant, P. (2005). *A cencury of water.* On Tap, 42-46.

19. Emburgas filtri SIA. (2014). *Polyurethane foam filters.* Retrieved February 25, 2015, from google: http://www.emburgasfiltri.lv/en/polyurethane-foam-filters

20. Environmental Protection Agency (EPA). (Thursday, October 8, 2009). Drinking Water Contaminant Candidate List 3—Final. *Federal Register daily journal of united states government/ Vol. 74, No. 194*, 51850-51862.

21. EPA,United States Environmental Protection Agency. (2000, february). *The History of Drinking Water.* united state: Office of Water.

22. Eyassu Woldesenbet, P. P. (n.d.). *Summary of Research Work*. Retrieved April 6, 2014, from google : http://me.lsu.edu/~woldesen/research.html

23. F. El Azhar, N. E. (2013). Feasibility of Nanofiltration process in dual stage in desalination of the seawater. *IOSR Journal of Applied Chemistry Volume 5, Issue 1*, 35-42.

24. Fishwick, P. (1995, October thursday). *fishwick/introsim/node1.html*. Retrieved augest/25 monday, 2014, from google: http://www.cise.ufl.ed

25. *Fluid flow through porous media*. (2015, January 27). Retrieved Jebruary 2, 2015, from Wikipedia, The Free Encyclopedia.: http://en.wikipedia.org

26. George Mulongo, J. M.-C. (2011). Water Bactericidal Properties of Nanosilver Polyurethane Composites. *Nanoscience and Nanotechnology 1(2)*, 40-42.

27. Grigg, Z. Z. (2006). A Criterion for Non-Darcy Flow in Porous Media. *Transport in Porous Media*, 57–69.

28. Hendrix, M. (December 2012). Water in Ethiopia: Drought, Disease and Death. *Global Majority E-Journal, Vol. 3, No. 2* , 110-120.

29. Hlushkou, D. (2004). *Numerical simulation of fluid flow and mass transport in (electro) chromatographic systems* . Magdeburg: BelarusianState University.

30. Hoek, C. M.-J. (2010). A review of the antibacterial effects of silver nanomaterials and potential implications for human health and the environment. *Journal of Nanopart Res*, 1531–1551.

31. J.G. Wang, C. L. (2003). Numerical solutions for flow in porous media. *International Journal for Numerical and Analytical Methods in Geomechanics*, 565–583.

32. Jesperson, K. (Summer 1996). *Search for Clean Water Continues.* Morgantown: National Drinking Water.

33. JRank. (n.d.). *carbon.* Retrieved september 22, 2014, from google: http://www.chemistryexplained.com

34. Lefebvre, J. P. (2006). Modeling of neutral solute and ion transport in charged nanofiltration membranes using computer simulation programs. In X. L. Horst Chmiel, *Handbook of Theoretical and Computational Nanotechnology, volume5* (p. 93−214). America: American Scientific Publishers.

35. Liu, W. L. (2012). Preparation and characterization of polyurethane foam/activated carbon composite adsorbents. *tournal of porous materials* , 567-572.

36. M.Karnib, H. A. (2013). The Antibacterial Activity of Activated Carbon, Silver, Silver Impregnated Activated Carbon and Silica Sand Nanoparticles against Pathogenic E. coliBL21. *international journal of current microbiology and applied sciences Volume 2Number 4*, 20-30.

37. Maciej Długosz, M. B. (2012). Hybrid calcium carbonate/polymer microparticles containing silver nanoparticles as antibacterial agents. *Journal Nanopart Resource 14:1313, research paper*, 1-8.

38. Marjan S. Ranđelović, A. R. (2012). New Composite Materials in the Technology for Drinking Water Purification from Ionic and Colloidal Pollutants. In M. S. Ranđelović, *Composites and Their Applications* (pp. 273-300). Niš, Serbia: InTech.

39. Mark W. Kennedy, K. Z. (2012). Determination and Verification of the Forchheimer Coefficients for Ceramic Foam Filters Using COMSOL CFD Modelling. *Except from the proceedings of the 2012 COMSOL conference* , (pp. 1-7). Milan.

40. Martinez, F. A. (December 2001). *Polyurethane foam based packing media for biofilers removing volatile organic compaunds from contaminated air,thesis.* Louisiana State: unpublished.

41. Mesner, B. D. (2010, december). Drinking Water Treatment Systems. *Drinking Water Facts…..*, pp. 1-8.

42. Mohammed Amine Kendouci, B. K. (2013). Simulation of water filtration in porous zone based on Darcy's law. *Energy Procedia 36*, 163 – 168 .

43. Mohan Noronha, V. M. (2003). Computer-Aided Simulation and Design of Nanofiltration Processes. *Ann. N.Y. Acad. Sci.984*, 142-158.

44. Moise´s L. Pinto, J. ˜. (2004). Synthesis and Characterization of Polyurethane Foam Matrices for the Support of Granular Adsorbent Materials. *Journal of Applied Polymer Science, Vol. 92*, 2045–2053.

45. Morrison, F. A., & Osterle, J. (1965). Electrokinetic energy conversion in ultrafine capillaries . *Journal of Chemical Physics vol.43 No.6*, 2111–2115.

46. Nguyen Thi Phuong Phong, N. V. (2009). Fabrication of antibacterial water filter by coating silvernanoparticles on flexible polyurethane foams. *Journal of Physics: Conference Series187*, 1-8.

47. ocw.mit.edu. (2006). *google.* Retrieved March 12, 2015, from Chapter 3 flow past a sphere II: Stokes` law, the Bernoulli equation, Turulance, Boundary layers, Flow separation: http://ocw.mit.edu

48. Pahlke, O. (2005). *Polyurethane (PUR) foams*. Retrieved Fbruaty 25, 2015, from google: http://www.pahlke-schaumstoffe

49. Palmeri, J., Blanc, P., Larbot, A., & David, P. (1999). Theory of pressure-driven transport of neutral solutes and ions in porous ceramic nanofiltration membranes. *journal of Membrane Science 160*, 141–170.

50. polygrow. (2010, april 1). *What is Polyurethane foam?* Retrieved september 18, 2014, from google: http://www.polygrow.nl/index.php?id=15

51. *polyureyhane.* (2014, september 17). Retrieved septembe 18, 2014, from google:

52. PRAKASH, V. (2010, may thursday/27). *National Institute of Science Education and Research, Bhubaneswar.* Retrieved august monday/25, 2014, from google: www.niser.ac.in

53. Prashant Jain, T. P. (2005). Potential of Silver Nanoparticle-Coated Polyurethane Foam As an Antibacterial Water Filter. *Biotechnology and Bioengineering, VOL. 90, NO. 1*, 59-63.

54. Pratsinis, G. A. (2010). Antibacterial Activity of Nanosilver Ions and Particles. *Environmental Science & Technology Vol. 44, No. 14*, 5649–5654.

55. Prevension, C. f. (n.d.). *Diarrhea: Common Illness, Global Killer,CS229489-A & B.* U.S: cdc.

56. Quang Huy Tran, V. Q.-T. (2013). Silver nanoparticles: synthesis, properties,toxicology, applications and perspectives: review. *Advances in natural science: Nanoscience and Nanotechnology 4 / 033001*, 1-20.

57. Safe drink water foundation/SDWF. (2014). *Bacteria.* Retrieved september 29, 2014, from google: http://www.safewater.org

58. *Simulation*. (2014, august monday/4). Retrieved august monday/25, 2014, from google: http://en.wikipedia.org/w/index.php?title=Simulation&oldid=619815570

59. T. Pradeep, A. (2009). Special Feature Noble metal nanoparticles for water purification: A critical review. *Thin Solid Films 517*, 6441–6478.

60. Thomas R.R. Pintelon, S. A. (2010). Validation of 3D Simulations of Reverse Osmosis Membrane Biofouling. *Biotechnology and Bioengineering, Vol. 106, No. 4,*, 677–689.

61. Thomson, T. (2005). *Polyurethanes as Specialty Chemicals Principles and Applications.* Boca Raton London New York Washington, D.C.: by CRC Press LLC .

62. U.S. Environmental Protection Egency. (2015, March 19). *Granular Activated Carbon.* Retrieved March 19, 2015, from google: http://iaspub.epa.gov

63. Wang, L. (2012). Molecular Dynamics Simulations of Liquid T ransport through Nanofiltration Membranes. *Open Access Dissertations and Theses,Paper 7371*.

64. WHO. (2013-2020). *Water Quality and Health Strategy.* WHO.

65. Winant, E. H. (2005, summer). century of water. *on Tap*, pp. 42-46.

66. Worled health organization. (2007). *Combating water borne disease at the house hold level.* Geneva, Switzerland: WHO Document Production Services.

67. Zimmerman, D. R. (2002-2003). Diffusion Equation for Fluid Flow in Porous Rocks. In D. R. Zimmerman, *Flow in Porous Media* (p. 160). London: unpublished.

Appendixes

Appendix A. Tables

Table 16: simulation result for different PPI foams

For pore diameter 0.166 mm or for 90 PPI polyurethane foam

Particle size	Average Velocity(m/s)		Ratio(b/a)	Average Velocity at 5cm height (m/s)	Flow rate (L/h)	Error%
	Pore hight-2.5mm (a)	Pore hight-5mm (b)				
0.15mm	0.00891	0.00716	0.8	0.000103	0.58	-71

For pore diameter 0.2mm or for 70 PPI polyurethane foam

Particle size	Velocity		Ratio(b/a)	At 50cm height	Flow rate (L/h)	Error (%)
	Pore hight-2.5mm (a)	Pore hight-5mm (b)				
0.19 mm	0.00359	0.00361	1	0.0361	94.88	+3062.6
0.18 mm	0.00756	0.00717	0.9	0.0009	4.6	+53.3
0.175mm	0.02212	0.01182	0.53	3.6*10^-8	0.00042	-99.9
0.17 mm	0.00863	0.00525	0.6	3.15 * 10^-6	0.024	-98.8
0.16 mm	0.01464	0.0046	0.3	5.1* 10^-13	0.0049	-99.75

For pore diameter 0.233 mm or for 60 PPI polyurethane foam

Particle size	Velocity		Ratio (b/a)	At 50cm height	Flow rate (L/h)	Error (%)
	Pore hight-2.5mm (a)	Pore hight-5mm (b)				
0.22 mm	0.00565	0.00437	0.77	3*10^-5	0.874	-56.3
0.21mm	0.01817	0.01014	0.56	1.67*10^-6	0.0084	-99.58
0.2 mm	0.03859	0.01995	0.51	5.46 * 10^-7	0.0038	-99.81

For pore diameter 0.2833 mm or for 50 PPI polyurethane foam

Particle size	Velocity		Ratio(b/a)	At 50 cm height	Flow rate (L/h)	Error (%)
	Pore hight-2.5mm (a)	Pore hight-5mm (b)				
0.25 mm	0.06824	0.03396	0.49	7.9 * 10^-9	4.8*10^-5	-99.99

For pore diameter 0.45 mm or for40 PPI polyurethane foam

Particle size	Velocity		Ratio(b/a)	At 50cm height	Flow Rate (L/h)	Error (%)
	Pore hight-2.5mm (a)	Pore hight-5mm (b)				
0.15 mm	0.22368	0.103	0.46	4*10^-8	0.00032	-99.98
0.16 mm	0.13521	0.07099	0.52	2.8*10^-8	0.008	-99.6

For pore diameter 0.6 mm or for 30 PPI polyurethane foam

Particle size	Velocity		Ratio(b/a)	At 50 cm height	Flow rate (L/h)	Error (%)
	Pore hight-2.5mm (a)	Pore hight-5mm (b)				
0.15mm	0.00344	0.00145	0.42	1.10^-10	0.48*10^-10	100
0.18	0.2751	0.1364	0.49	1.75 *10^-7	0.0022	-99.89
0.19	0.35367	0.16624	0.47	9.78*10^-8	0.00239	-99.88

For pore diameter 0.9 mm or for 20 PPI polyurethane foam

Particle size	Velocity		Ratio (b/a)	At 50 cm height	Flow rate (L/h)	Error (%)
	Pore Height 2.5mm (a)	Pore height 5mm (b)				
0.25 mm	0.22968	0.11208	0.49	1.46*10^-7	0.001	-99.95
0.2	0.21882	0.10416	0.48	9.22*10^-8	0.00167	-99.91

For pore diameter 1.95 mm or for 10 PPI polyurethane foam

Particle size		No. particles with maximum pore height 5mm				average ratio	At 50cm height	Flow rate (L/h)	Error (%)
		1	2	3	4				
1.2 mm	straight	27.05754	14.94035	11.17337	10.35341	0.74	1.59*10^-4	5.16	+72
	zigzag	27.05754	19.32311	11.1165	8.45983	0.72	5.3*10^-5	1.72	-14
1.3 mm	straight	16.58662	11.89097	8.24294	7.10456	0.75	1.66*10^-4	4.82	+60.6
	zigzag	16.59662	9.52033	7.90753	7.2395	0.77	4.77*10^-4	13.85	+333.3
1.4 mm	straight	10.14155	7.78619	4.84925		0.69	1.48*10^-4	3.75	+25
	zigzag	10.14155	8.60485	4.8912		0.7	2.28*10^-4	5.77	+92.3
1.5 mm	straight	6.40011	4.01409	3.23377		0.71	2.2*10^-4	4.69	+56.3
	zigzag	6.40011	5.53075	3.75804		0.76	1.7*10^-3	36.29	+1109.6
1.6 mm	straight	3.39327	2.21942	1.93293		0.76	9*10^-4	15.3	+343.3
	zigzag	3.39327	3.12359	2.34638		0.83	0.0126	215.3	+7076.6

Particle size	Height 2.5mm	Height 5mm	Ratio	At height 50mm	Flow rate (L/h)	Error (%)
1.4mm&0.25 mm combined	1.12117	0.7069	0.63	1.08*10^-4	1.39	-30.5
1.5 mm and 0.2mm combined	0.45133	0.22088	0.49	4.98*10^-6	0.06	-97

Table 17: Modified velocities and flow rates

No.	Particle size	Porosity PPI	Thickness of foam(cm)	Radius of foam (cm)	Velocity (m/s)	Flow Rate (L/h)	Error (%)
	0.15mm	90	3 to 3.6	20	3.91*10^-4	1.97 to 3.17	0 to ±5.6
3	0.18 mm	70	5	15	0.0009	2.59	0
4	0.175mm	70	1.5	20	4.9*10^-4	3.09	3
5	0.17 mm	70	1.6	20	3.11*10^-4	2.33	0
6	0.16 mm	70	1	20	1.18*10^-4	1.15	-42.5
7	0.22M	60	1.75 & 2	20	6.98*10^-4 & 1.04*10^-3	2.03 & 2.64	0
8	0.21mm	60	1.5 & 1.6	20	5.5*10^-4 & 7.4*10^-4	2.11 & 2.82	0
9	0.2 mm	60	1.75	20	3.46*10^-4	2.45	0
10	0.25mm	50	1.75	20	4.62*10^-4	2.79	0
11	0.15 mm	40	2.5	20	9.48*10^-5	2.35	0
12	0.16 mm	40	2.75	20	1.02*10^-5	2.24	0
13	0.15mm	30	1	20	1.07*10^-4	2.65	0
14	0.18 mm	30	2.5	20	2.19*10^-4	2.36	0
15	0.19 mm	30	2.5	20	1.86*10^-4	2.47	0
17	0.25 mm	20	2.5	20	1.83*10^-4	2.49	0

18	0.2 mm		20	2.4	20	2.05*10^-4	2.82	0
19	1.2mm	straight	10	5	15	1.59*10^-4	2.9	0
20		zigzag	10	4.88	20	7.38*10^-5	2.39	0
21	1.3mm	straight	10	5	15	1.66*10^-4	2.71	0
22	1.4mm	straight	10	5	15	1.48*10^-4	2.1	0
23		zigzag	10	5	15	2.28*10^-4	3.25	8.3
24	1.5mm	straight	10	5	15	2.2*10^-4	2.64	0
25	1.4mm&0.25mm combined		10	4.75	20	1.72*10^-4	2.59	0
26	1.5 mm and 0.2mm combined		10	2.4	20	5.14*10^-4	2.4	0

Table 18: Antimicrobial effects of Ag-NPs As compiled by Nguyen and Anh-Tuan Le [54]

Characterization of Ag-NPs			Microbial strains	Major outcomes
Type	Particle size	Surface stability		
1. Antibacterial effects				
Ag-NPs powder	12 nm	None	E. coli	Growth inhibitory concentration: 50–60 μg cm^{-3} (10^5CFU), and 20 μg cm^{-3} (10^4CFU)
Ag-NPs powder	1–100 nm	Carbon matrix	E. coli, v.cholera, P. concentration: aeruginosa and Salmonella typhus	Growth inhibitory concentration: 75 μg ml^{-1} P. aeruginosa and V. cholera were more resistant than E. coli and S. typhus
Ag-NPs	13.4 nm	None	E. coli and S. aureus	Minimum inhibitory [4 concentration: >3.3 nM (E. coli) and >33 nM
Ag-NPs in aqueous	10–15 nm	None	E. coli, ampicillin resistant E. coli, multi-	Growth inhibitory concentration:

media			drug resistant Salmonella typhiand S. aureaus	25 μg $ml^{-1}$for E. coli, ampicillin-resistant E. coli and multi-drug resistant strains of S. typhi Undetermined data for
Ag-NP in different shapes	Different shapes and size	None	E. coli	Growth inhibitory Concentration: 1 μg (truncated triangular particles) 50–100 μg (spherical particles) >100 μg (rod-shape particles)
Ag-NP in PDDA	26nM	Polymers/ surfactant	Standard strains, and isolated from human clinical samples	Minimum inhibitory concentration: 1.69–13.5 μg ml^{-1} 1 μg ml^{-1} SDS-modified Ag-NPs
Ag-NPs in culture media	100Nm	NA	Drug-resistant bacteria: erythromycin-resistant S. Pyogenes,-ampicillin-resistant E. coliO157 : H7, and multidrug resistant p.aeruginosa Drug-susceptible bacteria: Streptococcus sp., E. coli, and P. aeruginosa	Minimum inhibitory concentrations (in average): 79.4 nM for drug resistant bacteria and 71.5 nM for drug-susceptible bacteria Minimal bactericidal concentrations (in average): 83.3 nM for drug resistant bacteria and 74.3 nM for drug-susceptible bacteria
Ag-NPs powder	NA	NA	E. coli and S.aureus	Minimum inhibitory concentration: 100 μg ml^{-1}
Ag-NPs	9-10nM	Oleate ions	E coli and V. cholerae	Minimum inhibitory concentration:

				~3 μg ml^{-1} for both bacterial strains
Ag-NPs	8-50nM	SDS	E. coli, P aeruginosa and S. aureus	Minimum inhibitory concentration: <7 ppm
2. Antifungal effects				
Ag-NPs	~ 3 nm	None	44 strains of 6 fungal species from clinical isolates and ATCC strains of T mentagrophytes and C.albicans	IC_{80}: 1–7 μg ml^{-1}
Ag-NPs Coated plastic catheters	3-18nM	None	C. albicans	Growth inhibition of Ag-NPs - coated catheter (80–120 nm in thick) was almost complete for C. albicans
Ag-NPs	25nM	None and SDS	Candida spp.	Minimum inhibitory concentration: 210 μg ml^{-1} for naked Ag-NPs 50 μg ml^{-1} for Ag-NPs modified with SDS
Ag-NPs	~ 5 nm	None	C. albicans and Candida Glabrata	Minimum inhibitory concentration: 0.4–3.3 μg ml^{-1}
3. Antiviral effects				
Ag-NPs	1-10nM	Carbon, PVP BSA	HIV-1	Ag-NPs undergo a size-dependent interaction with HIV-1 (1–10 nm), and inhibit the virus from binding to host cells
Ag-NPs	10,50and 800n	None	HBV	Inhibition of HBV replication (Ag-NPs,10 nm)

	M			
Ag-NPs	NA	PVP, recombinant RSV fusion (F) protein, and BSA	RSV	44% inhibition of syncytial virus infection for PVP-coated fusion Ag-NPs
Ag-NPs	10-80nM	None, polysaccharide Coating	Monkey pox virus (MPV	Ag-NPs of approximately 10 nm inhibit MPV infection in vitro
Ag-NPs	11.2nM	Biogenic Ag^0	MNV-1	Addition of 31.25 mg biogenic Ag^0 m^{-2}on the filter caused a 3.8-log decline of the virus as compared with a 1.5-log decrease by the original filter
Ag-NPs	10nM	None	H1N1 influenza A virus	Efficient inhibitory activity on H1N1 influenza A virus

Note IC_{80}: 80% inhibitory concentration; SDS: sodium dodecyl sulfate; PDDA: poly (diallyldimethylammonium) chloride; PVP: poly (N -vinyl-2-pyrrolidone); BSA: bovine serum albumin; NA: not available

Table 19: Table of contaminants [19]

Chemical Contaminants

Substance Name	Use
1,1,1,2-Tetrachloroethane	It is an industrial chemical used in the production of other substances.
1,1-Dichloroethane	It is an industrial chemical used as a solvent.
1,2,3-Trichloropropane	It is an industrial chemical used in paint manufacture.
1,3-Butadiene	It is an industrial chemical used in rubber production.

1,3-Dinitrobenzene	It is an industrial chemical and is used in the production of other substances.
1,4-Dioxane	It is used as a solvent or solvent stabilizer in the manufacture and processing of paper, cotton, textile products, automotive coolant, cosmetics and shampoos.
17alpha-estradiol	It is an estrogenic hormone and is used in pharmaceuticals.
1-Butanol	It is used in the production of other substances, and as a paint solvent and food additive.
2-Methoxyethanol	It is used in consumer products, such as synthetic cosmetics, perfumes, fragrances, hair preparations, and skin lotions.
2-Propen-1-ol	It is used in the production of other substances, and in the manufacture of flavorings and perfumes.
3-Hydroxycarbofuran	It is a carbamate, and is a pesticide degradates. The parent, carbofuran, is used as an insecticide.
4,4'-Methylenedianiline	It is used in the production of other substances, and as a corrosion inhibitor and curing agent for polyurethanes.
Acephate	It is used as an insecticide.
Acetaldehyde	It is used in the production of other substances, and as a pesticide and food additive.
Acetamide	It is used as a solvent, solubilizer, plasticizer, and stabilizer.
Acetochlor	It is used as an herbicide for weed control on agricultural crops.
Acetochlor ethanesulfonic acid (ESA)	Acetochlor ESA is an acetanilide pesticide DE gradates. The parent, acetochlor, is used as an herbicide for weed control on agricultural crops.
Acetochlor oxanilic acid (OA)	Acetochlor OA is an acetanilide pesticide DE gradates. The parent, acetochlor, is used as an herbicide for weed control on agricultural crops.
Acrolein	It is used as an aquatic herbicide, rodenticide, and industrial chemical.
Alachlor ethanesulfonic acid (ESA)	Alachlor ESA is an acetanilide pesticide DE gradates. The parent, alachlor, is used as an herbicide for weed control on agricultural

	crops.
Alachlor oxanilic acid (OA)	Alachlor OA is an acetanilide pesticide degradates. The parent, alachlor, is used as an herbicide for weed control on agricultural crops.
alpha-Hexachlorocyclohexane	It is a component of benzene hexachloride (BHC) and was formerly used as an insecticide.
Aniline	It is used as an industrial chemical, as a solvent, in the synthesis of explosives, rubber products, and in isocyanates.
Bensulide	It is used as an herbicide.
Benzyl chloride	It is used in the production of other substances, such as plastics, dyes, lubricants, gasoline and pharmaceuticals.
Butylated hydroxyanisole	It is used as a food additive (antioxidant).
Captan	It is used as a fungicide.
Chlorate	Chlorate compounds are used in agriculture as defoliants or desiccants and may occur in drinking water related to use of disinfectants such as chlorine dioxide.
Chloromethane (Methyl chloride)	It is used as a foaming agent and in the production of other substances.
Clethodim	It is used as an herbicide.
Cobalt	It is a naturally-occurring element and was formerly used as cobaltus chloride in medicines and as a germicide.
Cumenehydroperoxide	It is used as an industrial chemical and is used in the production of other substances.
Cyanotoxins	Toxins naturally produced and released by cyanobacteria ("blue-green algae"). Various studies suggest three cyanotoxins for consideration: Anatoxin-a, Microcystin-LR, and Cylindrospermopsin.
Dicrotophos	It is used as an insecticide.
Dimethipin	It is used as an herbicide and plant growth regulator.
Dimethoate	It is used as an insecticide on field crops, (such as cotton), orchard crops, and vegetable crops, in forestry and for residential purposes.

Disulfoton	It is used as an insecticide.
Diuron	It is used as an herbicide.
Equilenin	It is an estrogenic hormone and is used in pharmaceuticals.
Equilin	It is an estrogenic hormone and is used in pharmaceuticals.
Erythromycin	It is used in pharmaceutical formulations as an antibiotic.
Estradiol (17-beta estradiol)	It is an estrogenic hormone and is used in pharmaceuticals.
Estriol	It is an estrogenic hormone and is used in veterinary pharmaceuticals.
Estrone	It is an estrogenic hormone and is used in veterinary and human pharmaceuticals.
Ethinyl Estradiol (17-alpha ethynyl estradiol)	It is an estrogenic hormone and is used in veterinary and human pharmaceuticals.
Ethoprop	It is used as an insecticide.
Ethylene glycol	It is used as antifreeze, in textile manufacture and is a cancelled pesticide.
Ethylene oxide	It is used as a fungicidal and insecticidal fumigant.
Ethylene thiourea	It is used in the production of other substances, such as for vulcanizing polychloroprene (neoprene) and polyacrylate rubbers, and as a pesticide.
Fenamiphos	It is used as an insecticide.
Formaldehyde	It has been used as a fungicide, may be a disinfection byproduct, and can occur naturally.
Germanium	It is a naturally-occurring element and is commonly used as germanium dioxide in phosphors, transistors and diodes, and in electroplating.
Halon 1011 (bromochloromethane)	It is used as a fire-extinguishing fluid and to suppress explosions, as well as a solvent in the manufacturing of pesticides. May also occur as a disinfection by-product in drinking water.
HCFC-22	It is used as a refrigerant, as a low-temperature solvent, and in fluorocarbon resins, especially in tetrafluoroethylene polymers.

Hexane	It is used as a solvent and is a naturally-occurring alkane.
Hydrazine	It is used in the production of other substances, such as rocket propellants, and as an oxygen and chlorine scavenging compound.
Mestranol	It is an estrogenic hormone and is used in veterinary and human pharmaceuticals.
Methamidophos	It is used as an insecticide.
Methanol	It is used as an industrial solvent, a gasoline additive and also as anti-freeze.
Methyl bromide (Bromomethane)	It has been used as a fumigant as a fungicide.
Methyl tert-butyl ether	It is used as an octane booster in gasoline, in the manufacture of isobutene and as an extraction solvent.
Metolachlor	It is used as an herbicide for weed control on agricultural crops.
Metolachlor ethanesulfonic acid (ESA)	Metolachlor ESA is an acetanilide pesticide degradates. The parent, metolachlor, is used as an herbicide for weed control on agricultural crops.
Metolachlor oxanilic acid (OA)	Metolachlor OA is an acetanilide pesticide degradates. The parent, metolachlor, is used as an herbicide for weed control on agricultural crops.
Molinate	It is used as an herbicide.
Molybdenum	It is a naturally-occurring element and is commonly used as molybdenum trioxide as a chemical reagent.
Nitrobenzene	It is used in the production of aniline, and also as a solvent in the manufacture of paints, shoe polishes, floor polishes, metal polishes, explosives, dyes, pesticides and drugs (such as acetaminophen), and in its re-distilled from (oil of mirbane) as an
Nitroglycerin	It is used in pharmaceuticals, in the production of explosives, and in rocket propellants.
N-Methyl-2-pyrrolidone	It is a solvent in the chemical industry, and is used for pesticide application and in food packaging materials.
N-nitrosodiethylamine	It is a nitrosamine used as an additive in gasoline and in lubricants,

(NDEA)	as an antioxidant, as a stabilizer in plastics, and also may be a disinfection byproduct.
N-nitrosodimethylamine (NDMA)	It is a nitrosamine and has been formerly used in the production of rocket fuels, is used as an industrial solvent and an anti-oxidant, and also may be a disinfection byproduct.
N-nitroso-di-n-propylamine	It is a nitrosamine and may be a disinfection byproduct.
N-Nitrosodiphenylamine	It is a nitrosamine chemical reagent that is used as a rubber and polymer additive and may be a disinfection byproduct.
N-nitrosopyrrolidine (NPYR)	It is a nitrosamine used as a research chemical and may be a disinfection byproduct.
Norethindrone (19-Norethisterone)	It is a progresteronic hormone used in pharmaceuticals.
n-Propylbenzene	It is used in the manufacture of methylstyrene, in textile dyeing, and as a printing solvent, and is a constituent of asphalt and naptha.
O-Toluidine	It is used in the production of other substances, such as dyes, rubber, pharmaceuticals and pesticides.
Oxirane, methyl-	It is an industrial chemical used in the production of other substances.
Oxydemeton-methyl	It is used as an insecticide.
Oxyfluorfen	It is used as an herbicide.
Perchlorate	It is both a naturally occurring and human-made chemical. Perchlorate is used to manufacture fireworks, explosives, flares and rocket propellant.
Perfluorooctane sulfonic acid (PFOS)	PFOS was used in firefighting foams and various surfactant uses; few of which are still ongoing because no alternatives are available.
Perfluorooctanoic acid (PFOA)	PFOA is used in the manufacture of fluoropolymers, substances which provide non-stick surfaces on cookware and waterproof, breathable membranes for clothing
Permethrin	It is used as an insecticide.

Profenofos	It is used as an insecticide and an acaricide.
Quinoline	It is used in the production of other substances, and as a pharmaceutical (anti-malarial) and as a flavoring agent.
RDX	It is used as an explosive.
Butylbenzene	It is used as a solvent for coating compositions, in organic synthesis, as a plasticizer and in surfactants.
Strontium	It is naturally-occurring element and is used as strontium carbonate in pyrotechnics, in steel production, as a catalyst and as a lead scavenger.
Tebuconazole	It is used as a fungicide.
Tebufenozide	It is used as an insecticide.
Tellurium	It is a naturally-occurring element and is commonly used as sodium tellurite in bacteriology and medicine.
Terbufos	It is used as an insecticide.
Terbufos sulfone	Terbufos sulfone is a phosphorodithioate pesticide degradates. The parent, terbufos, is used as an insecticide.
Thiodicarb	It is used as an insecticide.
Thiophanate-methyl	It is used as a fungicide.
Toluene diisocyanate	It is used in the manufacture of plastics.
Tribufos	It is used as an insecticide and as a cotton defoliant.
Triethylamine	It is used in the production of other substances, and as a stabilizer in herbicides and pesticides, in consumer products, in food additives, in photographic chemicals and in carpet cleaners.
Triphenyltin hydroxide	It is used as a pesticide.
Urethane	It is used as a paint ingredient.
Vanadium	It is a naturally-occurring element and is commonly used as vanadium pentoxide in the production of other substances and as a catalyst.
Vinclozolin	It is used as a fungicide.
Ziram	It is used as a fungicide.

Microbial contaminants

Microbial Contaminant Name	Information
Adenovirus	Virus most commonly causing respiratory illness, and occasionally gastrointestinal illness
Caliciviruses	Virus (includes Norovirus) causing mild self-limiting gastrointestinal illness
Campylobacter jejuni	Bacterium causing mild self-limiting gastroentestinal illness
Enterovirus	Group of viruses including polioviruses, coxsackieviruses and echoviruses that can cause mild respiratory illness
Escherichia coli (0157)	Toxin-producing bacterium causing gastrointestinal illness and kidney failure
Helicobacter pylori	Bacterium sometimes found in the environment capable of colonizing human gut that can cause ulcers and cancer
Hepatitis A virus	Virus that causes a liver disease and jaundice
Legionella pneumophila	Bacterium found in the environment including hot water systems causing lung diseases when inhaled
Mycobacterium avium	Bacterium causing lung infection in those with underlying lung disease, and disseminated infection in the severly immunocompromised

Appendix B

Figures of Simulation results

1. For 70PPI foam

Particle size	Flow result
0.16mm	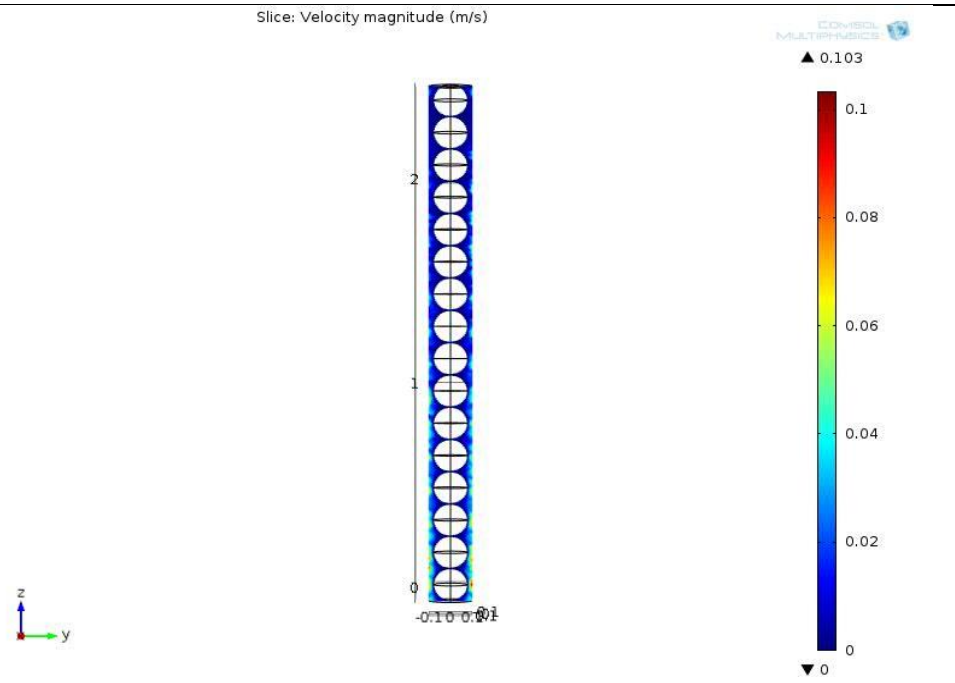
0.17mm	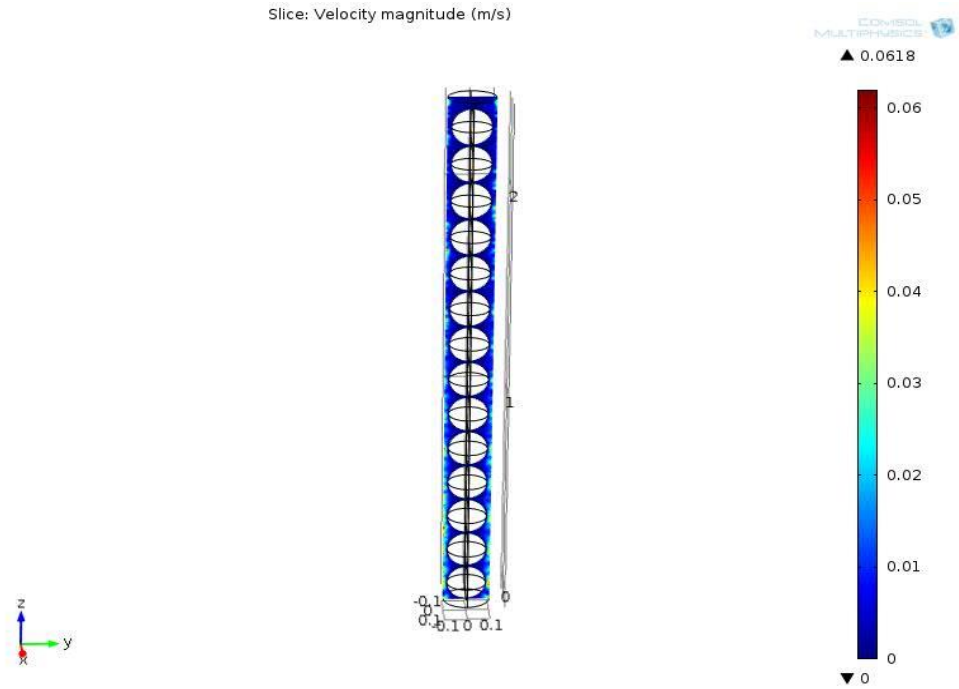

0.18mm	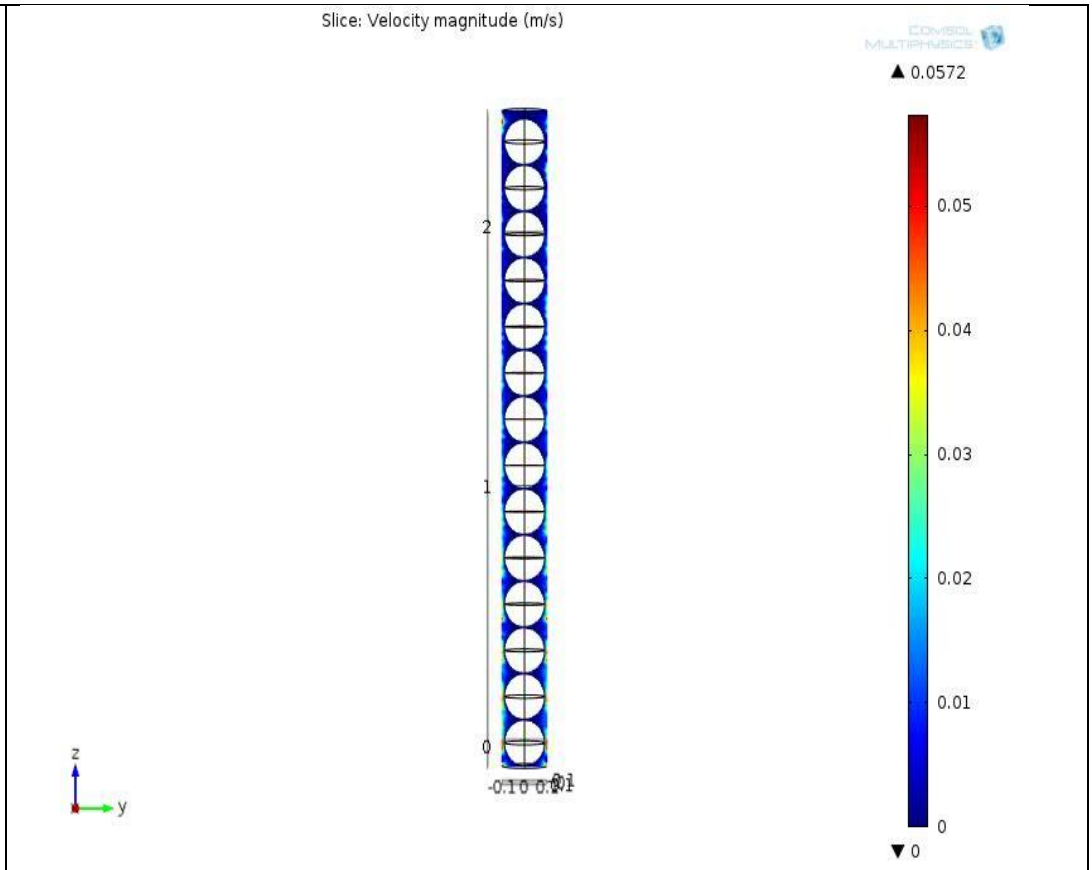 Slice: Velocity magnitude (m/s) ▲ 0.0572 0.05 0.04 0.03 0.02 0.01 0 ▼ 0 2 1 0 z y
0.19mm	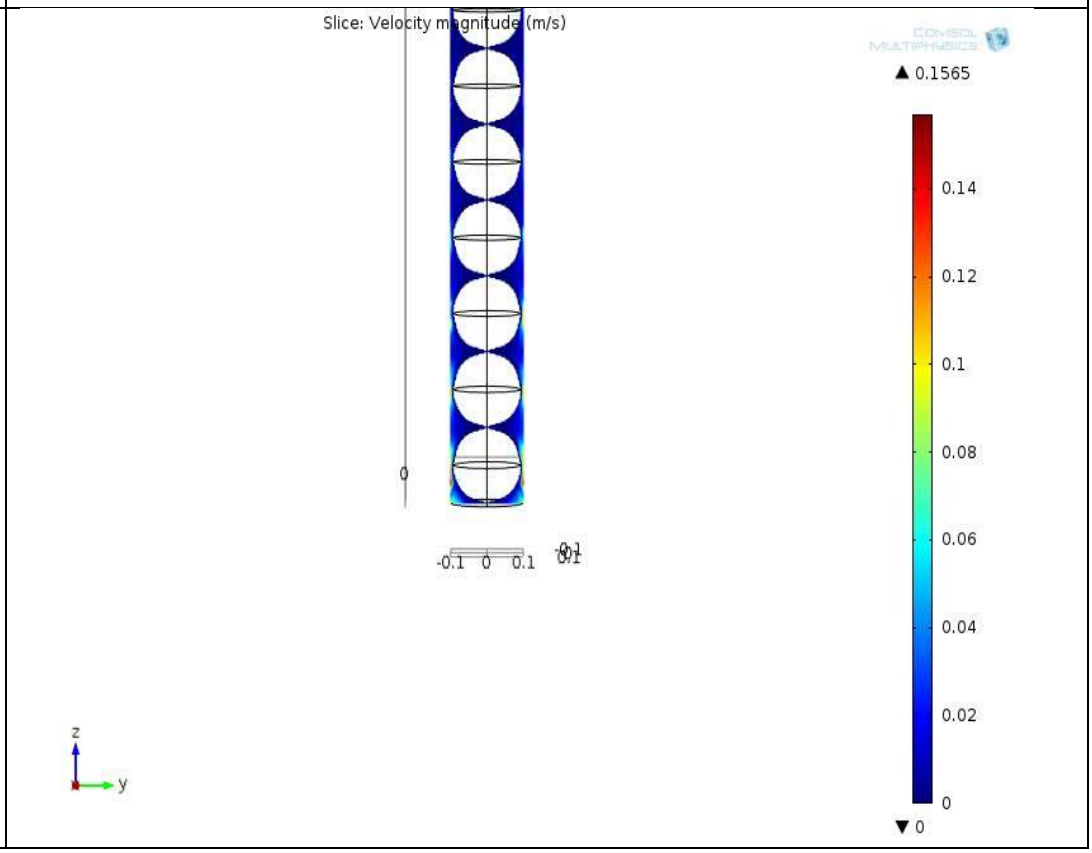 Slice: Velocity magnitude (m/s) ▲ 0.1565 0.14 0.12 0.1 0.08 0.06 0.04 0.02 0 ▼ 0 0 -0.1 0 0.1 z y

2. For 60 PPI

Particle size	Simulation result
0.22mm height 2.5mm	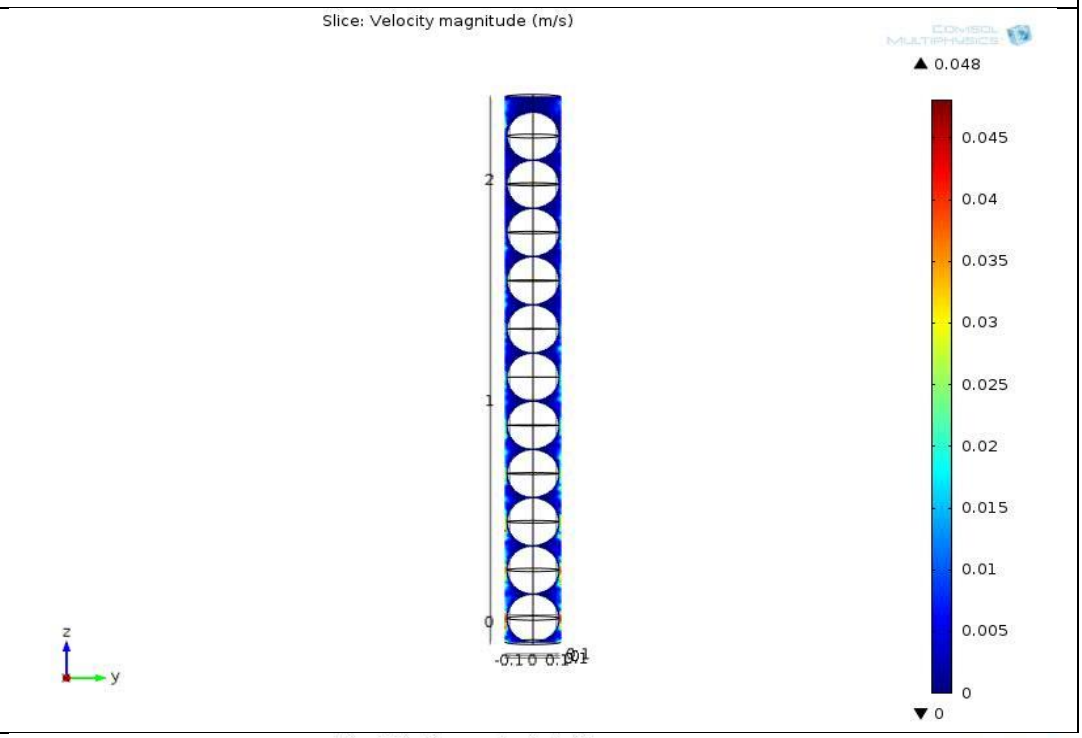
0.21 mm height 2.5 mm	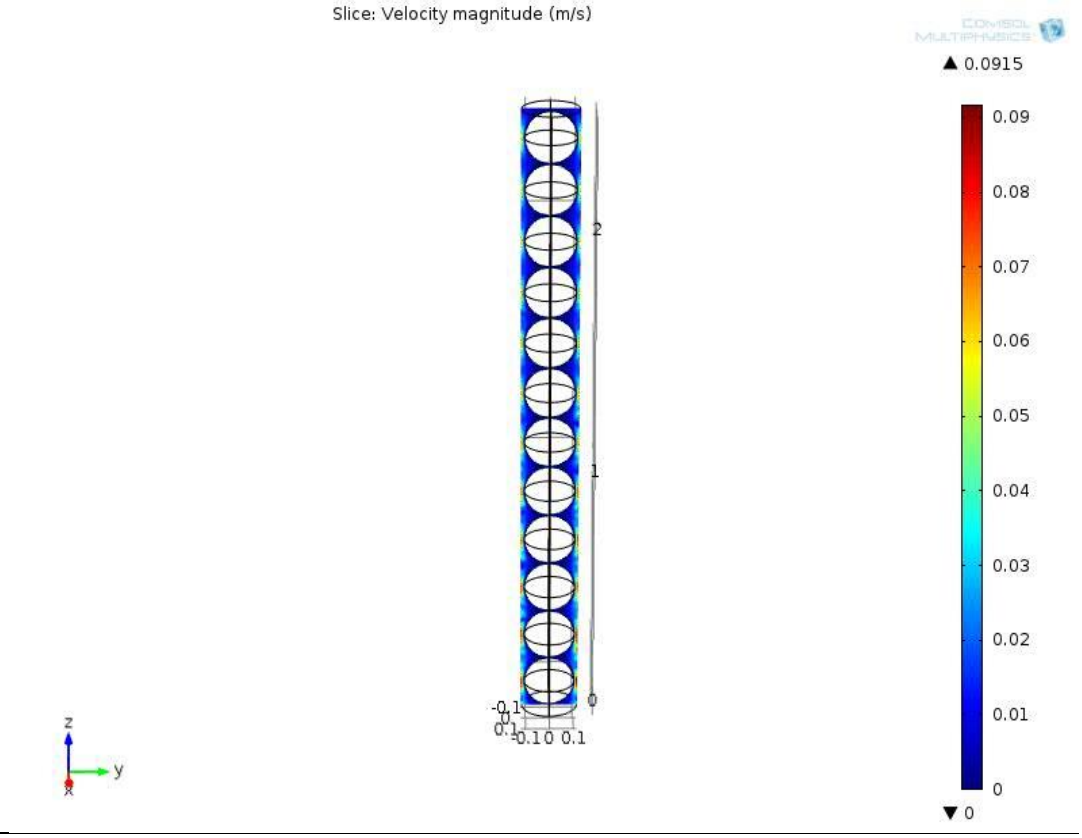

0.2mm height 2.5mm	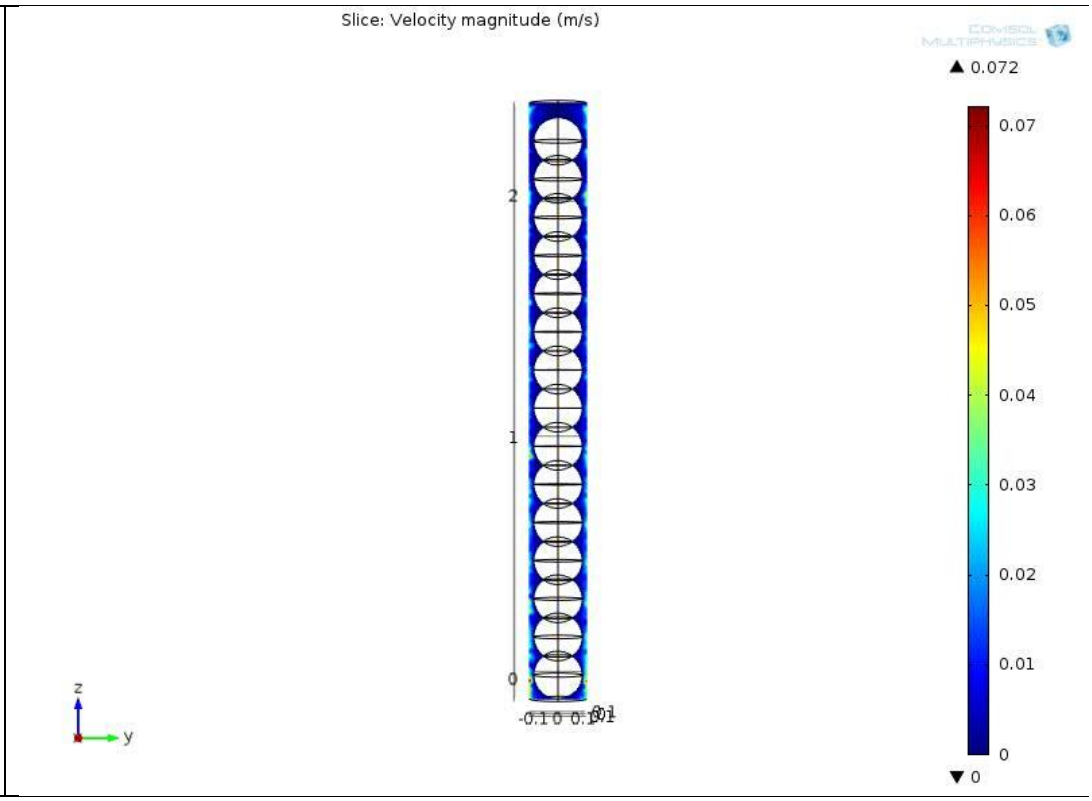

For 50PPI

0.25mm height 2.5mm	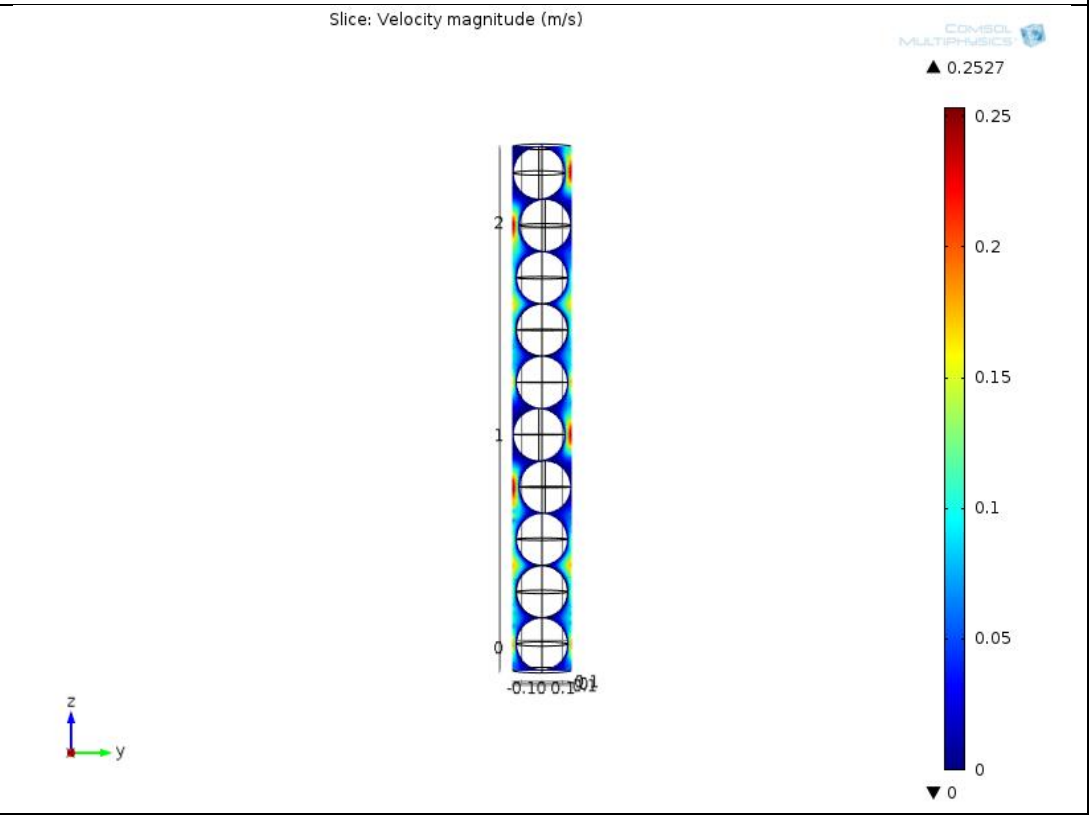

For 40 PPI

0.16mm height 2.5mm	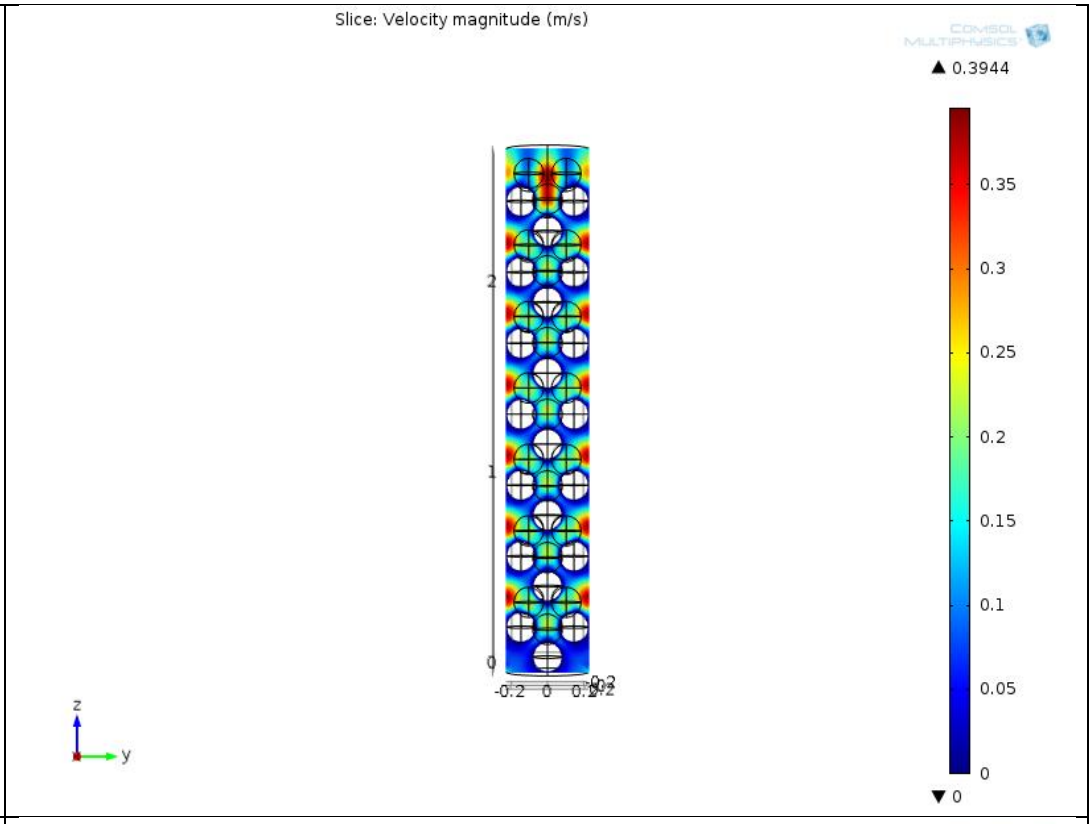
0.16mm arrangement	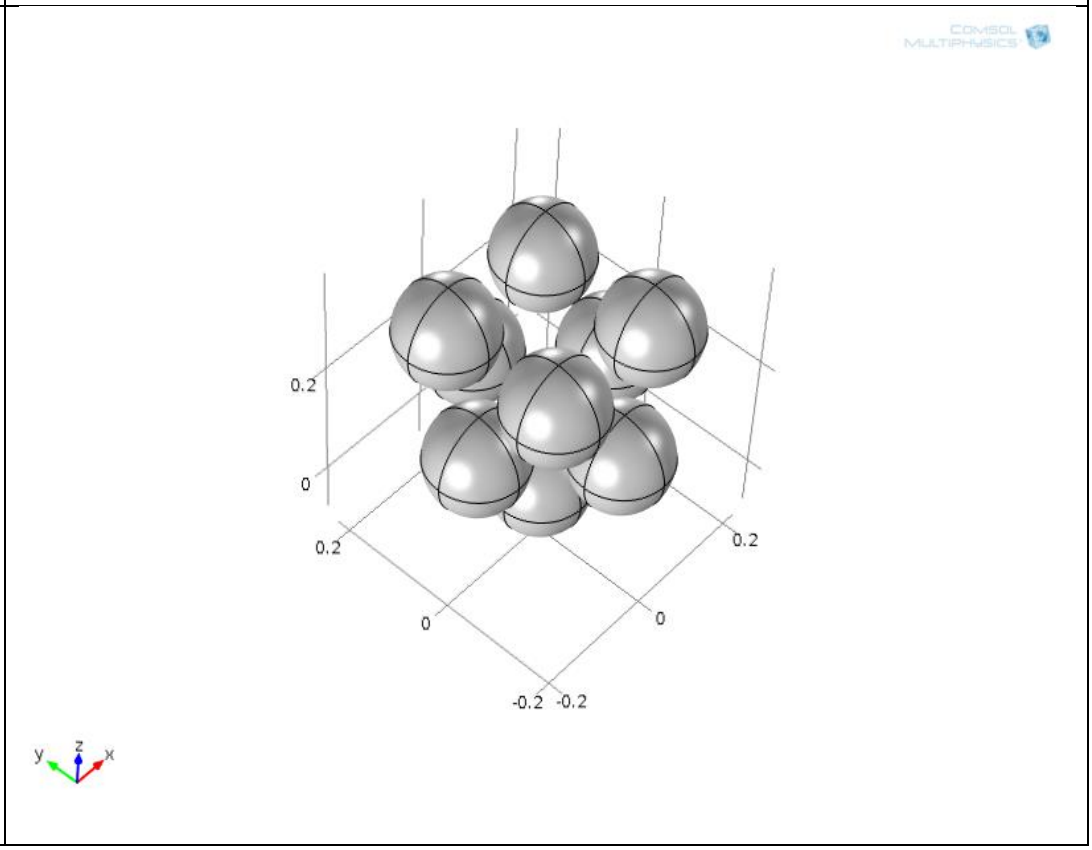

For 30 PPI

Particle diameter	Simulation result
0.15 mm height 2.5mm	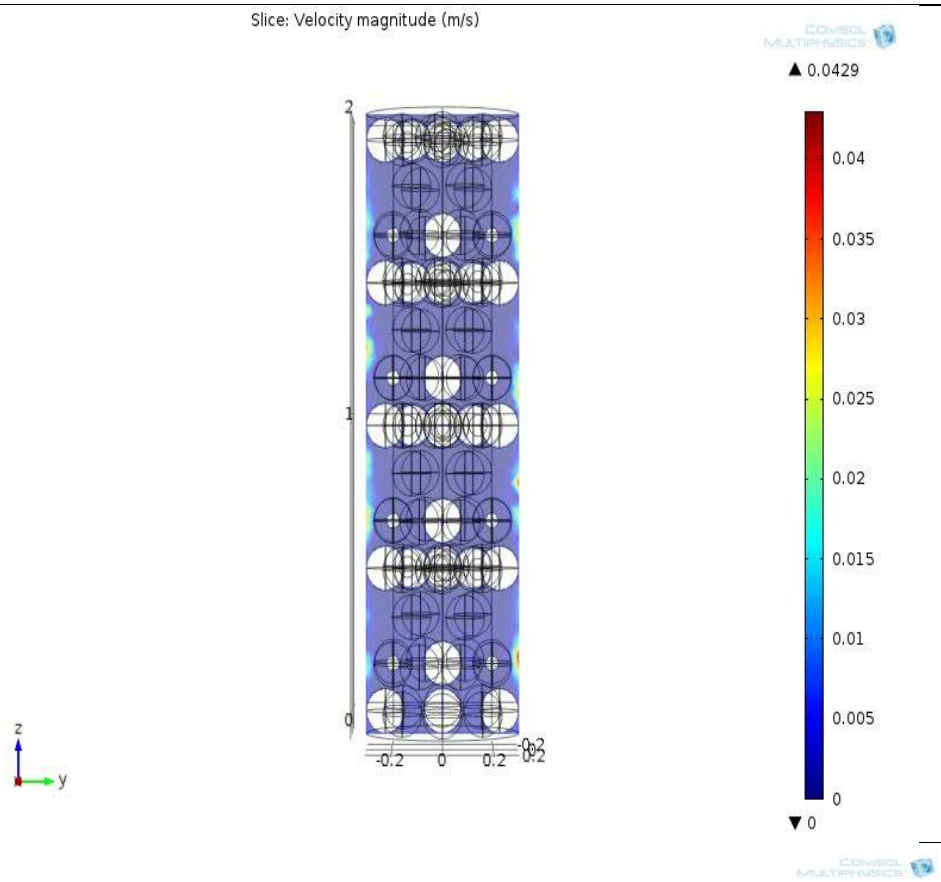
0.15 mm arrangement top view	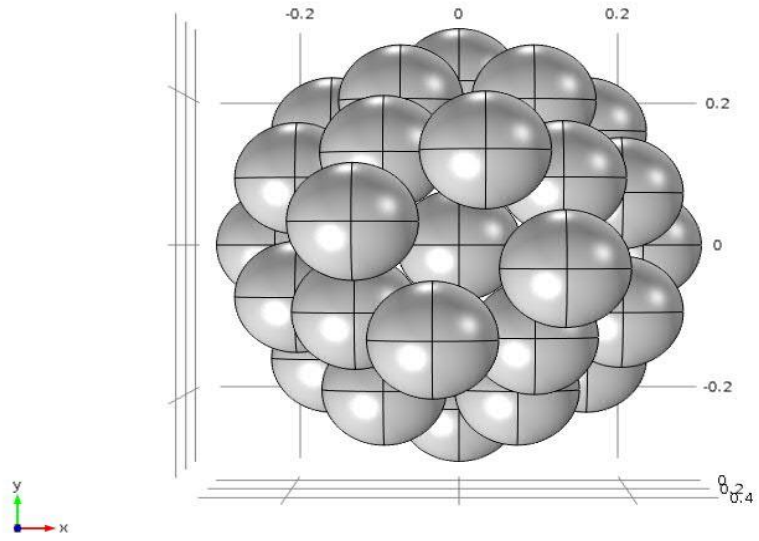

0.18 mm height 2.5 mm	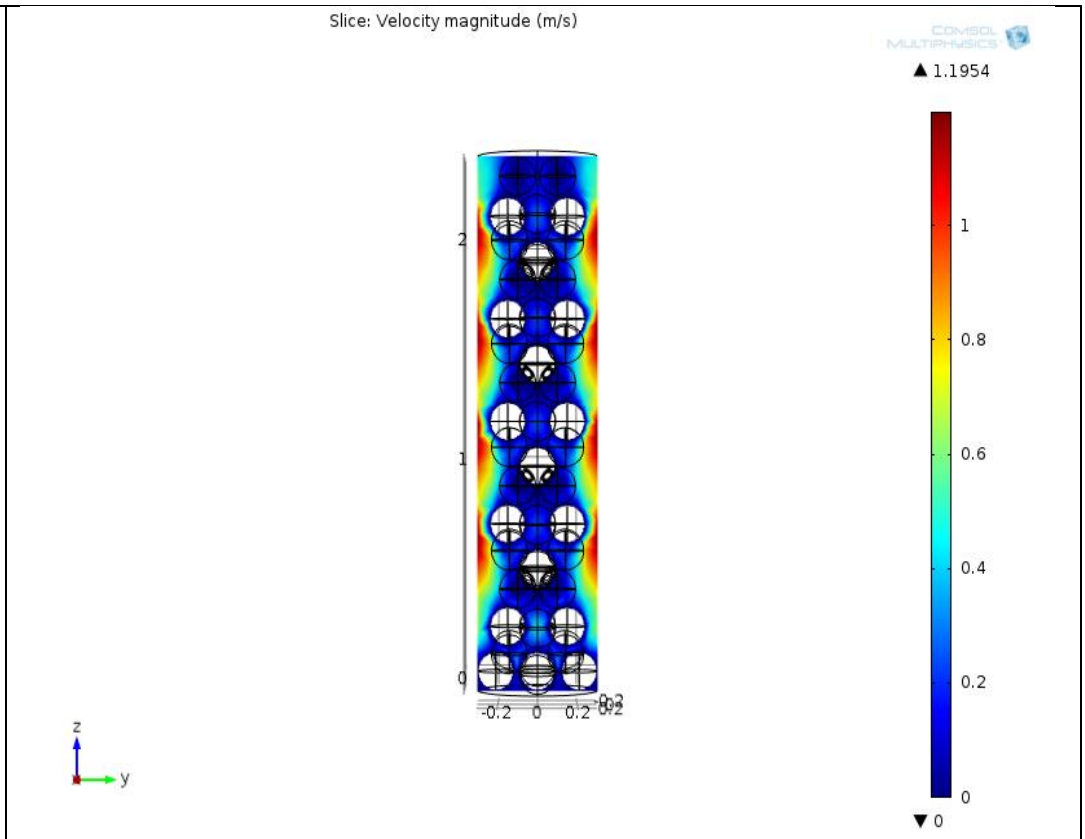
0.19mm height 2.2 mm	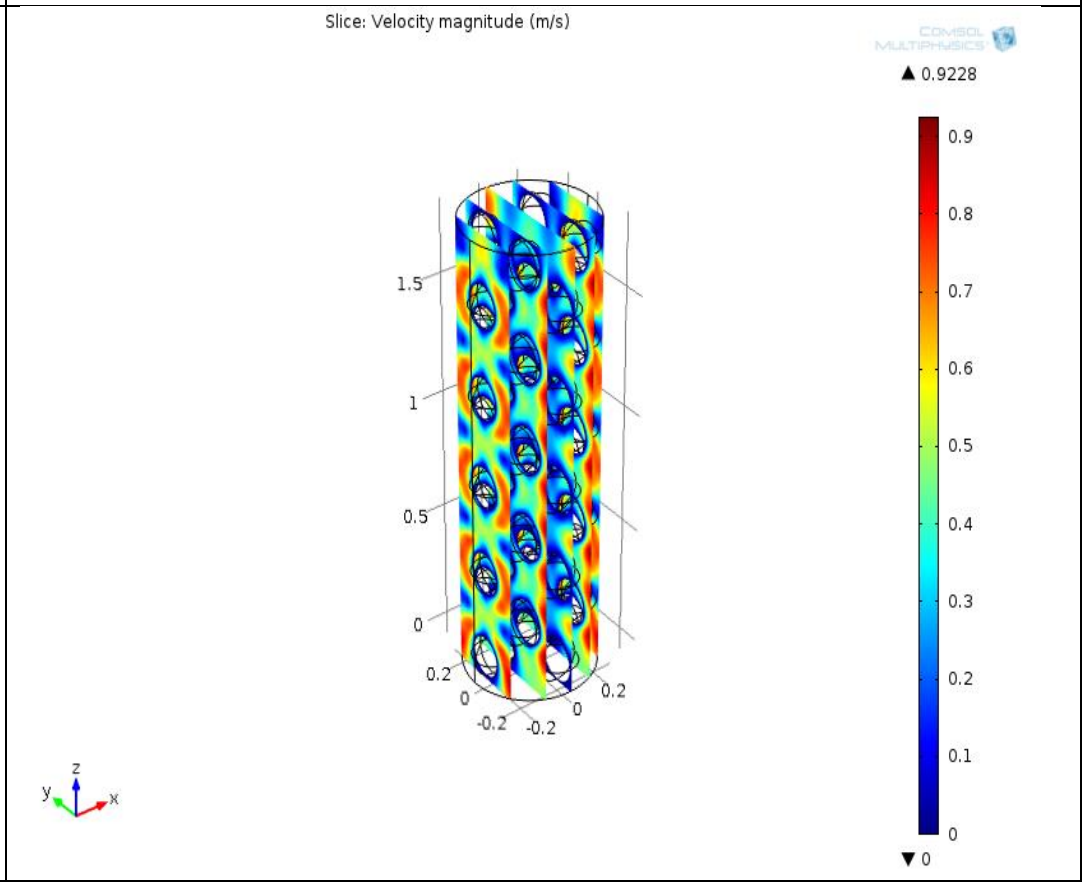

0.25 mm height 5mm	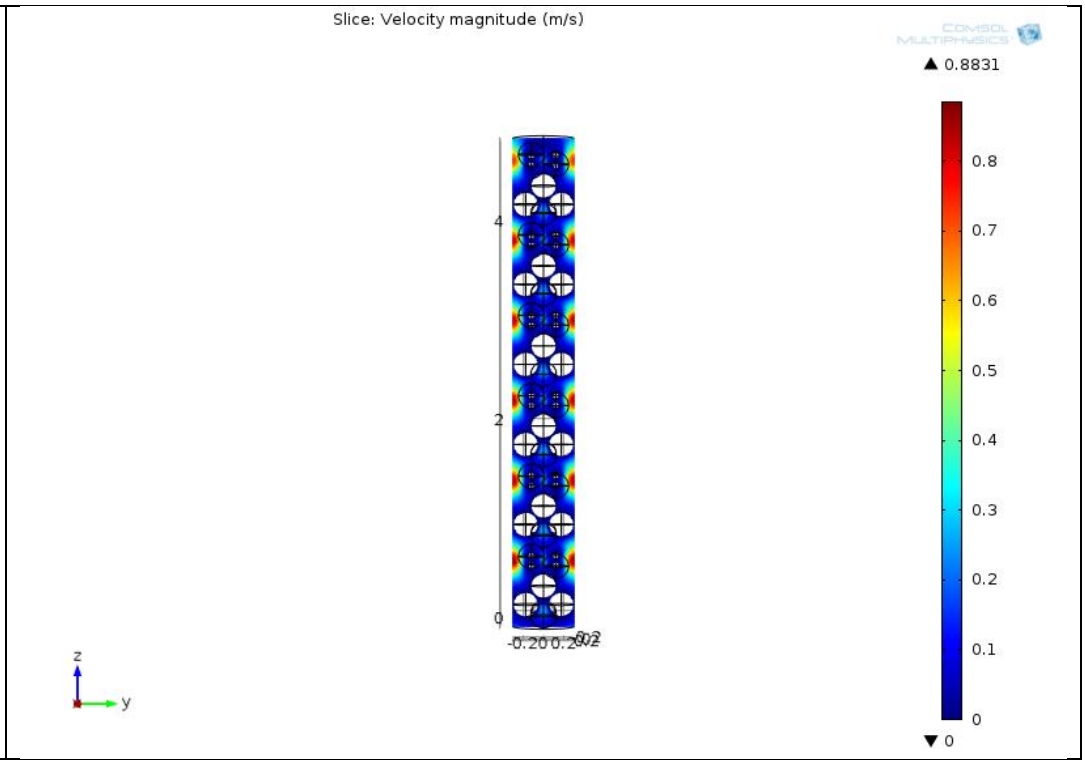

For 20 PPI

0.25 mm particle size in 0.9 mm pore size height 2.5mm	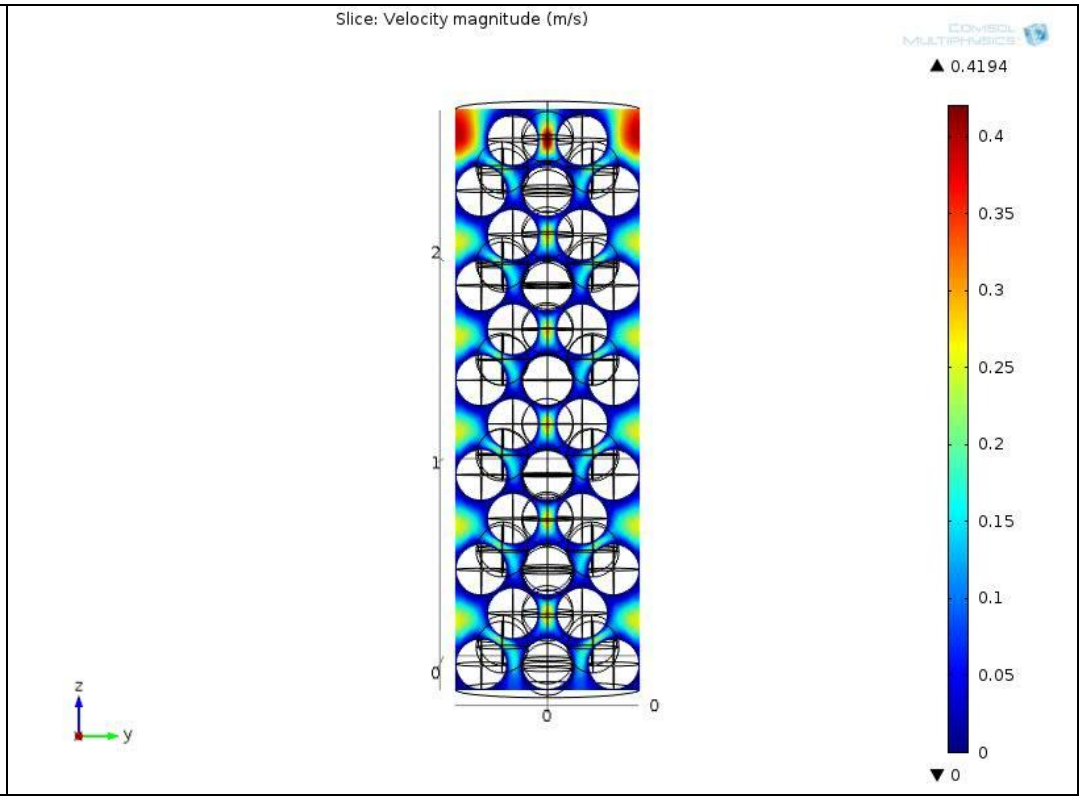

0.25 mm particle arrangement in 0.9mm pore diameter	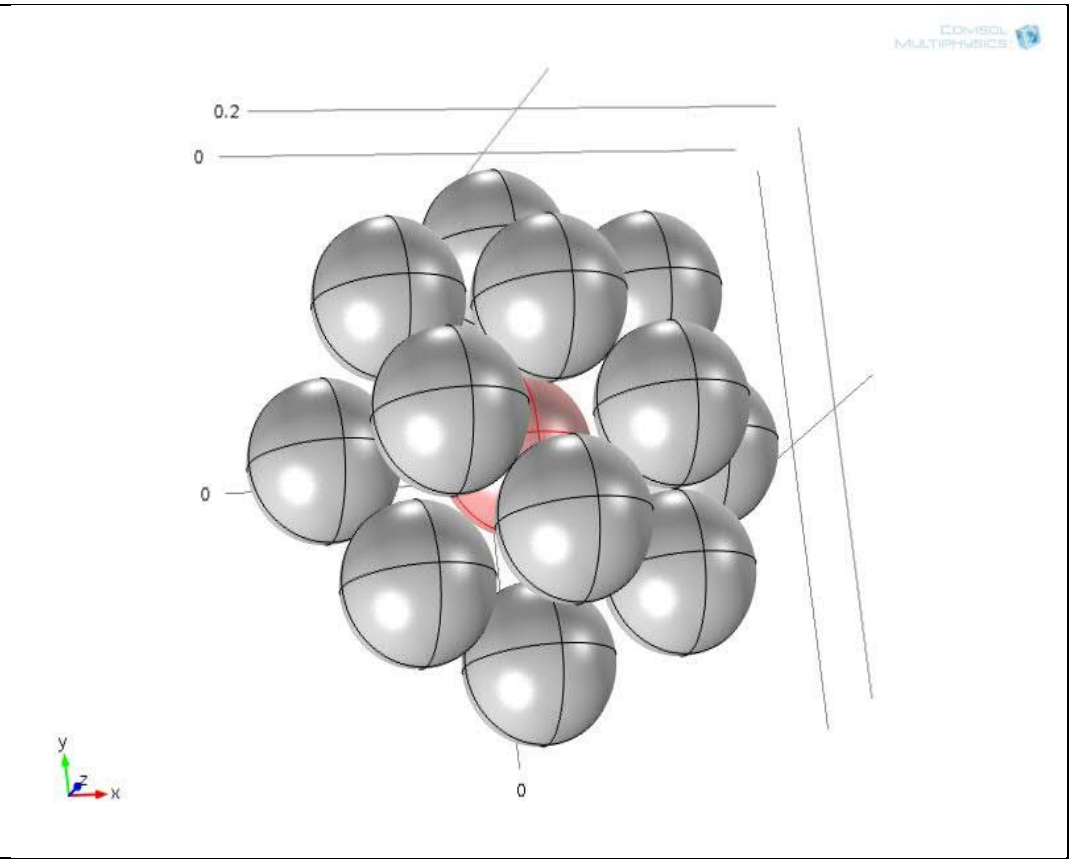

I declare that this thesis work is my original work and has not presented for a degree in any other university, and also all sources of the materials are well acknowledged.

Name: Tesfaye Gonite

Signature:_____

Thesis title: Simulation of Water Transport through Nano Foam Filter

Department: Dr. Daniel Tilahun

Signature: _____

Advisor: Professor Eyassu Woldesenbet

Signature:_____

Coo advisor: Dr. Daniel Tilahun

Signature:_____